CONTRIBUTION OF A MAJOR QUANTITATIVE TRAIT LOCUS TO MOUSE ADENOVIRUS TYPE 1 ENCEPHALITIS AND MORTALITY

by

Tien-Huei Hsu

A dissertation submitted in partial fulfillment
of the requirements for the degree of
Doctor of Philosophy
(Microbiology and Immunology)
in The University of Michigan
2012

Doctoral Committee:

Professor Katherine R. Spindler, Chair
Professor David T. Burke
Professor Michael J. Imperiale
Professor Bethany B. Moore
Associate Professor David Miller

Dedication

To my parents, to whom I owe everything.

Acknowledgments

This dissertation would not have been possible without the help, support and guidance of many people.

First and foremost, I thank my Ph.D. advisor, Kathy Spindler, for taking me into her lab. She is a successful woman in science, and that is great inspiration to me. I am grateful for her time, ideas, and funding which made my Ph.D. experience productive. I also thank her for her meticulous comments on abstracts, grant proposals, manuscripts, and this dissertation.

I am also deeply grateful for my committee members, who have given generously of their time, support and guidance, and whose insightful comments have guided the course of my dissertation work. The unique scientific perspectives they offered are greatly appreciated. Dave Miller asked key questions and offered great solutions. Dave Burke provided invaluable advice on the transgenic mouse work and other genetics questions. Beth Moore, whom I have known since 2005, is a constant source of excellent advice and encouraging words. Her unwavering confidence in my abilities has supported me in times of self-doubt. Mike Imperiale has continuously challenged me to think critically at every step; the rigorous training environment he provided is great preparation for my future work in science.

I am grateful to many others at the University of Michigan who have contributed to this work. Irene Althaus was integral in the construction of the congenic mouse strain. Oded Foreman analyzed the histology slides and helped score them. Matt Stier

performed the BAC sequencing and ligation detection assays. Tyson Luoma performed bioinformatics analysis of the CHORI BAC library sequencing data. Amanda Welton, Shanna Ashley, Jenny Imperiale, Brad Harlan, Carla Domanski, Kaveri Rajula, Michelle Passater, and Samantha Sayers helped with the husbandry and genotyping of the mouse strains. Wanda Filipiak and Maggie van Keuren from the UM Transgenic Animal Model Core prepared the transgenic mice. Thom Saunders provided advice on BAC transgenesis and gave us access to his pulsed-field gel apparatus. Richard Keep taught me how to use the flame photometer and also helped me with the interpretation of the edema results. Yasmina Laouar, Irina Grigorova and Mike Elfman helped with the design and analysis of flow cytometry experiments. Anuska Andjelkovic provided advice on the isolation of primary cells. Jason Weinberg offered critical feedback during lab meetings and on manuscripts. Shanna Ashley taught me many techniques when I first joined the lab.

I gratefully acknowledge all funding sources that have made my Ph.D. work possible. This work was supported by a NIH R01 AI068645 grant to Kathy. I was also funded by the Rackham Merit Fellowship, Genetics Training Grant, University of Michigan EDGE award Outstanding Graduate Student Fellowship, Rackham Graduate Student Research Grants, and the Dr. Frances Wang Chin Fellowship in Microbiology and Immunology. Travel to conferences was made possible by the following: Rackham travel grants, National Cancer Institute travel award, American Society for Virology travel grants, Genetics Training Grant travel awards, and the International Mammalian Genome Society Scholarship. The publication citation information for Chapters II, III, and IV are in the Notes sections at the end of each chapter.

Thank you to the Microbiology and Immunology department for the outstanding training and support I received. I am indebted to Phil King and Vic DiRita for their kindness, encouragement and excellent advice. The ladies of the M&I office have been amazing and made sure everything went smoothly for me. Heidi Thompson, in particular, has gone above and beyond with her support and encouragement.

I would also like to thank past and present members of the Spindler lab. Their friendship has sustained me through the most challenging periods of graduate school. I cherish dearly the conversations we've had, the laughter we've shared, and the faith they have in me.

I have made so many good friends in the past five years, many of whom I have already mentioned. I cannot imagine having a better group of people around me. I am fully aware of how lucky I am to have them in my life. This achievement would have been out of my reach without my friends, who were with me every step of the way.

I would also like to thank Stephen Lin, who is my port in stormy seas. His patient tolerance of my moods, unquestioning support of my decision to remain at the University of Michigan (though it meant five long years of being away from each other), and constant encouragement when my confidence wore thin, speak to his unwavering commitment to me.

Finally, I would like to thank my family for their love and support. Everything I am now is because of where I came from. My parents taught me to love learning for its own sake. They also taught me that one needs to persevere to gain what is worthwhile. Without intellectual curiosity, I would not have begun this journey; without discipline, I could not have completed it.

Table of Contents

List of Figures

Figure

List of Tables

Table

Abstract

Mice from susceptible mouse strains die from hemorrhagic encephalomyelitis following infection with mouse adenovirus type 1 (MAV-1). MAV-1 susceptibility quantitative trait locus, *Msq1*, was identified based on its strong linkage to the high brain viral load phenotype (a surrogate measure of susceptibility) following MAV-1 infection. *Msq1* accounts for ~40% of the phenotypic trait variance between resistant BALB/c and susceptible SJL mice after MAV-1 infection. To study the *in vivo* contribution of *Msq1*, we bred an interval-specific congenic mouse strain (C.SJL-Msq1^{SJL}), in which the SJL-derived allele *Msq1*^{SJL} is introgressed onto a BALB/c background. *Msq1*^{SJL} accounts for the high brain viral titers and blood-brain barrier disruption, yet does not account for the total extent of brain pathology, edema, inflammatory cell recruitment or mortality in SJL mice. In comparison, BALB/c mice showed no signs of disease in these assays. Infection of SJL- and C.SJL-Msq1^{SJL}-derived primary mouse brain endothelial cells resulted in loss of barrier properties, whereas BALB/c-derived cells retained their barrier properties. These results validate *Msq1* as an important host factor in MAV-1 infection, and refine the major role of the locus in development of MAV-1 encephalitis. They further suggest that additional host factors or gene interactions are involved in the mechanism of pathogenesis in MAV-1-infected SJL mice.

There are 14 *Ly6* or *Ly6*-related genes in Msq1, which spans from 74.68 to 75.43 Mb on mouse chromosome 15. *Ly6* genes are good candidate genes for MAV-1 susceptibility because their gene products are expressed on both myeloid and lymphoid cells and because they can be upregulated by both type I and II interferons. In addition, they have been identified as important host factors in other viral infections, including HIV, West Nile virus and Marek's disease virus. To identify the specific *Ly6* gene(s) that influence MAV-1 infection, transgenic mouse strains were made using bacterial artificial chromosomes derived from $Msq1^{129S6/SvEv}$. Thus far, 7 of the 8 transgenic mouse strains were phenotypically resistant to MAV-1 infection. Efforts to interpret the resistant phenotype are currently ongoing.

Chapter I

Introduction

Human adenoviruses

Human adenoviruses were first isolated from adenoid tissues in 1953 (Hilleman and Werner, 1954; Rowe et al., 1953). Adenovirus serotype classifications are determined based on the ability of different antisera to neutralize known human adenoviruses (Fields et al., 2007). However, recent whole genome sequencing of adenoviruses revealed the unreliability of using low-resolution techniques such as serum neutralization and hexon sequencing for adenovirus classifications (Singh et al., 2012; Walsh et al., 2010; Zhou et al., 2012). Accordingly, whole genome sequencing has now become the standard of adenovirus classification. To date, over 60 adenoviruses have been formally recognized based on a combination of serology, phylogenetics and whole genome sequencing (Singh et al., 2012).

Adenoviruses all share a similar structure to adenovirus 5 (Ad5), which was resolved to near atomic resolution in 2010 by cryo-electron microscopy (Liu et al., 2010) and x-ray crystallography (Reddy et al., 2010). Adenoviruses are medium-sized, non-enveloped, double-stranded DNA viruses that contain genomes ranging in size from 26 to 45 kb (Davison et al., 2003; Fields et al., 2007). Each viral particle has a diameter of ~90 nm, and a protein shell that consists of three major (hexon, penton, and fiber) and four minor (IIIa, VI, VIII, and IX) capsid proteins. The viral core includes four additional proteins (V, VII, μ, and terminal protein) and DNA.

Human adenoviruses are responsible for ~5 to 10% of early childhood respiratory infections (Fields et al., 2007). They have also been associated with acute respiratory disease in military recruits, who are susceptible to infection from the combination of overcrowding and exhaustion. In addition, adenoviruses can cause a variety of other clinical syndromes, including most commonly, keratoconjunctivitis and gastroenteritis (Goncalves et al., 2011; Sambursky et al., 2007). In immunocompetent hosts, human adenovirus infections are usually mild and self-limiting, or asymptomatic. However, in immunocompromised individuals, such as transplant, cancer, immunodeficient or AIDs patients, adenoviral infections often become disseminated and cause a broad range of clinical disease (Krilov, 2005). These include hemorrhagic cystitis, myocarditis, hepatitis, pneumonia, and encephalitis.

Encephalitis caused by human adenoviruses occurs most often in children during acute respiratory disease outbreaks and is most commonly associated with adenovirus type 7 (Gabrielson et al., 1966; Sakata et al., 1998; Simila et al., 1970). Other human adenoviruses that have been associated with central nervous system (CNS) disease include adenoviruses type 2 (West et al., 1985), type 3 (Okamoto et al., 2004), type 5 (Chatterjee et al., 2000), type 11 (Osamura et al., 1993), type 32 (Roos et al., 1972), type 31 and 49 (Schnurr et al., 1995). Although human adenovirus molecular biology has been extensively studied (Fields et al., 2007), we know little of the mechanisms of adenovirus neuroinvasion and brain pathogenesis, and even less about the contribution of host factors to susceptibility to adenoviral disease. Knowledge of these may help the development of therapeutic interventions to decrease disease severity.

Experimental animal models of human adenoviruses

Due to the species-specificity of adenoviruses, study of human adenoviruses has lacked good animal models (Wold and Horwitz, 2007). Human adenoviruses can infect cells of other species, including the mouse, but only at very high multiplicities of infection that are not physiologically relevant (Blair et al., 1989; Ganly et al., 2000; Jogler et al., 2006; Ternovoi et al., 2005; Younghusband et al., 1979). Human adenovirus infection is inhibited even in monkey cells, and requires either coinfection with SV40 or key adenovirus mutations to overcome the host-range barrier (Klessig and Grodzicker, 1979; Rabson et al., 1964). The exception to this species-specificity is porcine primary cell cultures, in which Ad5 is able to establish robust replication (Jogler et al., 2006). Nevertheless, animal models have been explored to study human adenovirus biology and pathology. Because mice are not permissive hosts for human adenovirus infections (Ginsberg et al., 1991), the suitability of other small laboratory rodents, including the cotton rat (Pacini et al., 1984) and the Syrian hamster (Hjorth et al., 1988), has been pursued.

The cotton rat has been used as a model organism for many human respiratory tract infections (Sadowski et al., 1987). Cotton rats are susceptible to at least 4 adenovirus types, including types 1, 2, 5, and 6 (Pacini et al., 1984). In addition, when adenovirus type 5 (Ad5) is intranasally inoculated into the cotton rat, pneumonia develops, similar to that seen in humans (Pacini et al., 1984; Prince et al., 1993). When a cotton rat fibrosarcoma cell line is compared with a human lung carcinoma cell line (A549) with regard to susceptibility to Ad5 infection, high progeny release is seen in A549 cells, while virus progeny release from the cotton rat fibrosarcoma cell line is 2 log

units lower (Toth et al., 2005). In addition, injection of an oncolytic adenovirus vector into tumors establishes infection in the tumors but not in normal tissues of the cotton rat; no viral progeny is detectable in blood, liver, or lung tissues by 2 days post injection.

The Syrian hamster is also permissive for Ad5 infection in the lung (Hjorth et al., 1988). In addition, Ad6 is able to establish a persistent infection in the brains of young adult hamsters (Yabe et al., 1988). A comparison study of a Syrian hamster kidney cell line with A549 cells revealed only a 1 log unit difference in viral replication between the cell lines, with lower virus yield in the Syrian hamster kidney cells (Thomas et al., 2006). Also, following intratumoral infection of the oncolytic adenovirus vector into hamster tumors, viral progeny was detected in blood, liver and lungs up to 7 days post injection. In another study, primary cell cultures from different laboratory animal species (including the cotton rat and the Syrian hamster) were infected with Ad5 and compared using a single-cycle virus burst assay (Jogler et al., 2006). Cotton rat primary cells required a one log unit higher virus inoculation than Syrian hamster cells for the production of infectious viral particles.

The results from these studies suggest that Syrian hamster cells and hamsters are more permissive to adenovirus infection than are cotton rats and cells derived from cotton rats. Therefore, Syrian hamsters seem to be a better animal model for human adenoviruses. However, a study examining parallel intracranial infections of cotton rats and Syrian hamsters with Ad5 and a glioma-targeting conditionally replicative adenovirus demonstrated that cotton rats are much more susceptible than Syrian hamsters (Sonabend et al., 2009). The different conclusions reached from these studies may result

from the differences in inoculation route and sensitivity of the assays used to detect presence of virus.

Mouse adenoviruses

Adenoviruses have also been isolated from other vertebrates besides humans. There are four different genera in the current adenovirus classification: *Mastadenovirus, Aviadenovirus*, *Atadenovirus*, and *Siadenovirus* (Davison et al., 2003; Harrach and Benkö, 2007). An additional fish adenovirus (obtained from white sturgeon) falls into a fifth clade, which may subsequently be classified as a separate genus. Non-human adenoviruses provide alternative approaches to studying adenoviral pathology in the natural host. Mice in particular are a convenient and powerful experimental model organism for *in vivo* study of adenovirus pathogenesis and the genetic components mediating susceptibility to adenoviruses. This is due to the availability of resources that include inbred mouse strains, immunological tools, and mouse cell lines that can be biochemically, immunologically and genetically manipulated.

Despite numerous independent isolations, only three mouse adenovirus types have thus far been identified, mouse adenovirus type 1 (MAV-1) (Hartley and Rowe, 1960), mouse adenovirus type 2 (MAV-2) (Hashimoto et al., 1966), and mouse adenovirus type 3 (MAV-3) (Klempa et al., 2009). Mouse adenoviruses cause different pathologies. MAV-1 causes a disseminated infection and in particular, replicates to high titers in the CNS and spleen of susceptible mouse strains (Charles et al., 1998; Guida et al., 1995; Kajon et al., 1998; Kring et al., 1995). MAV-2 mainly infects cells of the gastrointestinal tract (Takeuchi and Hashimoto, 1976), while MAV-3 predominantly infects heart tissues

(Klempa et al., 2009). Why there are significant differences in mouse adenovirus pathologies is currently unknown.

Like human adenoviruses, mouse adenoviruses belong to the *Mastadenovirus* genus (Davison et al., 2003); mouse adenoviruses have a similar structure and genomic organization to human adenoviruses (Hemmi et al., 2011; Klempa et al., 2009; Spindler et al., 2007). Phylogenetic and genetic analyses reveal that MAV-1 and MAV-3 are more similar to each other than to MAV-2 (Hemmi et al., 2011; Klempa et al., 2009). This is surprising given that MAV-1 and MAV-2 were both isolated from the house mouse (*Mus musculus*), while MAV-3 was isolated from the striped field mouse (*Apodemus agrarius*). Cross-neutralization of mouse adenoviruses is only partially effective. MAV-2 antisera are able to neutralize both MAV-2 and MAV-1. MAV-1 antisera neutralize MAV-1, but its neutralization of MAV-2 and MAV-3 is much weaker (Klempa et al., 2009; Lussier et al., 1987; Wigand et al., 1977). MAV-3 antisera neutralize MAV-3, but show no cross-neutralization of MAV-1 (Klempa et al., 2009). Cross-neutralization experiments with MAV-2 and MAV-3 have yet not been performed.

MAV-1 was first identified in 1960 as a contaminant in Friend murine leukemia cultures, and it has subsequently been successfully used in *in vivo* adenovirus pathogenesis studies (Spindler et al., 2007). MAV-1 infects both inbred and outbred strains of mice and targets endothelial cells and cells of the monocytic lineage, causing acute and persistent infections. Disease outcome of MAV-1 infection is dependent on the administered dose of virus, the route of infection, and the age and strain of mice (Guida et al., 1995; Kring et al., 1995; Spindler et al., 2001). In neonatal and suckling mice, MAV-1 infection results in a disseminated infection, resulting in death. MAV-1 can

cause fatal disease in both newborn and adult mice with inocula as low as 1 PFU (Hartley and Rowe, 1960; Spindler et al., 2001).

Host immune response to MAV-1 infection

Resistance to MAV-1 infection is thought to be mediated by host immune response. Exposure of resistant C3H/HeJ mice to a sublethal dose of gamma irradiation renders them susceptible to MAV-1 (Spindler et al., 2001). $RAG^{-/-}$ mice on a C57BL/6 background that are deficient for mature T- and B-cells succumb more readily to MAV-1 infection than wild-type C57BL/6 controls (Moore et al., 2003). SCID mice on a BALB/c background (BALB/c are a MAV-1-resistant strain) are also highly susceptible to MAV-1 infection and develop diffuse hepatic damage similar to that seen in human Reye syndrome (Charles et al., 1998; Pirofski et al., 1991).

Mice lacking α/β T cells develop high brain viral loads and eventually succumb to MAV-1 infection by 9 to 12 weeks post infection (Moore et al., 2003). In contrast, wild-type C57BL/6 control mice are able to clear viral infection. These data demonstrate that T cells are required for long-term viral clearance. However, MHC class I-deficient, MHC class II deficient, $CD8^{-/-}$, $CD4^{-/-}$, and perforin-deficient mice are able to clear virus, demonstrating that having either $CD4^{+}$ or $CD8^{+}$ T cells present is sufficient for viral clearance. Despite their increased susceptibility to MAV-1, mice lacking α/β T cells do not develop encephalomyelitis in response to MAV-1 infection, demonstrating that T cells contribute to the brain immunopathology. Mice lacking MHC class I and perforin do not show signs of acute disease and have less MAV-1-induced brain pathology. In contrast, MHC class II-deficient mice have similar pathology to infected susceptible

wild-type mice. These data suggest that $CD8^+$ T cells contribute significantly to MAV-1 encephalomyelitis.

Mice that are genetically deficient in NK cells and mice that are lacking both NK and T cells do not differ from wild type control mice in either viral loads or survival following MAV-1 infection. C57BL/6 and BALB/c mice that were depleted of NK cells and infected with MAV-1 have similar brain viral loads as mice that had not been depleted of NK cells, and no differences in survival were seen (Welton et al., 2008). Therefore, NK cells do not appear to have a role in control of MAV-1 replication in the brains of mice.

B cell-deficient mice are also highly susceptible to MAV-1 infection; they die earlier than T cell-deficient mice, suggesting that B cells (but not T cells) are required at the acute phase of infection (Moore et al., 2004). Bruton's tyrosine kinase knockout mice (Btk-/-), which have reduced serum immunoglobin and decreased levels of conventional B cells and peritoneal B-1 cells, also succumb to MAV-1 infection early in infection. Finally, treatment with MAV-1 immune serum (containing T cell independent antiviral IgM) protects Btk-/- mice against lethal infection.

Macrophages are recruited to the brains of C57BL/6 mice after MAV-1 infection (Gralinski et al., 2009). Macrophage depletion by treatment with clodronate-loaded liposomes results in increased spleen viral loads in treated BALB/c mice compared to untreated mice, suggesting that macrophages play a role in control of MAV-1 infection in the spleens of BALB/c mice (Ashley et al., 2009). However, high brain and spleen viral loads are seen in both treated and untreated SJL mice. These data suggest that macrophages do not control the dissemination of virus in SJL mice.

The blood-brain barrier (BBB) and MAV-1 encephalitis

The BBB is a highly regulated interface that separates the brain parenchyma from the peripheral circulation (Abbott et al., 2010). The exclusion of an intravenously injected dye from brain tissue was first observed by Paul Ehrlich in 1885. The BBB serves a critical function because the regulation of the extracellular environment of neurons is essential for their function. Concentrations of ions, chemicals and other solutes are normally controlled within very narrow ranges, and disruption of these levels can have neurotoxic effects.

A key component of the BBB is the endothelial cells that line the brain microvasculature. These cells are different from endothelial cells in the periphery due to the presence of intercellular tight junctions (Kniesel and Wolburg, 2000), the lack of fenestrations (Fenstermacher et al., 1988), increased mitochondrial count (Oldendorf et al., 1977), and the low rate of endocytosis (Sedlakova et al., 1999). Other cells that make up the BBB are astrocytes, pericytes, and neurons, which can modulate the integrity of the barrier by the secretion of cellular factors (Hawkins and Davis, 2005). With the addition of the extracellular matrix, these components make up the "neurovascular unit."

In certain cases, increased BBB permeability can be a pathological effect of the disease, such as during ischemic stroke (Ilzecka, 1996). In other diseases, BBB disruption may be the cause of pathology, such as in multiple sclerosis (Minagar and Alexander, 2003). Failure of the BBB during CNS disease has a critical effect on disease outcome. Increased permeability of the BBB has harmful consequences, such as the influx of neurotoxic compounds and fluid from the peripheral circulation. In addition, disruption of the BBB due to disease, such as from an encephalitic viral infection, is usually

accompanied by large immune cell infiltrate into the CNS (Charles et al., 2001; Dorries, 2001; Irani and Griffin, 1996). Inflammatory cell presence in the CNS is low in healthy individuals and limited to immune cell surveillance; influx of inflammatory cells into the brain parenchyma is usually a sign of disease (Wekerle et al., 1986). At this time, the mechanisms by which immune cells cross the BBB have not been well-defined, although immune cells are known to passage through and between brain endothelial cells (refer to Spindler and Hsu, 2012; Chapter III).

Key factors controlling BBB permeability include matrix metalloproteinases (MMPs) (Candelario-Jalil et al., 2009). MMPs are endoproteinases whose primary function is the remodeling of extracellular matrix. In the healthy individual, MMPs participate in repair and regenerative processes such as angiogenesis and tissue repair. However, during CNS disease, MMPs play a role in the degradation of basement membrane and extracellular matrix, as well as tight junction proteins, thereby facilitating leukocyte infiltration into the brain parenchyma (Hartung and Kieseier, 2000; Jin et al., 2010; Keogh et al., 2003; Reijerkerk et al., 2006; Wang et al., 2008). Uncovering the pathways by which BBB disruption occurs (e.g., through the regulation of the expression or degradation of tight junction proteins) has significant potential for the treatment of disease and the delivery of drugs to the CNS.

Viruses are the most common causes of encephalitis; encephalitic viruses disrupt the BBB through a variety of means (refer to Spindler and Hsu, 2012; Chapter III). MAV-1 causes a fatal encephalomyelitis in mice, its natural host (Guida et al., 1995; Kring et al., 1995). The occurrence of hemorrhagic encephalitis following MAV-1 infection is dependent on both the dose of MAV-1 inoculum and the mouse strain.

MAV-1 induces a dose-dependent breakdown of the BBB during acute infection of C57BL/6 mice, which have an intermediate susceptibility to MAV-1, but not in similarly infected (resistant) BALB/c mice (Gralinski et al., 2009; Guida et al., 1995). Lethal MAV-1 encephalitis is associated with high brain viral loads, accompanied by a large influx of inflammatory cells in the brain, followed by vascular dysfunction, leading to death (Guida et al., 1995; Moore et al., 2003; Spindler et al., 2001).

The primary site of MAV-1 infection in the brain is the endothelial cells of the microvasculature (Charles et al., 1998; Kajon et al., 1998). The infection of primary mouse brain endothelial cells results in the downregulation of tight junction mRNA and protein expression, which could be the precipitating event leading to BBB disruption (Gralinski et al., 2009). It had previously been suggested that there is a receptor for MAV-1 that is only expressed in the CNS of susceptible mouse strains (Charles et al., 1998). However, MAV-1 can also be detected in brain endothelia of resistant C3H/HeJ mice, although levels are higher in susceptible SJL mice (Spindler et al., 2001). In addition, MAV-1 replicates equally well in the brains of both susceptible SJL and resistant BALB/c mice after intracerebral inoculation (Spindler et al., 2007). These data suggest that the difference in mouse strain susceptibility cannot fully be accounted for by a difference in MAV-1 receptor expression in the brain endothelia of resistant and susceptible mouse strains.

Increased infiltration of $CD4^+$ and $CD8^+$ T cells, B cells, neutrophils, and macrophages is seen in brains of C57BL/6 mice after MAV-1 infection (Gralinski et al., 2009). However, the increased BBB permeability following MAV-1 infection appears to be largely independent of inflammation. Infection of C57BL/6 mice with a mutant early

region 3 (E3) null virus results in reduced cellular infiltrate, but have similar levels of blood-brain barrier breakdown compared to MAV-1-infected mice. Likewise, perforin-/- mice do not have visible inflammatory infiltrate in their brains following MAV-1 infection; however, levels of BBB breakdown are also comparable to that seen in wild-type C57BL/6 controls. These data suggest that BBB disruption during MAV-1 infection is not due to the presence of infiltrating inflammatory cells. Conversely, there is evidence that $CD8^+$ cytotoxic T cells are critical to the pathogenesis of MAV-1 in the brain during acute infection; mice lacking MHC class I genes do not show signs of acute disease (Moore et al., 2003). However, whether increased BBB permeability occurs in these mice is currently unknown.

Studies were performed to determine whether the difference in MAV-1 outcome is due to a difference in cytokine response between the two strains. In particular, MAV-1-susceptible C57BL/6 and MAV-1-resistant BALB/c mice mount Th1 and Th2 cytokine responses, respectively (Gorham et al., 1996). Following activation, naïve $CD4^+$ T cells differentiate into two types of functionally distinct effector cells, Th1 or Th2 cells (Mosmann et al., 2005). Th1 cells induce cell-mediated immunity, while Th2 cells mediate humoral immunity through antibody production. However, analysis of cytokine gene expression following MAV-1 infection did not show any significant differences between BALB/c and C57BL/6 mice in the nature of the cytokines induced in the two strains (Charles et al., 1998).

Genetic differences in chemokines and/or chemokine receptors can also underlie susceptibility to viral infection. Chemokines function as chemoattractants, recruiting specific leukocytes to the site of infection (Baggiolini, 1998). MAV-1 infection results in

an upregulation of the mRNA levels of chemokine receptors in both strains (Charles et al., 1999). However, IFNγ-induced protein 10 (CXCL10), monocyte chemoattractant protein 1 (CCL2), and T cell activation gene 3 (CCL1) steady-state mRNA levels are increased in the CNS of susceptible C57BL/6 mice but not in resistant BALB/c mice. These data suggest a role of chemokines in MAV-1-induced encephalitis. Even so, it has yet to be determined whether the observed chemokine expression differences contribute to the development of pathogenesis, or if they are merely a representation of a difference in the innate immune response brought about as a result of a productive viral infection in C57BL/6 mice.

CCL2 is a chemokine that decreases tight junction protein expression, resulting in loss of endothelial cell barrier properties (Song and Pachter, 2004; Stamatovic et al., 2005). CCL2 is involved in increasing blood-brain barrier permeability during HIV and dengue virus infections (Eugenin et al., 2006; Lee et al., 2006). However, treatment with anti-CCL2 does not prevent loss of barrier properties of an *ex vivo* BBB model in response to MAV-1 infection (Gralinski et al., 2009). In addition, infection with a MAV-1 early region 3 (E3) null mutant causes BBB disruption despite a lack of CCL2 induction. These data indicate that MAV-1-induced BBB disruption is CCL2-independent.

Ex vivo BBB model

The technique for the isolation of cerebral endothelial cells was first developed in 1973 (Joo and Karnushina, 1973). It remains a labor-intensive procedure involving the immediate removal of brains following euthanasia, separation of cerebellum from

cortexes, and the isolation of brain capillaries involving mechanical homogenization, density gradient separation, and enzymatic digestion (detailed protocol in Chapter VI). In addition, primary cultures are susceptible to bacterial contamination due to the many handling steps.

However, the major advantage of using primary brain endothelial cell cultures is that they mimic *in vivo* endothelial cell properties more closely than immortalized endothelial cell lines (Cecchelli et al., 1999). Primary brain endothelial cells grown to a confluent monolayer on a transwell membrane express complex tight junctions and achieve high transendothelial electrical resistance. Immortalized cell lines usually lack the necessary restrictive barrier properties that would allow us to perform permeability screening experiments (Roux and Couraud, 2005). However, the tightness of the endothelial cell barrier seen *ex vivo* still differs greatly from what is seen *in vivo* (Malina et al., 2009). This is because when endothelial cells are removed from their *in vivo* environment, they rapidly lose their characteristics (Risau and Wolburg, 1990). Co-cultures of primary endothelial cells with either glial cells (Malina et al., 2009) or astrocytes (Cecchelli et al., 1999) can increase the barrier properties of endothelial cells.

Data gathered from *ex vivo* studies should therefore not be directly compared to data from *in vivo* models. However, the *ex vivo* model still provides key insight into the effects of MAV-1 infection on brain endothelial cells, and specifically, their barrier properties, in the absence of other neural cell types. In addition, we can also control the subsequent introductions of specific cell types into *ex vivo* cell culture, which can help elucidate the contribution of each cell type to the loss of BBB integrity during MAV-1 infection.

Host determinants of susceptibility to pathogens

There are host genetic contributions to many infectious diseases, leading to diversity in rate of disease progression and outcome. However, the identification of the underlying genes has not been straightforward. While pathogen-specific genetic determinants of infection severity (virulence genes) have been widely studied, less is known about host determinants. Obtaining a better understanding of cellular and host pathways involved in susceptibility to infection may lead to a wider range of therapeutic options. There are a variety of methods to identify host genetic factors involved in viral infection (refer to Hsu and Spindler, 2012; Chapter II).

Although the majority of susceptibility loci have yet to be identified, significant progress has been made to identify genes involved in infection outcome through the development of powerful genetic tools. Quantitative trait locus/loci (QTL) mapping is a common approach used to identify genes involved in complex phenotypes, which include disease outcome (Flaherty et al., 2005). This is a "hypothesis-free" approach; a specific genomic region(s) that is strongly linked to a specific phenotype is isolated without prior knowledge of the functions of the genes contained within the region. This strategy allows researchers to dissect a complex phenotype without having to know the mechanism of the process. Although identifying a QTL does not identify the specific gene(s) involved in the complex trait, this approach drastically reduces the number of candidate genes involved. Identification of the gene(s) underlying the QTL requires further narrowing of the QTL for positional cloning to be feasible. A functional relationship between the candidate gene and the QTL will then need to be demonstrated. In addition, to understand

the molecular pathways that are influenced by the QTL, functional analyses of the gene(s) will need to be performed.

Resistance to *Mycobacterium bovis* and other *Mycobacterium* species, *Salmonella typhimurium* and *Leishmania donovani* was mapped to a single gene encoding the natural resistance associated macrophage protein 1 (*Nramp1*, now annotated as solute carrier family 11 member 1 [*Slc11a1*]) gene in mice via positional cloning (Bradley, 1977; Plant and Glynn, 1976; Skamene et al., 1982; Skamene et al., 1984; Vidal et al., 1993). Susceptible inbred mouse strains have a glycine to aspartate substitution, and this single amino acid change is sufficient to impair *Slc11a1* folding and processing, leading to loss of function of the protein (Malo et al., 1994). In comparison, in humans the contribution of *Slc11a1* is modest due to the increased genetic complexity of the human background and the likely contribution of additional genes (Remus et al., 2003).

Genes controlling resistance to viruses, such as the 2′,5′-oligoadenylate synthetase 1b gene associated with West Nile virus susceptibility (Lucas et al., 2003; Mashimo et al., 2002; Perelygin et al., 2002), and Ly49H, associated with mouse cytomegalovirus susceptibility (Brown et al., 2001; Lee et al., 2001), were also identified through positional cloning. Recently, expression quantitative trait loci that are associated with differences in host response phenotype were identified using mice that exhibit extreme phenotypic responses to influenza virus infection (Bottomly et al., 2012).

Mouse adenovirus type 1 susceptibility quantitative trait locus (*Msq1*)

Using the MAV-1/mouse model, we examined the genetic parameters for viral infection outcome. In adult mice, the 50% lethal dose (LD_{50}) difference between resistant

and susceptible mice can be on the order of >5 log units (Spindler et al., 2001). For example, SJL mice have an LD_{50} of $10^{-0.32}$, while the LD_{50} of BALB/c mice is $>10^{4.4}$. Other resistant strains include C3H/HeJ, DBA/J, A/J and 129/J; other susceptible strains include SWR, 129S6/SvEv and PL/J mice (Spindler et al., 2001; Spindler et al., 2010). High viral loads are found in the spleen and brains of susceptible mouse strains after MAV-1 infection, while significantly lower viral loads are found in the respective organs of resistant mice.

An unbiased genetic approach was used to identify the QTL underlying susceptibility to MAV-1 infection. Backcross mice were generated for mapping analysis and phenotyped for MAV-1 infection outcome (Welton et al., 2005). Results from the initial crosses between inbred mouse strains suggest that the susceptibility phenotype is semi-dominant. Crosses between resistant and susceptible mice produce F_1 progeny that have an intermediate susceptibility to MAV-1. To identify QTL, F_1 mice were genotyped for simple sequence length polymorphism markers distributed evenly throughout the genome. QTL were mapped by identifying genomic markers that are linked to the high brain viral load phenotype. Since we need to determine the susceptibility of individual mice, LD_{50} assays cannot be used for mapping studies. Therefore, brain viral load is used as a surrogate measure of susceptibility.

Through this process we identified a major QTL on mouse chromosome 15 (Chr 15) and another minor effect modifier on Chr 5 that are strongly linked to the susceptibility (high brain viral load) phenotype. The Chr 15 QTL has a logarithm of odds score of 21, and it contributes to ~40% of the trait variance (brain viral load) between resistant BALB/c and susceptible SJL mice. The Chr 15 major QTL is designated *Msq1*.

Additional analysis of recombinant and backcross mice allowed further reduction of *Msq1* from ~2.5 Mb to 0.75 Mb; currently Msq1 spans from 74.68 to 75.43 Mb on Chr 15 (Fig. 1.1).

Distinguishing the effects on susceptibility due to *Msq1* from effects caused by other genes within the SJL background can be difficult. We wanted to be able to examine the role of the QTL in isolation of other contributing variables in the mouse strain that may also affect susceptibility. We accomplished this by introgressing $Msq1^{SJL}$ into the genome of resistant BALB/c mice, to create an interval-specific congenic mouse strain for the QTL (Fig. 1.2). We investigated the *in vivo* contribution of the introgressed locus to MAV-1 infection outcome in Chapter IV.

Since the congenic strategy does not help decrease the number of candidate genes, we used bacterial artificial chromosome (BAC) transgenesis to further reduce the size of *Msq1*. BAC transgenesis has been successfully used to reduce the size of QTLs and to identify and confirm genes of interest (Ferraro et al., 2007; Hillebrandt et al., 2005; Tomida et al., 2009; Vidal et al., 1993). Using the BAC transgenesis approach, relatively large segments (150 to 200 kb) of donor mouse genetic material can be introduced as transgenes into a recipient strain. We describe results from the BAC transgenesis approach in Chapter V.

Transgenic mice

The term “transgenic” was coined to refer to mice that were genetically modified by the stable introduction of foreign genetic material into early stage embryos (Gordon and Ruddle, 1981). This technique was first demonstrated in 1981, almost concurrently,

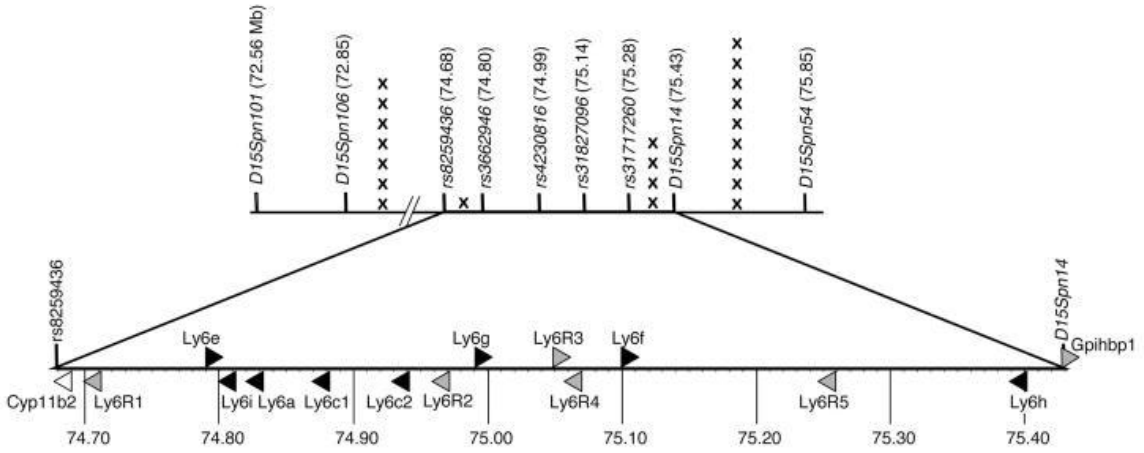

Figure 1.1. ***Msq1*****.** SSLP and SNP markers used in fine mapping backcross progeny are indicated in the top line, in parentheses are the physical positions of each marker. The number of backcrossed mice with genotypic recombination are indicated with an "X" at their respective locations. The lower line is an expansion of the deduced critical interval with predicted candidate genes (figure taken from Spindler et al., 2010).

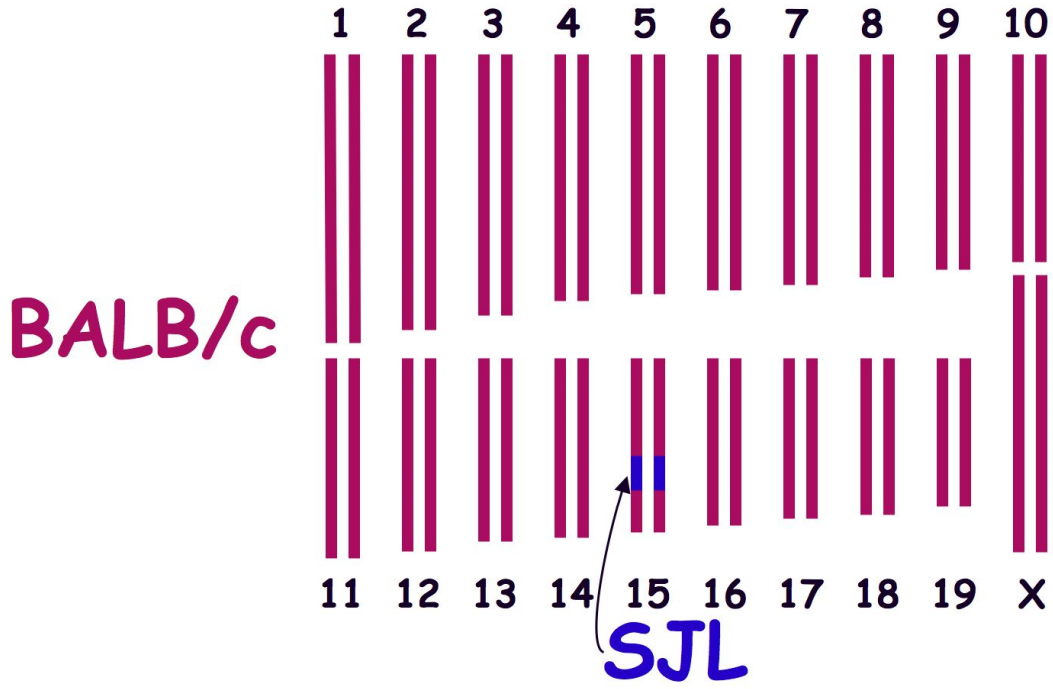

Figure 1.2. Genotype of C.SJL-Msq1 mice.

by multiple labs (Brinster et al., 1981; Costantini and Lacy, 1981; Gordon and Ruddle, 1981; Harbers et al., 1981; Wagner et al., 1981). Transgenic mice are an important and powerful tool that can be used for a number of applications, including the study of gene function and regulation in the context of a whole animal (Deal et al., 2006; Dunnick et al., 2005; Jones et al., 2003; Oliver et al., 2004).

Genetic material, usually entire genes or large genetic regions, is microinjected into the male pronuclei of fertilized embryos (Fig. 1.3) (Nagy, 2003). The embryos are then implanted into the uterus of foster mothers and carried to term. Separate transgenic mouse lines are established from each transgenic founder mouse. This is done because no two transgenic founders are the same. Integration of the transgene into the genome is a random event; the transgene in each transgenic founder mouse is integrated at a unique chromosomal location. Also, copy numbers of integrated transgenes can differ among transgenic founders. In general, transgenes tend to be inserted in multiple copies and form head-to-tail concatmers (Brinster et al., 1981; Gordon and Ruddle, 1981).

To clone a transgene, it must first be in a vector that will enable it to be taken up by a cell. The vector can also contain other useful properties, such as an origin of replication or a selective marker for propagation in a non-mammalian host. There are many different types of vectors that have varying DNA carrying capacities. One cloning system that has been used to create transgenic mice is yeast artificial chromosomes (YACs) (Burke et al., 1987). However, several limitations exist, including the difficulty of isolating intact YAC DNA, and the high levels of chimerism and clonal instability in the system (Bauchwitz and Costantini, 1998; Gnirke et al., 1993).

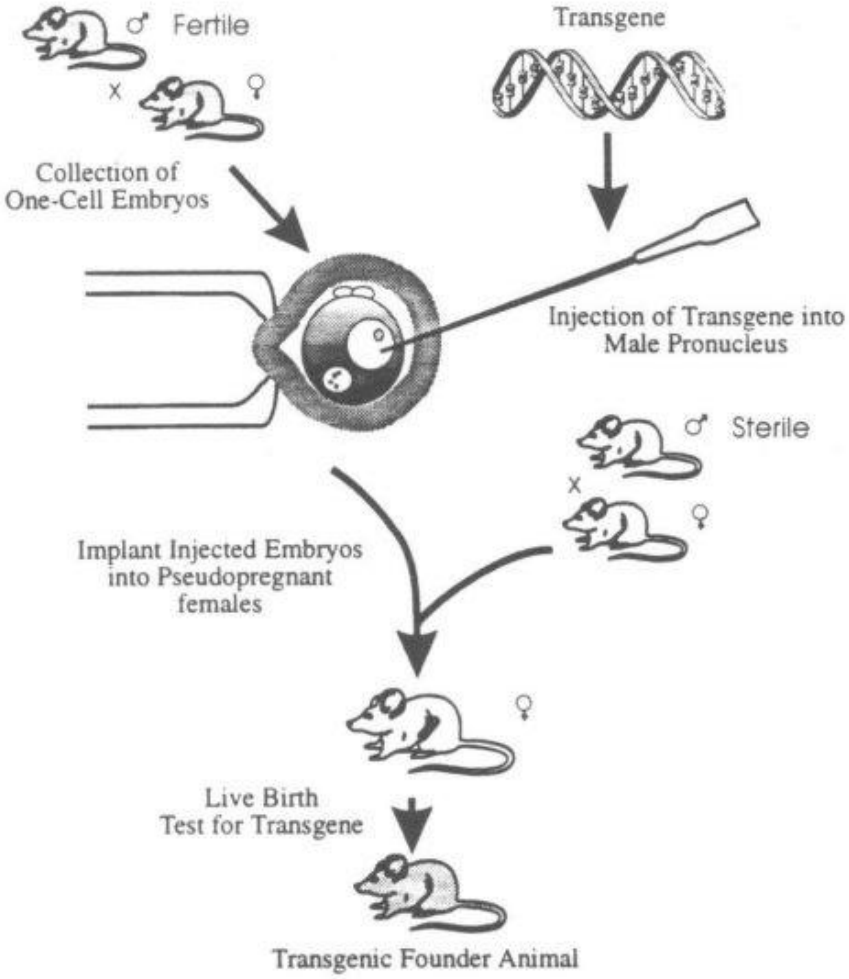

Figure 1.3. Production of transgenic mice by microinjection of exogenous DNA into the pronuclei of fertilized eggs (figure taken from Richardson et al., 1997).

Alternatively, bacterial artificial chromosomes are large-insert DNA clones (based on the *Escherichia coli* fertility plasmid) that can stably accommodate up to 300 kb of genomic DNA for over 100 generations of growth in *E.coli* without the occurrence of rearrangements (Ioannou et al., 1994; Monaco and Larin, 1994; Shizuya et al., 1992). Isolation of BACs is also easier than YACs, because the BAC plasmids are supercoiled in *E.coli* and are thus resistant to shearing.

BACs usually hold ~150 to 200 kb of genomic DNA. Therefore, they are thought to contain all the necessary regulatory elements needed to confer physiological transgene expression, with similar developmental timing and expression patterns as endogenous genes (Giraldo and Montoliu, 2001). Thus, they are usually informative with regard to the physiological effects of candidate genes. In studies examining BAC transgene expression, ~80% of BACs produce detectable transgene expression (Van Keuren et al., 2009). However, for the small number of genes that exceed 200 kb, transgene expression is less consistent.

BACs were initially used for genome sequencing projects; many organisms that have been sequenced, including humans and mice, have dense BAC contigs that cover the majority of their genomes (Hoskins et al., 2000; McPherson et al., 2001; Mozo et al., 1999; Osoegawa et al., 2000). For that reason, an investigator can obtain a selection of BACs that covers a region of interest from public repositories with relative ease. In addition, the development of recombineering methods to modify BAC DNA has increased the usefulness of the technique (Court et al., 2002; Yang et al., 1997); researchers can now achieve inducible transgene expression and target the expression of

BAC transgenes to specific cell types (Belteki et al., 2005; Okita et al., 2007; Sun et al., 2003).

Chapter outlines

We included two previously published review articles as chapters of this dissertation to provide background for our work. Chapter II, *Identifying host factors that regulate viral infection*, reviews state-of-the-art high-throughput techniques that are currently used to identify the role of host factors during viral infection (Hsu and Spindler, 2012). Chapter III, *Viral disruption of the blood-brain barrier*, gives a broad overview of the types of viruses that cause encephalitis, and what we know about the mechanisms by which they do so (Spindler and Hsu, 2012).

In Chapter VI, susceptible SJL, resistant BALB, and an interval-specific congenic strain containing SJL-derived *Msq1* introgressed onto a BALB/c background were infected with MAV-1 and assayed for known MAV-1 disease manifestations in the brain. These include survival, viral loads, blood-brain barrier disruption, edema, mouse brain endothelial cell barrier properties, pathology and inflammatory cell recruitment. We determined the extent to which *Msq1* influences each of these MAV-1 infection phenotypes. We also examined whether the susceptibility difference seen between strains is due to a difference in MAV-1 receptor expression through use of primary mouse brain endothelial cells derived from resistant and susceptible mice. Our results showed that *Msq1* is a critical host genetic factor that controls many, but not all, aspects of MAV-1 infection.

In Chapter V, we describe our attempt to narrow the *Msq1* susceptibility QTL through a BAC transgenesis approach. We introduce BAC transgenes, generated from a susceptible 129S6/SvEv background, into a resistant strain background to produce transgenic founder lines for each BAC. This was done for 8 different BACs. The transgenic progeny were then phenotyped to determine if the susceptibility phenotype can be complemented. If the susceptibility phenotype is conferred to the resistant background, this would provide formal genetic proof that the gene(s) of interest have been transferred.

Finally, in Chapter VI, we summarize the work in this dissertation and discuss implications. We also propose future directions for the research.

References

Abbott, N.J., Patabendige, A.A., Dolman, D.E., Yusof, S.R., and Begley, D.J. (2010). Structure and function of the blood-brain barrier. *Neurobiol Dis* 37, 13-25.

Ashley, S.L., Welton, A.R., Harwood, K.M., Van Rooijen, N., and Spindler, K.R. (2009). Mouse adenovirus type 1 infection of macrophages. *Virology* 390, 307-314.

Baggiolini, M. (1998). Chemokines and leukocyte traffic. *Nature* 392, 565-568.

Bauchwitz, R., and Costantini, F. (1998). YAC transgenesis: a study of conditions to protect YAC DNA from breakage and a protocol for transfection. *Biochim Biophys Acta* 1401, 21-37.

Belteki, G., Haigh, J., Kabacs, N., Haigh, K., Sison, K., Costantini, F., Whitsett, J., Quaggin, S.E., and Nagy, A. (2005). Conditional and inducible transgene expression in mice through the combinatorial use of Cre-mediated recombination and tetracycline induction. *Nucleic Acids Res* 33, e51.

Blair, G.E., Dixon, S.C., Griffiths, S.A., and Zajdel, M.E. (1989). Restricted replication of human adenovirus type 5 in mouse cell lines. *Virus Res* 14, 339-346.

Bottomly, D., Ferris, M.T., Aicher, L.D., Rosenzweig, E., Whitmore, A., Aylor, D.L., Haagmans, B.L., Gralinski, L.E., Bradel-Tretheway, B.G., Bryan, J.T., Threadgill, D.W., de Villena, F.P., Baric, R.S., Katze, M.G., Heise, M., and McWeeney, S.K. (2012). Expression quantitative trait loci for extreme host response to influenza a in pre-collaborative cross mice. *G3 (Bethesda)* 2, 213-221.

Bradley, D.J. (1977). Regulation of Leishmania populations within the host. II. genetic control of acute susceptibility of mice to Leishmania donovani infection. *Clin Exp Immunol* 30, 130-140.

Brinster, R.L., Chen, H.Y., Trumbauer, M., Senear, A.W., Warren, R., and Palmiter, R.D. (1981). Somatic expression of herpes thymidine kinase in mice following injection of a fusion gene into eggs. *Cell* 27, 223-231.

Brown, M.G., Dokun, A.O., Heusel, J.W., Smith, H.R., Beckman, D.L., Blattenberger, E.A., Dubbelde, C.E., Stone, L.R., Scalzo, A.A., and Yokoyama, W.M. (2001). Vital involvement of a natural killer cell activation receptor in resistance to viral infection. *Science* 292, 934-937.

Burke, D.T., Carle, G.F., and Olson, M.V. (1987). Cloning of large segments of exogenous DNA into yeast by means of artificial chromosome vectors. *Science* 236, 806-812.

Candelario-Jalil, E., Yang, Y., and Rosenberg, G.A. (2009). Diverse roles of matrix metalloproteinases and tissue inhibitors of metalloproteinases in neuroinflammation and cerebral ischemia. *Neuroscience* 158, 983-994.

Cecchelli, R., Dehouck, B., Descamps, L., Fenart, L., Buee-Scherrer, V.V., Duhem, C., Lundquist, S., Rentfel, M., Torpier, G., and Dehouck, M.P. (1999). In vitro model for evaluating drug transport across the blood-brain barrier. *Adv Drug Deliv Rev* 36, 165-178.

Charles, P.C., Chen, X., Horwitz, M.S., and Brosnan, C.F. (1999). Differential chemokine induction by the mouse adenovirus type-1 in the central nervous system of susceptible and resistant strains of mice. *J Neurovirol* 5, 55-64.

Charles, P.C., Guida, J.D., Brosnan, C.F., and Horwitz, M.S. (1998). Mouse adenovirus type-1 replication is restricted to vascular endothelium in the CNS of susceptible strains of mice. *Virology* 245, 216-228.

Charles, P.C., Trgovcich, J., Davis, N.L., and Johnston, R.E. (2001). Immunopathogenesis and immune modulation of Venezuelan equine encephalitis virus-induced disease in the mouse. *Virology* 284, 190-202.

Chatterjee, N.K., Samsonoff, W.A., Balasubramaniam, N., Rush-Wilson, K., Spargo, W., and Church, T.M. (2000). Isolation and characterization of adenovirus 5 from the brain of an infant with fatal cerebral edema. *Clin Infect Dis* 31, 830-833.

Costantini, F., and Lacy, E. (1981). Introduction of a rabbit beta-globin gene into the mouse germ line. *Nature* 294, 92-94.

Court, D.L., Sawitzke, J.A., and Thomason, L.C. (2002). Genetic engineering using homologous recombination. *Annu Rev Genet* 36, 361-388.

Davison, A.J., Benko, M., and Harrach, B. (2003). Genetic content and evolution of adenoviruses. *J Gen Virol* 84, 2895-2908.

Deal, K.K., Cantrell, V.A., Chandler, R.L., Saunders, T.L., Mortlock, D.P., and Southard-Smith, E.M. (2006). Distant regulatory elements in a Sox10-beta GEO BAC transgene are required for expression of Sox10 in the enteric nervous system and other neural crest-derived tissues. *Dev Dyn* 235, 1413-1432.

Dorries, R. (2001). The role of T-cell-mediated mechanisms in virus infections of the nervous system. *Curr Top Microbiol Immunol* 253, 219-245.

Dunnick, W.A., Shi, J., Graves, K.A., and Collins, J.T. (2005). The 3' end of the heavy chain constant region locus enhances germline transcription and switch recombination of the four gamma genes. *J Exp Med* 201, 1459-1466.

Eugenin, E.A., Osiecki, K., Lopez, L., Goldstein, H., Calderon, T.M., and Berman, J.W. (2006). CCL2/monocyte chemoattractant protein-1 mediates enhanced transmigration of human immunodeficiency virus (HIV)-infected leukocytes across the blood-brain barrier: a potential mechanism of HIV-CNS invasion and NeuroAIDS. *J Neurosci* 26, 1098-1106.

Fenstermacher, J., Gross, P., Sposito, N., Acuff, V., Pettersen, S., and Gruber, K. (1988). Structural and functional variations in capillary systems within the brain. *Ann N Y Acad Sci* 529, 21-30.

Ferraro, T.N., Golden, G.T., Dahl, J.P., Smith, G.G., Schwebel, C.L., MacDonald, R., Lohoff, F.W., Berrettini, W.H., and Buono, R.J. (2007). Analysis of a quantitative trait locus for seizure susceptibility in mice using bacterial artificial chromosome-mediated gene transfer. *Epilepsia* 48, 1667-1677.

Fields, B.N., Knipe, D.M., and Howley, P.M. (2007). "Fields Virology." 5th ed. Wolters Kluwer Health/Lippincott Williams & Wilkins, Philadelphia.

Flaherty, L., Herron, B., and Symula, D. (2005). Genomics of the future: identification of quantitative trait loci in the mouse. *Genome Res* 15, 1741-1745.

Gabrielson, M.O., Joseph, C., and Hsiung, G.D. (1966). Encephalitis associated with adenovirus type 7 occurring in a family outbreak. *J Pediatr* 68, 142-144.

Ganly, I., Mautner, V., and Balmain, A. (2000). Productive replication of human adenoviruses in mouse epidermal cells. *J Virol* 74, 2895-2899.

Ginsberg, H.S., Moldawer, L.L., Sehgal, P.B., Redington, M., Kilian, P.L., Chanock, R.M., and Prince, G.A. (1991). A mouse model for investigating the molecular pathogenesis of adenovirus pneumonia. *Proc Natl Acad Sci U S A* 88, 1651-1655.

Giraldo, P., and Montoliu, L. (2001). Size matters: use of YACs, BACs and PACs in transgenic animals. *Transgenic Res* 10, 83-103.

Gnirke, A., Huxley, C., Peterson, K., and Olson, M.V. (1993). Microinjection of intact 200- to 500-kb fragments of YAC DNA into mammalian cells. *Genomics* 15, 659-667.

Goncalves, G., Gouveia, E., Mesquita, J.R., Almeida, A., Ribeiro, A., Rocha-Pereira, J., and Sao Jose Nascimento, M. (2011). Outbreak of acute gastroenteritis caused by adenovirus type 41 in a kindergarten. *Epidemiol Infect* 139, 1672-1675.

Gordon, J.W., and Ruddle, F.H. (1981). Integration and stable germ line transmission of genes injected into mouse pronuclei. *Science* 214, 1244-1246.

Gorham, J.D., Guler, M.L., Steen, R.G., Mackey, A.J., Daly, M.J., Frederick, K., Dietrich, W.F., and Murphy, K.M. (1996). Genetic mapping of a murine locus controlling development of T helper 1/T helper 2 type responses. *Proc Natl Acad Sci U S A* 93, 12467-12472.

Gralinski, L.E., Ashley, S.L., Dixon, S.D., and Spindler, K.R. (2009). Mouse adenovirus type 1-induced breakdown of the blood-brain barrier. *J Virol* 83, 9398-9410.

Guida, J.D., Fejer, G., Pirofski, L.A., Brosnan, C.F., and Horwitz, M.S. (1995). Mouse adenovirus type 1 causes a fatal hemorrhagic encephalomyelitis in adult C57BL/6 but not BALB/c mice. *J Virol* 69, 7674-7681.

Harbers, K., Jahner, D., and Jaenisch, R. (1981). Microinjection of cloned retroviral genomes into mouse zygotes: integration and expression in the animal. *Nature* 293, 540-542.

Harrach, B., and Benkö, M. (2007). Phylogenetic analysis of adenovirus sequences. *Methods Mol Med* 131, 299-334.

Hartley, J.W., and Rowe, W.P. (1960). A new mouse virus apparently related to the adenovirus group. *Virology* 11, 645-647.

Hartung, H.P., and Kieseier, B.C. (2000). The role of matrix metalloproteinases in autoimmune damage to the central and peripheral nervous system. *J Neuroimmunol* 107, 140-147.

Hashimoto, K., Sugiyama, T., and Sasaki, S. (1966). An adenovirus isolated from the feces of mice I. Isolation and identification. *Jpn J Microbiol* 10, 115-125.

Hawkins, B.T., and Davis, T.P. (2005). The blood-brain barrier/neurovascular unit in health and disease. *Pharmacol Rev* 57, 173-185.

Hemmi, S., Vidovszky, M.Z., Ruminska, J., Ramelli, S., Decurtins, W., Greber, U.F., and Harrach, B. (2011). Genomic and phylogenetic analyses of murine adenovirus 2. *Virus Res* 160, 128-135.

Hillebrandt, S., Wasmuth, H.E., Weiskirchen, R., Hellerbrand, C., Keppeler, H., Werth, A., Schirin-Sokhan, R., Wilkens, G., Geier, A., Lorenzen, J., Kohl, J., Gressner, A.M., Matern, S., and Lammert, F. (2005). Complement factor 5 is a quantitative trait gene that modifies liver fibrogenesis in mice and humans. *Nat Genet* 37, 835-843.

Hilleman, M.R., and Werner, J.H. (1954). Recovery of new agent from patients with acute respiratory illness. *Proc Soc Exp Biol Med* 85, 183-188.

Hjorth, R.N., Bonde, G.M., Pierzchala, W.A., Vernon, S.K., Wiener, F.P., Levner, M.H., Lubeck, M.D., and Hung, P.P. (1988). A new hamster model for adenoviral vaccination. *Arch Virol* 100, 279-283.

Hoskins, R.A., et al. (2000). A BAC-based physical map of the major autosomes of Drosophila melanogaster. *Science* 287, 2271-2274.

Hsu, T.-H., and Spindler, K.R. (2012). Identifying host factors that regulate viral infection. *PLoS Pathog* 8, e1002772.

Ilzecka, J. (1996). The structure and function of blood-brain barrier in ischaemic brain stroke process. *Ann Univ Mariae Curie Sklodowska Med* 51, 123-127.

Ioannou, P.A., Amemiya, C.T., Garnes, J., Kroisel, P.M., Shizuya, H., Chen, C., Batzer, M.A., and de Jong, P.J. (1994). A new bacteriophage P1-derived vector for the propagation of large human DNA fragments. *Nat Genet* 6, 84-89.

Irani, D.N., and Griffin, D.E. (1996). Regulation of lymphocyte homing into the brain during viral encephalitis at various stages of infection. *The Journal of Immunology* 156, 3850-3857.

Jin, R., Yang, G., and Li, G. (2010). Molecular insights and therapeutic targets for blood-brain barrier disruption in ischemic stroke: critical role of matrix metalloproteinases and tissue-type plasminogen activator. *Neurobiol Dis* 38, 376-385.

Jogler, C., Hoffmann, D., Theegarten, D., Grunwald, T., Uberla, K., and Wildner, O. (2006). Replication properties of human adenovirus in vivo and in cultures of primary cells from different animal species. *J Virol* 80, 3549-3558.

Jones, J.M., Datta, P., Srinivasula, S.M., Ji, W., Gupta, S., Zhang, Z., Davies, E., Hajnoczky, G., Saunders, T.L., Van Keuren, M.L., Fernandes-Alnemri, T., Meisler, M.H., and Alnemri, E.S. (2003). Loss of Omi mitochondrial protease activity causes the neuromuscular disorder of mnd2 mutant mice. *Nature* 425, 721-727.

Joo, F., and Karnushina, I. (1973). A procedure for the isolation of capillaries from rat brain. *Cytobios* 8, 41-48.

Kajon, A.E., Brown, C.C., and Spindler, K.R. (1998). Distribution of mouse adenovirus type 1 in intraperitoneally and intranasally infected adult outbred mice. *J Virol* 72, 1219-1223.

Keogh, B., Sheahan, B.J., Atkins, G.J., and Mills, K.H. (2003). Inhibition of matrix metalloproteinases ameliorates blood-brain barrier disruption and neuropathological lesions caused by avirulent Semliki Forest virus infection. *Vet Immunol Immunopathol* 94, 185-190.

Klempa, B., Kruger, D.H., Auste, B., Stanko, M., Krawczyk, A., Nickel, K.F., Uberla, K., and Stang, A. (2009). A novel cardiotropic murine adenovirus representing a distinct species of mastadenoviruses. *J Virol* 83, 5749-5759.

Klessig, D.F., and Grodzicker, T. (1979). Mutations that allow human Ad2 and Ad5 to express late genes in monkey cells map in the viral gene encoding the 72K DNA binding protein. *Cell* 17, 957-966.

Kniesel, U., and Wolburg, H. (2000). Tight junctions of the blood-brain barrier. *Cell Mol Neurobiol* 20, 57-76.

Krilov, L.R. (2005). Adenovirus infections in the immunocompromised host. *Pediatr Infect Dis J* 24, 555-556.

Kring, S.C., King, C.S., and Spindler, K.R. (1995). Susceptibility and signs associated with mouse adenovirus type 1 infection of adult outbred Swiss mice. *J Virol* 69, 8084-8088.

Lee, S.H., Girard, S., Macina, D., Busa, M., Zafer, A., Belouchi, A., Gros, P., and Vidal, S.M. (2001). Susceptibility to mouse cytomegalovirus is associated with deletion of an activating natural killer cell receptor of the C-type lectin superfamily. *Nat Genet* 28, 42-45.

Lee, Y.R., Liu, M.T., Lei, H.Y., Liu, C.C., Wu, J.M., Tung, Y.C., Lin, Y.S., Yeh, T.M., Chen, S.H., and Liu, H.S. (2006). MCP-1, a highly expressed chemokine in dengue haemorrhagic fever/dengue shock syndrome patients, may cause permeability change, possibly through reduced tight junctions of vascular endothelium cells. *J Gen Virol* 87, 3623-3630.

Liu, H., Jin, L., Koh, S.B., Atanasov, I., Schein, S., Wu, L., and Zhou, Z.H. (2010). Atomic structure of human adenovirus by cryo-EM reveals interactions among protein networks. *Science* 329, 1038-1043.

Lucas, M., Mashimo, T., Frenkiel, M.P., Simon-Chazottes, D., Montagutelli, X., Ceccaldi, P.E., Guenet, J.L., and Despres, P. (2003). Infection of mouse neurones by West Nile virus is modulated by the interferon-inducible 2'-5' oligoadenylate synthetase 1b protein. *Immunol Cell Biol* 81, 230-236.

Lussier, G., Smith, A.L., Guenette, D., and Descoteaux, J.P. (1987). Serological relationship between mouse adenovirus strains FL and K87. *Lab Anim Sci* 37, 55-57.

Malina, K.C.-K., Cooper, I., and Teichberg, V.I. (2009). Closing the gap between the in-vivo and in-vitro blood–brain barrier tightness. *Brain Research* 1284, 12-21.

Malo, D., Vogan, K., Vidal, S., Hu, J., Cellier, M., Schurr, E., Fuks, A., Bumstead, N., Morgan, K., and Gros, P. (1994). Haplotype mapping and sequence analysis of the mouse Nramp gene predict susceptibility to infection with intracellular parasites. *Genomics* 23, 51-61.

Mashimo, T., Lucas, M., Simon-Chazottes, D., Frenkiel, M.P., Montagutelli, X., Ceccaldi, P.E., Deubel, V., Guenet, J.L., and Despres, P. (2002). A nonsense mutation in the gene encoding 2'-5'-oligoadenylate synthetase/L1 isoform is associated with West Nile virus susceptibility in laboratory mice. *Proc Natl Acad Sci U S A* 99, 11311-11316.

McPherson, J.D., et al. (2001). A physical map of the human genome. *Nature* 409, 934-941.

Minagar, A., and Alexander, J.S. (2003). Blood-brain barrier disruption in multiple sclerosis. *Mult Scler* 9, 540-549.

Monaco, A.P., and Larin, Z. (1994). YACs, BACs, PACs and MACs: artificial chromosomes as research tools. *Trends Biotechnol* 12, 280-286.

Moore, M.L., Brown, C.C., and Spindler, K.R. (2003). T cells cause acute immunopathology and are required for long-term survival in mouse adenovirus type 1-induced encephalomyelitis. *J Virol* 77, 10060-10070.

Moore, M.L., McKissic, E.L., Brown, C.C., Wilkinson, J.E., and Spindler, K.R. (2004). Fatal disseminated mouse adenovirus type 1 infection in mice lacking B cells or Bruton's tyrosine kinase. *J Virol* 78, 5584-5590.

Mosmann, T.R., Cherwinski, H., Bond, M.W., Giedlin, M.A., and Coffman, R.L. (2005). Two types of murine helper T cell clone. I. Definition according to profiles of lymphokine activities and secreted proteins. 1986. *J Immunol* 175, 5-14.

Mozo, T., Dewar, K., Dunn, P., Ecker, J.R., Fischer, S., Kloska, S., Lehrach, H., Marra, M., Martienssen, R., Meier-Ewert, S., and Altmann, T. (1999). A complete BAC-based physical map of the Arabidopsis thaliana genome. *Nat Genet* 22, 271-275.

Nagy, A. (2003). "Manipulating the mouse embryo : a laboratory manual." 3rd ed. Cold Spring Harbor Laboratory Press, Cold Spring Harbor, N.Y.

Okamoto, K., Fukuda, M., Shigemi, R., and Takaoka, T. (2004). [Two cases of acute encephalitis/encephalopathy associated with adenovirus type 3 infection]. *No To Hattatsu* 36, 487-491.

Okita, K., Ichisaka, T., and Yamanaka, S. (2007). Generation of germline-competent induced pluripotent stem cells. *Nature* 448, 313-317.

Oldendorf, W.H., Cornford, M.E., and Brown, W.J. (1977). The large apparent work capability of the blood-brain barrier: a study of the mitochondrial content of capillary endothelial cells in brain and other tissues of the rat. *Ann Neurol* 1, 409-417.

Oliver, E.R., Saunders, T.L., Tarle, S.A., and Glaser, T. (2004). Ribosomal protein L24 defect in belly spot and tail (Bst), a mouse Minute. *Development* 131, 3907-3920.

Osamura, T., Mizuta, R., Yoshioka, H., and Fushiki, S. (1993). Isolation of adenovirus type 11 from the brain of a neonate with pneumonia and encephalitis. *Eur J Pediatr* 152, 496-499.

Osoegawa, K., Tateno, M., Woon, P.Y., Frengen, E., Mammoser, A.G., Catanese, J.J., Hayashizaki, Y., and de Jong, P.J. (2000). Bacterial artificial chromosome libraries for mouse sequencing and functional analysis. *Genome Res* 10, 116-128.

Pacini, D.L., Dubovi, E.J., and Clyde, W.A. (1984). A new animal model for human respiratory tract disease due to adenovirus. *Journal of Infectious Diseases* 150, 92-97.

Perelygin, A.A., Scherbik, S.V., Zhulin, I.B., Stockman, B.M., Li, Y., and Brinton, M.A. (2002). Positional cloning of the murine flavivirus resistance gene. *Proc Natl Acad Sci U S A* 99, 9322-9327.

Pirofski, L., Horwitz, M.S., Scharff, M.D., and Factor, S.M. (1991). Murine adenovirus infection of SCID mice induces hepatic lesions that resemble human Reye syndrome. *Proc Natl Acad Sci U S A* 88, 4358-4362.

Plant, J., and Glynn, A.A. (1976). Genetics of resistance to infection with Salmonella typhimurium in mice. *J Infect Dis* 133, 72-78.

Prince, G.A., Porter, D.D., Jenson, A.B., Horswood, R.L., Chanock, R.M., and Ginsberg, H.S. (1993). Pathogenesis of adenovirus type 5 pneumonia in cotton rats (Sigmodon hispidus). *J Virol* 67, 101-111.

Rabson, A.S., O'Conor, G.T., Berezesky, I.K., and Paul, F.J. (1964). Enhancement of adenovirus growth in African green monkey kidney cell cultures by Sv40. *Proc Soc Exp Biol Med* 116, 187-190.

Reddy, V.S., Natchiar, S.K., Stewart, P.L., and Nemerow, G.R. (2010). Crystal structure of human adenovirus at 3.5 A resolution. *Science* 329, 1071-1075.

Reijerkerk, A., Kooij, G., van der Pol, S.M., Khazen, S., Dijkstra, C.D., and de Vries, H.E. (2006). Diapedesis of monocytes is associated with MMP-mediated occludin disappearance in brain endothelial cells. *FASEB J* 20, 2550-2552.

Remus, N., Alcais, A., and Abel, L. (2003). Human genetics of common mycobacterial infections. *Immunol Res* 28, 109-129.

Richardson, A., Heydari, A.R., Morgan, W.W., Nelson, J.F., Sharp, Z.D., and Walter, C.A. (1997). Use of transgenic mice in aging research. *ILAR J* 38, 125-136.

Risau, W., and Wolburg, H. (1990). Development of the blood-brain barrier. *Trends Neurosci* 13, 174-178.

Roos, R., Chou, S.M., Rogers, N.G., Basnight, M., and Gajdusek, D.C. (1972). Isolation of an adenovirus 32 strain from human brain in a case of subacute encephalitis. *Proc Soc Exp Biol Med* 139, 636-640.

Roux, F., and Couraud, P.O. (2005). Rat brain endothelial cell lines for the study of blood-brain barrier permeability and transport functions. *Cell Mol Neurobiol* 25, 41-58.

Rowe, W.P., Huebner, R.J., Gilmore, L.K., Parrott, R.H., and Ward, T.G. (1953). Isolation of a cytopathogenic agent from human adenoids undergoing spontaneous degeneration in tissue culture. *Proc Soc Exp Biol Med* 84, 570-573.

Sadowski, W., Semkow, R., Wilczynski, J., Krus, S., and Kantoch, M. (1987). [The cotton rat (Sigmodon hispidus) as an experimental model for studying viruses in human respiratory tract infections. I. Para-influenza virus type 1, 2 and 3, adenovirus type 5 and RS virus]. *Med Dosw Mikrobiol* 39, 33-42.

Sakata, H., Taketazu, G., Nagaya, K., Shirai, M., Sugai, R., Ikegami, K., and Maruyama, S. (1998). Outbreak of severe infection due to adenovirus type 7 in a paediatric ward in Japan. *Journal of Hospital Infection* 39, 207-211.

Sambursky, R.P., Fram, N., and Cohen, E.J. (2007). The prevalence of adenoviral conjunctivitis at the Wills Eye Hospital Emergency Room. *Optometry* 78, 236-239.

Schnurr, D., Bollen, A., Crawford-Miksza, L., Dondero, M.E., and Yagi, S. (1995). Adenovirus mixture isolated from the brain of an AIDS patient with encephalitis. *J Med Virol* 47, 168-171.

Sedlakova, R., Shivers, R.R., and Del Maestro, R.F. (1999). Ultrastructure of the blood-brain barrier in the rabbit. *J Submicrosc Cytol Pathol* 31, 149-161.

Shizuya, H., Birren, B., Kim, U.J., Mancino, V., Slepak, T., Tachiiri, Y., and Simon, M. (1992). Cloning and stable maintenance of 300-kilobase-pair fragments of human DNA in Escherichia coli using an F-factor-based vector. *Proc Natl Acad Sci U S A* 89, 8794-8797.

Simila, S., Jouppila, R., Salmi, A., and Pohjonen, R. (1970). Encephalomeningitis in children associated with an adenovirus type 7 epidemic. *Acta Paediatr Scand* 59, 310-316.

Singh, G., Robinson, C.M., Dehghan, S., Schmidt, T., Seto, D., Jones, M.S., Dyer, D.W., and Chodosh, J. (2012). Overreliance on the hexon gene, leading to misclassification of human adenoviruses. *J Virol* 86, 4693-4695.

Skamene, E., Gros, P., Forget, A., Kongshavn, P.A., St Charles, C., and Taylor, B.A. (1982). Genetic regulation of resistance to intracellular pathogens. *Nature* 297, 506-509.

Skamene, E., Gros, P., Forget, A., Patel, P.J., and Nesbitt, M.N. (1984). Regulation of resistance to leprosy by chromosome 1 locus in the mouse. *Immunogenetics* 19, 117-124.

Sonabend, A.M., Ulasov, I.V., Han, Y., Rolle, C.E., Nandi, S., Cao, D., Tyler, M.A., and Lesniak, M.S. (2009). Biodistribution of an oncolytic adenovirus after intracranial

injection in permissive animals: a comparative study of Syrian hamsters and cotton rats. *Cancer Gene Ther* 16, 362-372.

Song, L., and Pachter, J.S. (2004). Monocyte chemoattractant protein-1 alters expression of tight junction-associated proteins in brain microvascular endothelial cells. *Microvasc Res* 67, 78-89.

Spindler, K.R., Fang, L., Moore, M.L., Hirsch, G.N., Brown, C.C., and Kajon, A. (2001). SJL/J mice are highly susceptible to infection by mouse adenovirus type 1. *J Virol* 75, 12039-12046.

Spindler, K.R., and Hsu, T.H. (2012). Viral disruption of the blood-brain barrier. *Trends Microbiol* doi:10.1016/j.tim.2012.03.009.

Spindler, K.R., Moore, M.L., and Cauthen, A.N. (2007). Mouse adenoviruses. 2nd ed. *In* "The mouse in biomedical research. American College of Laboratory Animal Medicine series", Vol. 2, pp. 49-65. 4 vols. Elsevier, Amsterdam ; Boston.

Spindler, K.R., Welton, A.R., Lim, E.S., Duvvuru, S., Althaus, I.W., Imperiale, J.E., Daoud, A.I., and Chesler, E.J. (2010). The major locus for mouse adenovirus susceptibility maps to genes of the hematopoietic cell surface-expressed LY6 family. *J Immunol* 184, 3055-3062.

Stamatovic, S.M., Shakui, P., Keep, R.F., Moore, B.B., Kunkel, S.L., Van Rooijen, N., and Andjelkovic, A.V. (2005). Monocyte chemoattractant protein-1 regulation of blood-brain barrier permeability. *J Cereb Blood Flow Metab* 25, 593-606.

Sun, H., Yang, T.L., Yang, A., Wang, X., and Ginsburg, D. (2003). The murine platelet and plasma factor V pools are biosynthetically distinct and sufficient for minimal hemostasis. *Blood* 102, 2856-2861.

Takeuchi, A., and Hashimoto, K. (1976). Electron microscope study of experimental enteric adenovirus infection in mice. *Infect Immun* 13, 569-580.

Ternovoi, V.V., Le, L.P., Belousova, N., Smith, B.F., Siegal, G.P., and Curiel, D.T. (2005). Productive replication of human adenovirus type 5 in canine cells. *J Virol* 79, 1308-1311.

Thomas, M.A., Spencer, J.F., La Regina, M.C., Dhar, D., Tollefson, A.E., Toth, K., and Wold, W.S. (2006). Syrian hamster as a permissive immunocompetent animal model for the study of oncolytic adenovirus vectors. *Cancer Research* 66, 1270-1276.

Tomida, S., Mamiya, T., Sakamaki, H., Miura, M., Aosaki, T., Masuda, M., Niwa, M., Kameyama, T., Kobayashi, J., Iwaki, Y., Imai, S., Ishikawa, A., Abe, K., Yoshimura, T., Nabeshima, T., and Ebihara, S. (2009). Usp46 is a quantitative trait gene regulating mouse immobile behavior in the tail suspension and forced swimming tests. *Nat Genet* 41, 688-695.

Toth, K., Spencer, J.F., Tollefson, A.E., Kuppuswamy, M., Doronin, K., Lichtenstein, D.L., La Regina, M.C., Prince, G.A., and Wold, W.S. (2005). Cotton rat tumor model for the evaluation of oncolytic adenoviruses. *Hum Gene Ther* 16, 139-146.

Van Keuren, M.L., Gavrilina, G.B., Filipiak, W.E., Zeidler, M.G., and Saunders, T.L. (2009). Generating transgenic mice from bacterial artificial chromosomes: transgenesis efficiency, integration and expression outcomes. *Transgenic Res* 18, 769-785.

Vidal, S.M., Malo, D., Vogan, K., Skamene, E., and Gros, P. (1993). Natural-resistance to infection with intracellular parasites - isolation of a candidate for Bcg. *Cell* 73, 469-485.

Wagner, T.E., Hoppe, P.C., Jollick, J.D., Scholl, D.R., Hodinka, R.L., and Gault, J.B. (1981). Microinjection of a rabbit beta-globin gene into zygotes and its subsequent expression in adult mice and their offspring. *Proc Natl Acad Sci U S A* 78, 6376-6380.

Walsh, M.P., Seto, J., Jones, M.S., Chodosh, J., Xu, W., and Seto, D. (2010). Computational analysis identifies human adenovirus type 55 as a re-emergent acute respiratory disease pathogen. *J Clin Microbiol* 48, 991-993.

Wang, P., Dai, J., Bai, F., Kong, K.F., Wong, S.J., Montgomery, R.R., Madri, J.A., and Fikrig, E. (2008). Matrix metalloproteinase 9 facilitates West Nile virus entry into the brain. *J Virol* 82, 8978-8985.

Wekerle, H., Linington, C., Lassmann, H., and Meyermann, R. (1986). Cellular immune reactivity within the CNS. *Trends in Neurosciences* 9, 271-277.

Welton, A.R., Chesler, E.J., Sturkie, C., Jackson, A.U., Hirsch, G.N., and Spindler, K.R. (2005). Identification of quantitative trait loci for susceptibility to mouse adenovirus type 1. *J Virol* 79, 11517-11522.

Welton, A.R., Gralinski, L.E., and Spindler, K.R. (2008). Mouse adenovirus type 1 infection of natural killer cell-deficient mice. *Virology* 373, 163-170.

West, T.E., Papasian, C.J., Park, B.H., and Parker, S.W. (1985). Adenovirus type 2 encephalitis and concurrent Epstein-Barr virus infection in an adult man. *Arch Neurol* 42, 815-817.

Wigand, R., Gelderblom, H., and Ozel, M. (1977). Biological and biophysical characteristics of mouse adenovirus, strain FL. *Arch Virol* 54, 131-142.

Wold, W.S.M., and Horwitz, M.S. (2007). Adenoviruses. 5 ed. *In* "Fields Virology", pp. 2395-2436. Lippincott-Raven, Philadelphia.

Yabe, Y., Matsumoto, K., and Ogura, H. (1988). Lifelong persistent infection of hamster brain by human adenovirus type 6. *Acta Med Okayama* 42, 45-47.

Yang, X.W., Model, P., and Heintz, N. (1997). Homologous recombination based modification in Escherichia coli and germline transmission in transgenic mice of a bacterial artificial chromosome. *Nat Biotechnol* 15, 859-865.

Younghusband, H.B., Tyndall, C., and Bellett, A.J. (1979). Replication and interaction of virus DNA and cellular DNA in mouse cells infected by a human adenovirus. *J Gen Virol* 45, 455-467.

Zhou, X., Robinson, C.M., Rajaiya, J., Dehghan, S., Seto, D., Jones, M.S., Dyer, D.W., and Chodosh, J. (2012). Analysis of human adenovirus type 19 associated with epidemic keratoconjunctivitis and its reclassification as adenovirus type 64. *Invest Ophthalmol Vis Sci* 53, 2804-2811.

Chapter II

Identifying host factors that regulate viral infection

The host side of viral infection

One goal of virology research is to identify viral and host factors involved in infection, in order to develop antiviral therapies. Drugs targeting viral proteins have certain key disadvantages. They often affect only a specific viral species or subtype (Anderson et al., 2009). Also, the low-fidelity polymerases of many medically important viruses, including HIV and influenza, make them prone to rapid mutations leading to development of drug resistance. Consequently, combination therapy is a standard pharmacological regimen for some viral diseases. However, combination therapy increases the cost of treatment and the number of side effects, which can lead to poor patient compliance. In addition, viruses encode few proteins, limiting the number of available targets.

Targeting host proteins is a practical alternative. Viruses use host proteins at multiple stages of their life cycles. Identifying host functions subverted by viruses will further our understanding of viral life cycles and may provide a catalog of novel drug targets that are unlikely to mutate following therapy. Furthermore, targeting the host may result in therapies with a broader range than traditional antivirals. Exciting progress has been made in recent years in this field; the development of new genomic and proteomic tools enables identification of interacting host factors at an unprecedented scale and level

of detail. Together with the use of bioinformatics, these approaches hold promise for accelerating our understanding of virus-host interactions.

Genomics techniques to identify host factors

Host genetic background can significantly influence the outcome of viral infection. Genetic studies identify host factors required for successful viral infection through phenotypic effects such as susceptibility. The ability to manipulate experimental animals has expanded our knowledge of host factors involved in infection. For example, inbred mice that exhibit inherent phenotypic differences in their susceptibility profiles can be bred to generate progeny whose genotypes and phenotypes can be determined. Linkage analysis tools can then be used to identify a candidate region, and potential disease susceptibility genes can be prioritized for positional cloning.

Through genetic mapping, mouse cytomegalovirus (MCMV) susceptibility was determined to be associated with the loss of an activating natural killer cell receptor (Brown et al., 2001; Lee et al., 2001). A genetic approach was also used to identify the *Flv* gene, subsequently identified as *Oas1b*, a member of the OAS/RNASEL innate immune system, which is responsible for controlling resistance to West Nile virus infection in mice (Mashimo et al., 2002; Perelygin et al., 2002). A quantitative trait locus (QTL) strongly linked to susceptibility to mouse adenovirus type 1 was identified and reduced rapidly from a 18 Mb region to only 0.75 Mb through positional cloning involving backcross mice, polymorphic markers and single nucleotide polymorphism haplotype identity (Welton et al., 2005). To develop a genetically diverse panel of inbred mouse strains, a community effort was made to create the Collaborative Cross (CC),

(Collaborative Cross Consortium, 2012). In a recent study, 44 pre-CC mouse strains were used to identify 21 QTLs associated with regulation of host response to influenza infection (Bottomly et al., 2012). Pre-CC mice are in the process of becoming inbred CC strains; this study clearly demonstrates that CC mice have greater phenotypic diversity than standard inbred mouse strains. Pre-CC mice were also used to create Diversity Outbred (DO) mice (Svenson et al., 2012). DO mice are maintained through outcrossing to maintain allelic diversity; CC mice are inbred to generate stable clones. Complementary use of CC and DO mice will allow researchers to identify genes important in complex traits such as susceptibility to viral infection. These strategies identify pre-existing variants in host susceptibility genes.

In contrast, novel germline mutations can be created using mutagens, such as *N*-ethyl-*N*-nitrosourea (Crozat et al., 2006). MCMV resistant mice were mutagenized and selected for susceptibility to MCMV. Genes associated with resistance were then identified through positional cloning and sequencing. This same approach was recently used to identify a mouse gene, *Eif2ak4* (encoding GCN2), involved in susceptibility to MCMV and human adenovirus (Won et al., 2012).

Efforts to determine human homologs of susceptibility genes identified in mouse models are underway to translate these findings to human disease. In humans, genome-wide linkage analysis studies have been limited to chronic infectious diseases, due to the difficulty in recruiting families with multi-case acute viral infections. A whole genome scan conducted with Gambian families identified a major susceptibility locus to chronic hepatitis B infection that contains a cluster of cytokine receptor genes (Frodsham et al., 2006).

Genome-wide association studies (GWAS) have been used to identify human susceptibility loci. Whole genomes of a large human population can be scanned to identify genetic variations frequently associated with susceptibility to infection by a particular pathogen or with severity of disease. The HLA-viral peptide interaction was identified through GWAS as a major genetic factor responsible for HIV control (Pereyra et al., 2010). GWAS have limited ability to detect variants with small effect or low frequencies. However, next generation sequencing is likely to enable identification of rare mutations associated with host susceptibility (Moorhouse and Sharma, 2011).

Direct protein-based techniques to identify host factors

Many methods can be used to identify physical interactions between viral and host proteins. One of the earliest of these was co-immunoprecipitation of viral and cellular protein complexes with specific antisera to viral and host proteins. The tumor suppressor protein p53 was first identified by co-immunoprecipitation in complexes with adenovirus E1B 55kDa protein and in complexes with SV40 large T antigen (Sarnow et al., 1982). The tumor suppressor protein Rb co-immunoprecipitates with adenovirus E1A protein (Harlow et al., 1986). These findings provided critical evidence that oncogenic viruses promote tumorigenesis by inactivating tumor suppressor proteins.

Additional techniques used to detect interactions of viral and host proteins include yeast-two-hybrid (Y2H), tandem affinity purification, virus overlay protein binding assay (VOPBA), glutathione S-transferase protein purification, and co-immunoprecipitation followed by mass spectrometry analysis. Y2H is amenable to high-throughput screening and has identified host-viral protein interactions for a variety of viruses, including HIV

(Lake et al., 2003) , hepatitis C virus (Flajolet et al., 2000), herpesviruses (Uetz et al., 2006) and T7 bacteriophage (Bartel et al., 1996). When the Y2H approach is adapted to high-throughput format, a single "bait" can be tested against multiple "preys" for physical interaction. VOPBA screens for interacting proteins by electrophoresing cellular contents, blotting to a membrane, and "probing" with virus. VOPBA has been used to identify virus receptors for human adenovirus (Wu et al., 2001), respiratory syncytial virus (Tayyari et al., 2011), lymphocytic choriomeningitis virus and Lassa fever virus (Cao et al., 1998). Results from Y2H and VOPBA can be validated by co-immunoprecipitations of co-transfected proteins, but the techniques are limited to direct protein-protein interactions.

Gene silencing techniques can assist in defining effects of cellular factors on viral infection that are both direct and indirect. Genome-scale RNA interference (RNAi) screening is a high-throughput method used to investigate diverse biological processes, including host factors involved in viral pathogenesis. One study identified >250 host factors involved in HIV infection (Bushman et al., 2009). However, because it is technically challenging to develop complete RNAi libraries of the human genome, important candidates may be missed (Shan, 2010). RNAi screens are highly sensitive to experimental variation, and the overlap of positive hits between similar studies can vary (Goff, 2008). Also, because RNAi screens are resource intensive, often few time points are examined, limiting knowledge of dynamic changes during viral infection.

Molecular imaging techniques are increasingly being used to visualize transient or dynamic interactions. Live cell imaging microscopy techniques have advanced significantly, allowing detection of single molecules in the absence of artifacts caused by

fixation methods. Events of influenza entry were dissected using real-time microscopy, providing new insights into cellular endocytic pathways (Lakadamyali et al., 2003). Two different host proteins that interact with the Sindbis virus at different stages of infection were identified using a GFP-tagged viral protein, further demonstrating the usefulness of imaging approaches (Cristea et al., 2006).

Data repositories

Data generated from high-throughput techniques have furthered our understanding of the virus-host interface, and efforts are being made to identify and analyze candidate drug targets. To maximize the benefits of these screens, data need to be accessibly stored and modeled into networks. Several online repositories, including VirHostNet (Navratil et al., 2009), VirusMINT (Chatr-aryamontri et al., 2009) and BiologicalNetworks (Baitaluk et al., 2006), enable modeling of current data to gain broad understanding of protein and gene networks involved in viral infection. Multi-scale data integration approaches allow for simultaneous analysis of different datasets, such as phylogeny, literature searches, virulence and epidemiological data. However, there has been no standardization of where data should be deposited, and participation is voluntary.

Concluding remarks

Various techniques have facilitated identification of host factors involved in viral infection. Verification of these candidates through biochemical, genetic and immunological methods may progressively become the rate-limiting step. Virologists will increasingly need to collaborate with other scientists to realize the full potential of the

collected data. Use of simulations and models will enable better depiction of infection events. Structural biology can also be used to visualize protein interfaces at high resolution. The identification of host proteins through the many approaches described in this review is only a starting point for exploring function and mechanism, with the aim of uncovering cellular pathways affecting viral replication that can be targeted for drug development.

Notes

This work was reprinted with permission from:

Hsu, T.-H., and K.R. Spindler. Identifying host factors that regulate viral infection. 2012. PLoS Pathogens. doi:10.1371/journal.ppat.1002772

We apologize to those in the field whose work we were unable to cite due to space limitations. We thank David Burke, Michael Imperiale and Jason Weinberg for comments on the manuscript. This work was supported by NIH R01 AI068645 and NIH R01 AI091721 to K.R.S., and a NIH National Research Service Award T32 GM07544 to T.-H.H.

References

Anderson, J., Kräusslich, H.-G., and Bartenschlager, R. (2009). "Antiviral strategies." Handbook of experimental pharmacology Springer, Berlin.

Baitaluk, M., Sedova, M., Ray, A., and Gupta, A. (2006). BiologicalNetworks: visualization and analysis tool for systems biology. *Nucleic Acids Res* 34, W466-471.

Bartel, P.L., Roecklein, J.A., SenGupta, D., and Fields, S. (1996). A protein linkage map of Escherichia coli bacteriophage T7. *Nat Genet* 12, 72-77.

Bottomly, D., Ferris, M.T., Aicher, L.D., Rosenzweig, E., Whitmore, A., Aylor, D.L., Haagmans, B.L., Gralinski, L.E., Bradel-Tretheway, B.G., Bryan, J.T., Threadgill, D.W., de Villena, F.P., Baric, R.S., Katze, M.G., Heise, M., and McWeeney, S.K. (2012). Expression quantitative trait Loci for extreme host response to influenza a in pre-collaborative cross mice. *G3 (Bethesda)* 2, 213-221.

Brown, M.G., Dokun, A.O., Heusel, J.W., Smith, H.R., Beckman, D.L., Blattenberger, E.A., Dubbelde, C.E., Stone, L.R., Scalzo, A.A., and Yokoyama, W.M. (2001). Vital involvement of a natural killer cell activation receptor in resistance to viral infection. *Science* 292, 934-937.

Bushman, F.D., Malani, N., Fernandes, J., D'Orso, I., Cagney, G., Diamond, T.L., Zhou, H., Hazuda, D.J., Espeseth, A.S., Konig, R., Bandyopadhyay, S., Ideker, T., Goff, S.P., Krogan, N.J., Frankel, A.D., Young, J.A., and Chanda, S.K. (2009). Host cell factors in HIV replication: meta-analysis of genome-wide studies. *PLoS Pathog* 5, e1000437.

Cao, W., Henry, M.D., Borrow, P., Yamada, H., Elder, J.H., Ravkov, E.V., Nichol, S.T., Compans, R.W., Campbell, K.P., and Oldstone, M.B. (1998). Identification of alpha-dystroglycan as a receptor for lymphocytic choriomeningitis virus and Lassa fever virus. *Science* 282, 2079-2081.

Chatr-aryamontri, A., Ceol, A., Peluso, D., Nardozza, A., Panni, S., Sacco, F., Tinti, M., Smolyar, A., Castagnoli, L., Vidal, M., Cusick, M.E., and Cesareni, G. (2009). VirusMINT: a viral protein interaction database. *Nucleic Acids Res* 37, D669-673.

Collaborative Cross Consortium (2012). The genome architecture of the collaborative cross mouse genetic reference population. *Genetics* 190, 389-401.

Cristea, I.M., Carroll, J.W., Rout, M.P., Rice, C.M., Chait, B.T., and MacDonald, M.R. (2006). Tracking and elucidating alphavirus-host protein interactions. *J Biol Chem* 281, 30269-30278.

Crozat, K., Georgel, P., Rutschmann, S., Mann, N., Du, X., Hoebe, K., and Beutler, B. (2006). Analysis of the MCMV resistome by ENU mutagenesis. *Mamm Genome* 17, 398-406.

Flajolet, M., Rotondo, G., Daviet, L., Bergametti, F., Inchauspe, G., Tiollais, P., Transy, C., and Legrain, P. (2000). A genomic approach of the hepatitis C virus generates a protein interaction map. *Gene* 242, 369-379.

Frodsham, A.J., Zhang, L., Dumpis, U., Taib, N.A., Best, S., Durham, A., Hennig, B.J., Hellier, S., Knapp, S., Wright, M., Chiaramonte, M., Bell, J.I., Graves, M., Whittle, H.C., Thomas, H.C., Thursz, M.R., and Hill, A.V. (2006). Class II cytokine receptor gene cluster is a major locus for hepatitis B persistence. *Proc Natl Acad Sci U S A* 103, 9148-9153.

Goff, S.P. (2008). Knockdown screens to knockout HIV-1. *Cell* 135, 417-420.

Harlow, E., Whyte, P., Franza, B.R., Jr., and Schley, C. (1986). Association of adenovirus early-region 1A proteins with cellular polypeptides. *Mol Cell Biol* 6, 1579-1589.

Lakadamyali, M., Rust, M.J., Babcock, H.P., and Zhuang, X. (2003). Visualizing infection of individual influenza viruses. *Proc Natl Acad Sci U S A* 100, 9280-9285.

Lake, J.A., Carr, J., Feng, F., Mundy, L., Burrell, C., and Li, P. (2003). The role of Vif during HIV-1 infection: interaction with novel host cellular factors. *J Clin Virol* 26, 143-152.

Lee, S.H., Girard, S., Macina, D., Busa, M., Zafer, A., Belouchi, A., Gros, P., and Vidal, S.M. (2001). Susceptibility to mouse cytomegalovirus is associated with deletion of an activating natural killer cell receptor of the C-type lectin superfamily. *Nat Genet* 28, 42-45.

Mashimo, T., Lucas, M., Simon-Chazottes, D., Frenkiel, M.P., Montagutelli, X., Ceccaldi, P.E., Deubel, V., Guenet, J.L., and Despres, P. (2002). A nonsense mutation in the gene encoding 2'-5'-oligoadenylate synthetase/L1 isoform is associated with West Nile virus susceptibility in laboratory mice. *Proc Natl Acad Sci U S A* 99, 11311-11316.

Moorhouse, M.J., and Sharma, H.S. (2011). Recent advances in i-Gene tools and analysis: microarrays, next generation sequencing and mass spectrometry. *Indian J Biochem Biophys* 48, 215-225.

Navratil, V., de Chassey, B., Meyniel, L., Delmotte, S., Gautier, C., Andre, P., Lotteau, V., and Rabourdin-Combe, C. (2009). VirHostNet: a knowledge base for the management and the analysis of proteome-wide virus-host interaction networks. *Nucleic Acids Res* 37, D661-668.

Perelygin, A.A., Scherbik, S.V., Zhulin, I.B., Stockman, B.M., Li, Y., and Brinton, M.A. (2002). Positional cloning of the murine flavivirus resistance gene. *Proc Natl Acad Sci U S A* 99, 9322-9327.

Pereyra, F., et al. (2010). The major genetic determinants of HIV-1 control affect HLA class I peptide presentation. *Science* 330, 1551-1557.

Sarnow, P., Ho, Y.S., Williams, J., and Levine, A.J. (1982). Adenovirus E1b-58kd tumor antigen and SV40 large tumor antigen are physically associated with the same 54 kd cellular protein in transformed cells. *Cell* 28, 387-394.

Shan, G. (2010). RNA interference as a gene knockdown technique. *Int J Biochem Cell Biol* 42, 1243-1251.

Svenson, K.L., Gatti, D.M., Valdar, W., Welsh, C.E., Cheng, R., Chesler, E.J., Palmer, A.A., McMillan, L., and Churchill, G.A. (2012). High-resolution genetic mapping using the mouse diversity outbred population. *Genetics* 190, 437-447.

Tayyari, F., Marchant, D., Moraes, T.J., Duan, W., Mastrangelo, P., and Hegele, R.G. (2011). Identification of nucleolin as a cellular receptor for human respiratory syncytial virus. *Nat Med* 17, 1132-1135.

Uetz, P., Dong, Y.A., Zeretzke, C., Atzler, C., Baiker, A., Berger, B., Rajagopala, S.V., Roupelieva, M., Rose, D., Fossum, E., and Haas, J. (2006). Herpesviral protein networks and their interaction with the human proteome. *Science* 311, 239-242.

Welton, A.R., Chesler, E.J., Sturkie, C., Jackson, A.U., Hirsch, G.N., and Spindler, K.R. (2005). Identification of quantitative trait loci for susceptibility to mouse adenovirus type 1. *J Virol* 79, 11517-11522.

Won, S., Eidenschenk, C., Arnold, C.N., Siggs, O.M., Sun, L., Brandl, K., Mullen, T.M., Nemerow, G.R., Moresco, E.M., and Beutler, B. (2012). Increased susceptibility to DNA virus infection in mice with a GCN2 mutation. *J Virol* 86, 1802-1808.

Wu, E., Fernandez, J., Fleck, S.K., Von Seggern, D.J., Huang, S., and Nemerow, G.R. (2001). A 50-kDa membrane protein mediates sialic acid-independent binding and infection of conjunctival cells by adenovirus type 37. *Virology* 279, 78-89.

Chapter III

Viral disruption of the blood-brain barrier

Abstract

The blood-brain barrier (BBB) provides significant protection against microbial invasion of the brain. However, the BBB is not impenetrable, and mechanisms by which viruses breach it are becoming clearer. *In vivo* and *in vitro* model systems are enabling identification of host and viral factors contributing to breakdown of the unique BBB tight junctions. Key mechanisms of tight junction damage from inside and outside cells are disruption of the actin cytoskeleton and matrix metalloproteinase activity, respectively. Viral proteins acting in BBB disruption are described for HIV-1, currently the most studied encephalitic virus; other viruses are also discussed.

Viral entry to the brain

Viral encephalitis is a potentially deadly sequela of viral infection for which there are few treatment options. It is frequently associated with blood-brain barrier (BBB; see Table 3.2. Glossary) disruption, enabling entry of virus, inflammatory cells, and deleterious molecules into the brain parenchyma. Members of at least 11 virus families, including DNA viruses, retroviruses, and RNA viruses, cause encephalitis with significant morbidity and mortality (Knipe and Howley, 2007). There are a variety of means by which viruses enter the brain, primarily via neuronal transport or by crossing of one of several barriers to the central nervous system (CNS), including the BBB or the

blood-cerebrospinal fluid barrier (choroid plexus). Several recent reviews covered viral entry via axonal transport and the resulting neuronal damage (Griffin, 2011; McGavern and Kang, 2011; Salinas et al., 2010). This review will focus on CNS entry mechanisms used by viruses that breach the BBB. Cell culture and animal studies of viral encephalitis have recently progressed through approaches used in studies of pathogenic conditions of the CNS such as ischemic stroke and multiple sclerosis. We first present background information on the structure, function, and disruption of the BBB, followed by a discussion of specific mechanisms by which viruses breach the BBB.

Components of the BBB

The BBB is a physical, metabolic, and transport barrier between the peripheral circulation and the CNS (Abbott et al., 2010). The function of the barrier is contributed by features specific to brain microvascular endothelial cells, which form the walls of brain capillaries, and the interactions of these cells with other components of the neurovascular unit (NVU), especially astrocyte endfeet and extracellular matrix (Hawkins and Davis, 2005). The NVU also includes pericytes, microglia, and neurons (Fig. 3.1). Brain endothelial cells form extremely tight cell-cell junctions that are distinct from tight junctions of endothelia and epithelia elsewhere in the body, due to brain endothelial cells' morphology, biochemistry, and interactions with other cells of the NVU (Abbott et al., 2010; Engelhardt and Sorokin, 2009; Hawkins and Davis, 2005). Brain endothelial cells lack fenestrations, have high numbers of mitochondria, are very thin, and have a low rate of pinocytosis, characteristics that relate to their specialized function. For example, high mitochondrial content in the NVU relative to other tissues is likely important for the

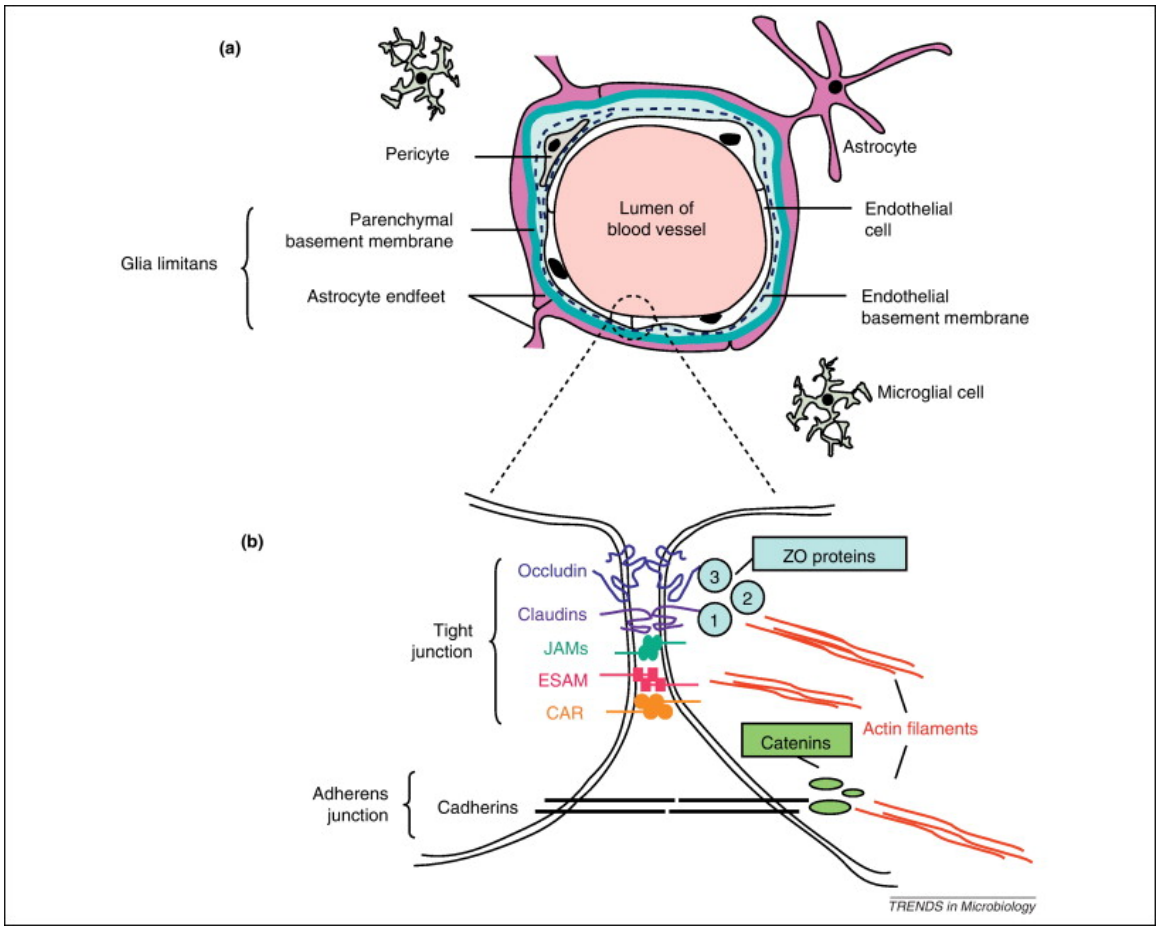

Figure 3.1. The neurovascular unit and junctions between endothelial cells. Top, cross-section of a brain microvessel, showing cells of the neurovascular unit. Neurons and their contacts with astrocytes are not shown. Cells in the lumen (bloodstream) include red blood cells, lymphocytes, monocytes, and neutrophils (not shown). Note the two basement membranes; the space between them is known as the perivascular space. Bottom, enlargement of an endothelial cell-cell junction. Major molecules of the tight junction and adherens junction are shown; no order of the tight junction proteins within the tight junction is implied by the figure. Abbreviations: JAMs, junctional adhesion molecules; ESAM, endothelial cell-selective adhesion molecule; CAR, Coxsackie and adenovirus receptor; ZO, zona occludens. The figure is based on figures in (Engelhardt and Sorokin, 2009; Francis et al., 2003).

energy required to maintain the structure and function of the BBB. Endothelial cells and associated pericytes are ensheathed by an endothelial cell basal lamina (vascular basement membrane). The composition of the endothelial basement membrane is distinct from that of a second basal lamina, the parenchymal basal lamina. This parenchymal basal lamina together with the astrocyte endfeet is termed the glia limitans. The perivascular space has been compared to a castle moat, between the vascular basement membrane (outer castle wall) and the glia limitans (inner wall) (Engelhardt and Coisne, 2011). Leukocytes accumulate in this cerebrospinal fluid-filled perivascular space (moat), where immune surveillance occurs. When leukocytes are presented with their cognate antigens, they are activated and cross the glia limitans into the brain parenchyma. Brain endothelial cells have active transporters expressed on their apical and basal surfaces that exclude potentially detrimental molecules or enable passage of essential nutrients such as glucose and amino acids into the brain parenchyma. Intact brain endothelium *in vivo* is characterized by a very high transendothelial electrical resistance (TEER) due to its complex tight junctions, which result in both the effective block of passage of macromolecules and restricted diffusion of ions and polar solutes. The consequence of these features of brain endothelial cells is a restrictive barrier with controlled entry of plasma components.

Tight junctions in the brain

The complexes holding brain endothelial cells together are adherens junctions and tight junctions (Fig. 3.1) (Abbott et al., 2010). The adherens junctions, composed of transmembrane cadherin proteins linked to the cell cytoskeleton by catenins, provide

structural support and are important for the development of tight junctions. Tight junction complexes consist of both integral transmembrane proteins and peripheral membrane proteins. The integral transmembrane tight junction proteins include occludin, claudins, junctional adhesion molecules (JAMs), endothelial cell-selective adhesion molecule (ESAM), and the Coxsackie and adenovirus receptor (CAR) (Abbott et al., 2010; Lehner et al., 2011). Occludin and claudins have external loops that mediate intercellular adhesion by interaction with occludin and claudins of neighboring cells (Hawkins and Davis, 2005). The tight junction proteins that span the gap between cells can be altered in their localization or cleaved during BBB damage resulting from viral infections and other pathological conditions.

Cytosolic tails of the transmembrane tight junction proteins are associated with any of a large number of peripheral membrane (cytosolic) tight junction proteins, which can serve adaptor, scaffolding, signaling, or transcriptional activator functions (Lehner et al., 2011). In particular, claudins and occludin interact with zona occludens (ZO)-1, -2, and -3, which in turn link to the actin cytoskeleton. The endothelial cytoskeleton is critical for integrity of tight junctions: actin stress fibers and microtubules contribute to tension force and isometric cellular contraction required for barrier function (Stamatovic et al., 2008). Disruption of the endothelial cytoskeleton can contribute to or be a result of tight junction dysfunction. Disruption of occludin, claudin-5 and ZO-1 is an indicator of functional breakdown of the BBB (Candelario-Jalil et al., 2009). The mechanisms that specific viruses use to alter tight junction proteins are discussed below.

BBB disruption by viruses

BBB disruption can be both a cause and effect of viral and non-viral CNS disease such as stroke, cancer, traumatic brain injury, and multiple sclerosis (Hawkins and Davis, 2005). Viruses known to cause disruption of the BBB or endothelial junctions include HIV-1, human T-cell leukemia virus (HTLV-1), lymphocytic choriomeningitis virus (LCMV), West Nile virus (WNV), and mouse adenovirus type 1 (MAV-1) (Table 3.1) (Afonso et al., 2008; Gralinski et al., 2009; Knipe and Howley, 2007; Strazza et al., 2011). HIV-1, simian immunodeficiency virus (SIV-1), feline immunodeficiency virus, and WNV are thought to invade the brain parenchyma by a 'Trojan horse' mechanism, through diapedesis of infected

immune cells that either cross the BBB paracellularly (between cells) or transcellularly (through cells) (Fletcher et al., 2011; Ivey et al., 2009a; Verma et al., 2009). WNV cell-free viruses and virus-like particles (VLPs) may transit human endothelial cells via a transcellular pathway that does not affect the integrity of the BBB (Hasebe et al., 2010; Verma et al., 2009). Important mechanisms of BBB disruption associated with paracellular entry of viruses that are discussed in this review include alterations in expression or phosphorylation of tight junction proteins, disruption of the basal lamina, and disruption of the actin cytoskeleton. Only in a few cases have viral gene products been directly implicated in BBB disruption (e.g., HIV-1, see below); in the absence of such mechanisms, indirect effects of viruses on the immune system are likely causes of barrier disruption.

There are many modulators of transcellular and paracellular BBB permeability,

Table 3.1. Viruses and their effects on the BBB

Virus	Effects on BBB	Ref
Herpes simplex virus	Increased MMP2 and MMP9 activity	71
HIV-1	Alteration of tight junction protein expression, which is likely CCL2-dependent	12, 33, 35, 36
	Increased MMP2 and MMP9 expression in *in vitro* culture supernatants	33
	Activation of Ras signaling	41-44
	Inhibition of tight junction protein expression with concomitant increase in MMP9 cleavage of tight junction proteins due to Tat	45, 46
	Higher vessel permeability due to presence of secreted gp120	47
	Increased expression of MMP2 and MMP9 with decreased expression of claudin-5 and laminin due to oxidative stress	49
HTLV-1	Alteration of tight junction protein expression	14
	Increased barrier permeability of cells and higher migration of infected lymphocytes in *in vitro* co-culture model	14
Japanese encephalitis virus (JEV)	Increased MMP9 expression	60
Lymphocytic choriomeningitis virus (LCMV)	$CD8^{+}$T cell-dependent BBB disruption	68
Mouse adenovirus type 1 (MAV-1)	Alteration of tight junction protein expression	13
Rabies virus	$CD4^{+}$ T cell-dependent BBB disruption	66, 67
SIV	Alteration of tight junction protein expression associated with increased FAK expression	39
Theiler's virus	Alteration of tight junction protein expression	68, 69
West Nile virus (WNV)	Increased tight junction protein expression	16
	Increased MMP expression and activity	59, 62
	Increased TLR3-dependent inflammatory response leading to increased BBB disruption	61
Various viruses	Increased ROS and RNS production	27

including vasogenic factors, growth factors, cytokines and chemokines, matrix metalloproteinases (MMPs), free radicals, and lipid mediators (Stamatovic et al., 2008). Accordingly, the mechanisms used by infectious agents to compromise the BBB vary. In some cases BBB disruption may be caused directly by microbial products, but in most cases, multiple factors are likely to play a role. For example, induction of cytokines and chemokines upon viral infection of brain cells and leukocytes homing to the brain could cumulatively contribute to BBB disruption.

Disruption of tight junctions and basal lamina by secreted MMPs

MMPs are key mediators of tight junction protein alterations leading to BBB dysfunction (Feng et al., 2011; Yang et al., 2007). These zinc-dependent enzymes have proteolytic activity that acts on the extracellular matrix, such as basal laminae in the NVU. MMP activity induced in pathological conditions causes BBB disruption not only by basement membrane degradation, but also by cleavage of tight junction proteins occludin and claudin-5 (Bojarski et al., 2004; Giebel et al., 2005; Gurney et al., 2006; Reijerkerk et al., 2006). MMPs can also cleave cytokines, modulating their activity and thus inflammation (Candelario-Jalil et al., 2009). MMPs are synthesized as inactive enzymes (zymogens), and their activity is regulated at four levels: gene expression, activation of proenzyme, enzyme inactivation by association with endogenous inhibitors (tissue inhibitors of metalloproteinases, TIMPs), and cellular compartmentalization (Lehner et al., 2011). Activation of MMPs occurs by cleavage by other MMPs or proteases, or by direct or indirect exposure to oxidative stress.

Increased production of reactive oxygen species (ROS) correlates with increased

MMP activity during brain injury, and markers of oxidative stress colocalize with active MMPs (Wakisaka et al., 2010). Non-viral inducers of ROS alter tight junction protein expression and phosphorylation, stimulate increased MMP activity, and increase permeability of the BBB (Haorah et al., 2007). Viral infections of the CNS can directly increase ROS and reactive nitrogen species (RNS) through stimulation of intracellular signaling by virion components or cytotoxic effects of viral nonstructural proteins (Valyi-Nagy and Dermody, 2005). The host inflammatory response to viral infection can also generate ROS and RNS, which in turn stimulate inflammatory cytokines and MMP secretion by cells of the NVU. Thus viral infections of the CNS have the potential to cause BBB disruption by inducing oxidative damage that alters MMP activity.

Some MMPs are membrane-bound (membrane-type MMPs, MT-MMPs), with extracellular catalytic domains (Yang et al., 2011). However, most MMPs are secreted, although they may stay localized to the cell surface by association with MT-MMPs or other cell surface molecules. In the neuroinflammatory response, the primary secreted MMPs are MMP2, MMP3, and MMP9 (Candelario-Jalil et al., 2009). MMP9 and MMP3 are inducible MMPs involved in inflammatory responses in the brain, whereas MMP2 is constitutively expressed by astrocytes, present in zymogen form throughout the brain, and activated upon host response to injury. MMP2, MMP3, and MMP9 all cleave tight junction proteins (Bojarski et al., 2004; Giebel et al., 2005; Gurney et al., 2006). All cell types in the NVU are able to produce MMPs, and in pathological conditions (including viral infections), alterations in MMP mRNA and enzymatic activity have been found in endothelial cells, astrocytes, and microglia of the NVU, and in macrophages and neutrophils recruited from the circulation (Yang et al., 2011).

Disruption of tight junctions by alterations to the actin cytoskeleton and peripheral membrane tight junction protein complexes

Tight junctions can also be disrupted from within cells. Changes to the actin cytoskeleton are likely to occur upon alterations to the tight junction proteins, resulting in paracellular permeability changes (Lai et al., 2005; Stamatovic et al., 2008). ROS play a role in disrupting tight junctions from within cells, by induction of the small GTPase RhoA, PI3 kinase and protein kinase B (PKB/Akt) signaling pathways with a concomitant rearrangement of the actin cytoskeleton, altered localization of occludin and claudin-5, and altered BBB integrity (Schreibelt et al., 2007). Other evidence that BBB disruption can be initiated from within cells is that alteration of the actin cytoskeleton induced by hypoxic stress is correlated with changes in BBB permeability and ZO-1 localization (Hicks et al., 2010). Furthermore, the tight junction proteins occludin, ZO-1, ZO-2, and claudin-5 are phosphoproteins; changes in their phosphorylation result in changes in localization and/or interaction, affecting BBB permeability (Stamatovic et al., 2008). Expression of monocyte chemoattractant protein-1 (CCL2) alters the actin cytoskeleton and localization of tight junction proteins in brain endothelium, disrupting the BBB (Stamatovic et al., 2003). HIV-1 alteration of tight junction proteins is dependent on CCL2 (Eugenin et al., 2006). Many virus infections alter the integrity of the cytoskeleton (Taylor et al., 2011), but the role of this in viral disruption of the BBB has not been well studied.

Breaching of the BBB by retroviruses

HIV-1 is one of the most-studied viruses with respect to viral and host processes

involved in encephalitis and disruption of the BBB. Accordingly, for HIV-1 encephalitis there are data for many of the mechanisms of barrier disruption described above, particularly alterations of tight junction protein expression (Strazza et al., 2011). Both transcellular and paracellular diapedesis of infected leukocytes are involved in HIV-1 transit across the BBB (Ivey et al., 2009a). Retroviral-associated neural disease caused by human T cell leukemia virus (HTLV-1) is also characterized by alteration of tight junction protein expression (Afonso et al., 2008).

Alteration of BBB function by HIV-1 infection is seen both in patients and *in vitro* models. Post-mortem brain samples of HIV-1-positive patients with encephalitis or HIV-1-associated dementia show increased monocyte infiltration and fragmented or reduced expression of the tight junction proteins ZO-1, occludin, and claudin-5; such disruption is not seen in controls (HIV-1 patients without encephalitis, HIV-1 seronegative patients, or cases who die of non-HIV-1 causes) (Boven et al., 2000; Dallasta et al., 1999). *In vitro* culture systems for HIV-1 infection studies use primary human brain-derived microvascular or umbilical vein-derived endothelial cells, often co-cultured across transwell inserts with astrocytes (Eugenin et al., 2006). Compared with uninfected activated peripheral blood mononuclear cells, HIV-1-infected cells introduced into culture systems cross the endothelial cell monolayers, altering tight junction protein expression and increasing permeability and MMP2 and MMP9 expression.

An important recent development in the study of human encephalitic pathogens, particularly lentiviruses, has been the use of the immortalized, well-characterized brain endothelial cell line hCMEC/D3, obtained by expressing human telomerase reverse transcriptase (hTERT) and simian virus 40 (SV40) large T antigen (Weksler et al., 2005).

This new cell line recapitulates important characteristics of primary human brain endothelial cells and has been successfully used in *in vitro* BBB studies with pathogenic microbes (Afonso et al., 2008; Fletcher et al., 2011; Zougbédé et al., 2011). For example, hCMEC/D3 cells infected by co-culture with a HTLV-1-producing cell line have higher permeability than when co-cultured with a control line not producing viral particles; and migration of infected lymphocytes across hCMEC/D3 cells is higher than migration of control lymphocytes (Afonso et al., 2008). Another culture system is Rhesus macaque brain microvessels, which when incubated with SIV-infected leukocytes show a significant loss of ZO-1 expression associated with increased expression of focal adhesion kinase (FAK) (Ivey et al., 2009b).

In addition to host components, viral proteins contribute to changes in BBB function during HIV-1 infection (Strazza et al., 2011). Three HIV-1 proteins have been implicated in altering BBB integrity, Tat, gp120, and Nef. Tat is a multifunctional viral protein that acts as a transactivator, enhancing initiation and elongation of viral transcription. Tat is secreted from infected cells, and it can enter other cells and affect their function. There is evidence for several mechanisms by which Tat contributes to BBB disruption. A key target of Tat is vascular endothelium, where it activates inflammation and angiogenesis. Specifically, Tat acts on endothelial cells, inducing proliferation, expression of adhesion molecules, release of proteolytic enzymes, and adhesion to the extracellular matrix via focal adhesions (Avraham et al., 2004). Introduction of Tat into human brain microvascular endothelial cells results in altered expression of tight junction proteins and activation of Ras signaling (Andras et al., 2005; Gandhi et al., 2010; Mahajan et al., 2008; Zhong et al., 2008). Similarly, injection of Tat

into mice results in altered expression of tight junction proteins occludin and ZO-1, accumulation of inflammatory cells, and activation of mitogen-activated protein kinase (MAPK) (Strazza et al., 2011). Tat interacts with MMP pathways, and may thus alter BBB function during HIV infection. For example, Tat was recently reported to inhibit endothelial cell occludin expression and promote its cleavage by MMP9, by a RhoA-dependent pathway (Xu et al., 2011). MMP9 mRNA, protein, and enzymatic activity levels are increased when astrocytes are treated with Tat (Ju et al., 2009). This upregulation of expression is dependent on MAPK, NF-κB (nuclear factor-kappa B) and Tat-induced tumor necrosis factor-alpha production. It should be noted that the physiological relevance of effects of Tat seen *in vitro* is controversial, because it is not clear whether sufficient levels of extracellular Tat in the circulation are achieved, even in microenvironments (Strazza et al., 2011).

Another HIV-1 protein that affects BBB integrity is gp120, a virion envelope protein (Strazza et al., 2011). gp120 can be found in patient serum, and it crosses brain endothelial cells in culture by adsorptive endocytosis, giving it access to cells in the NVU. A transgenic mouse model in which gp120 is secreted was used to examine the role of circulating gp120 (Toneatto et al., 1999). Compared to wild-type controls, transgenic mice had more brain blood vessels with permeability to albumin, indicating damage to the BBB. Additional experiments with endothelial cells from both transgenic or control mice, incubated with serum from transgenic mice, showed that the effect is gp120-dependent (Cioni and Annunziata, 2002). In another animal model, injection of gp120 alters the BBB in rats, increasing expression of MMP2 and MMP9 and decreasing expression of claudin-5 and laminin, a component of the BBB basal lamina; oxidative

stress is implicated as a contributing mechanism (Louboutin et al., 2010). A role for gp120 in BBB disruption is also supported by *in vitro* evidence that gp120 added to cultured human brain endothelial cells enhances monocyte migration, increases permeability, decreases TEER, and disrupts expression of tight junction proteins ZO-1, ZO-2, and occludin (but not claudins or actin) (Kanmogne et al., 2005; Kanmogne et al., 2007). A proteasomal mechanism is apparently involved in the gp120-induced degradation of the ZO proteins, but how that is initiated and the mechanism for degradation of other tight junction proteins remain unknown (Nakamuta et al., 2008). Taken together, these *in vivo* and *in vitro* data suggest that circulating gp120 in HIV-infected humans may contribute to BBB disruption.

Nef is a third HIV-1 protein implicated in damage of the BBB. Nef is a pleiotropic accessory protein, whose best characterized activities are alteration of antigen presentation by major histocompatibility complex class I (MHC-I) and downregulation of CD4 (Wonderlich et al., 2011). Nef is expressed in astrocytes of AIDS patients, particularly those with moderate to severe dementia (Ranki et al., 1995). Nef expression activates cultured astrocytes, elevating expression of markers associated with brain inflammation (Kohleisen et al., 1999). Nef also increases sensitivity of cultured astrocytes to hydrogen peroxide, a ROS (Masanetz and Lehmann, 2011). It is hypothesized that Nef may contribute to pathology in HIV-1-infected people through this mechanism, particularly in the absence of adequate functional glutathione peroxidase. HIV-1 infection of astrocyte cultures in an endothelial cell co-culture model increases permeability of the endothelium, causing endothelial cell apoptosis, altered astrocyte endfoot formation, and signaling between uninfected and infected cells in a gap junction-

dependent mechanism (Eugenin et al., 2011). This bystander effect of HIV-1-infected astrocytes on neighboring cells has *in vivo* support from experiments with astrocytes of SIV-infected macaques. HIV-1 infection of astrocytes also increases their production of pro-MMP2 and pro-MMP9 (Ju et al., 2009; Lévêque et al., 2004). Due to the importance of astrocyte endfeet in BBB integrity, it will be interesting to learn whether Nef is responsible for these reported HIV-1 effects in astrocytes, thereby contributing to disruption of BBB integrity. Taken together, studies on Tat, gp120, and Nef indicate that BBB disruption during viral infection can be attributed to specific viral proteins. Similar analysis of viral protein involvement for other viruses will increase our understanding of virus-host interations in encephalitis.

Breaching of the BBB by RNA viruses

Flaviviridae are among the best-studied RNA viruses that compromise the BBB. As described above, WNV traffics across the BBB both by a Trojan horse mechanism and as a cell-free virus (Verma et al., 2009). Remarkably, transit of cell-free virus or VLPs does not alter permeability of the BBB, and rather than a decrease in tight junction protein expression in cultured brain endothelial cells (as seen in other virus infections), there is an increase at the time of peak viral replication (Hasebe et al., 2010; Verma et al., 2009). WNV infection of cultured brain cortical astrocytes, but not endothelial cells, increases MMP mRNA, protein, and activity, and increases expression of TIMPs (Verma et al., 2010). Incubation of WNV-infected astrocyte supernatant with brain endothelial cells results in degradation of tight junction proteins, with a concomitant loss of TEER and barrier integrity. Infection of cultured rat astrocytes with another flavivirus, Japanese

encephalitis virus (JEV), increases MMP9 expression in a NF-κB-, MAPK- and ROS-dependent manner (Tung et al., 2010).

In vivo, WNV infection of wild-type mice results in BBB permeability that is greater than in mice deficient for Toll-like receptor 3 (TLR3) (Wang et al., 2004). The *Tlr3*$^{-/-}$ mice are more resistant to lethal WNV infection, indicating that the TLR3-mediated inflammatory response increases the ability of WNV to enter the brain. WNV infection increases activity and mRNA expression of MMP9 in mouse brains; and from experiments with MMP9-/- mice, MMP9 has been shown to disrupt the BBB and lead to virus entry into the brain (Wang et al., 2008). This study also showed that MMP9 protein is elevated in cerebrospinal fluid of WNV-infected patients compared to uninfected controls. Interestingly, lethal WNV infection in some mouse strains or hamsters occurs without BBB breakdown (Morrey et al., 2008). The mechanism for this is not understood, but the authors note that lymphocytic cells may traffic to the CNS by routes other than the BBB. As with WNV, infection of mice with JEV results in deformation of tight junctions and increased permeability of Evans blue dye in the brain (Liu et al., 2008).

The dissociation of BBB permeability from lethality occurs in infection by another RNA virus, rabies virus. Rabies virus is a neurotropic negative-sense RNA virus that enters the brain via retrograde axonal transport rather than by disrupting the BBB (Knipe and Howley, 2007). Nonetheless, in rabies virus infections of mice, increased BBB permeability and inflammation occur differentially in various parts of the brain, accompanied by clearance of virus and a lack of neurological sequelae (Phares et al., 2006). The BBB disruption is dependent on $CD4^+$ T cells, and mice in which there is more extensive BBB permeability and CNS inflammation survive a lethal rabies virus

infection better (Phares et al., 2007; Roy and Hooper, 2007). This indicates that in rabies virus infection, BBB disruption enables infiltration of immune effectors critical for survival.

Effects of two other RNA viruses on CNS vascular pathology have recently been reviewed. Some strains of Theiler's murine encephalomyelitis virus, a positive-sense RNA virus, induce acute encephalitis with alterations in tight junction protein expression (Kang and McGavern, 2010; Suidan et al., 2008). In meningitis caused by LCMV, a negative-sense RNA virus, virus-specific $CD8^+$ T cells are required for induction of disease; they are recruited into the CNS, resulting in increased vascular permeability and BBB disruption (Kang and McGavern, 2010). However, uncal herniation due to ventricular leakage and edema, rather than the BBB damage, appear to be the cause of the fatal choriomeningitis (Kang and McGavern, 2010; Matullo et al., 2010). Thus, similar to WNV and rabies, LCMV-induced BBB disruption itself is not lethal; instead ventricular failure is likely responsible for mortality.

Breaching of the BBB by DNA viruses

The mechanisms that DNA viruses use to enter the brain include both neural spread and breaching of the BBB. Herpes simplex virus-1 (HSV-1) causes rare but severe encephalitis, responsible for the majority of sporadic fatal viral encephalitis cases in the United States (Sellner et al., 2006). Similar to rabies virus, HSV-1 enters the brain via a neuronal route, and in HSV-1 encephalitis (HSE) BBB damage is seen. In a mouse model of HSE, MMP2 and MMP9 activity are increased, and *in situ* zymography indicates that MMP9 activity is centered around meninges and parenchymal blood vessels in the brain

(Sellner et al., 2006).

MAV-1 causes a fatal encephalomyelitis in susceptible strains of mice, its natural host (Guida et al., 1995; Kring et al., 1995). The virus infects endothelial cells and causes significant histopathology in brain vasculature (Guida et al., 1995; Kajon et al., 1998; Kring et al., 1995). MAV-1 infection induces increased BBB permeability that is largely independent of inflammation (Gralinski et al., 2009). Primary mouse brain endothelial cells infected with MAV-1 have decreased TEER, tight junction mRNA and protein levels compared to mock-infected cells. MAV-1 replication in the brain is limited to perivascular regions, leading to the hypothesis that the virus crosses the BBB by direct endothelial cell infection. However, entry into the CNS by a Trojan horse mechanism via monocytes, which are also infected by MAV-1, cannot be ruled out (Ashley et al., 2009; Kajon et al., 1998). Although MAV-1 infection results in inflammatory cell infiltration in the brain, in infected mice in which inflammation is greatly reduced, BBB disruption is equivalent to that in control mice (Gralinski et al., 2009). MAV-1 may thus stimulate an innate host response in infected endothelial cells that induces BBB disruption prior to and/or independent of cellular inflammation, possibly by increasing MMP activity of cells in the NVU and circulation.

Other virus-tight junction interactions: comparative lessons

Endothelia and epithelia share some features, such as tight and adherens junctions, although their permeabilities vary. For example, skin epithelium is a tighter barrier than intestinal epithelium (Moens and Veldhoen, 2012); and due to the unique properties of brain endothelial cells discussed above, the complex tight junctions of brain

endothelium are nearly impenetrable compared to other less structurally organized endothelia. Some aspects of tight junction regulation are shared between endothelia and epithelia, including modulation by phosphorylation and oxidative stress (Liu et al., 2012). The protein compositions of tight junctions of endothelia and epithelia are generally similar. However, BBB tight junctions have specific claudins (i.e., claudins 3, 5, and 12) that are key to maintenance of barrier function (Abbott et al., 2010; Hawkins and Davis, 2005; Nitta et al., 2003).

Viruses interact not only with tight junctions in the brain, but also tight junctions of airway and intestinal epithelial cells (Bergelson, 2009). Some components of tight junctions or adherens junctions are viral attachment receptors or entry factors. For example, JAM-1 is a receptor for reovirus (Barton et al., 2001) and feline calicivirus (Makino et al., 2006); occludin is required for Coxsackievirus B3 entry (Coyne et al., 2007); and claudin-1 and occludin are hepatitis C virus (HCV) entry factors (Evans et al., 2007; Ploss et al., 2009). Nectin-4, an adherens junction protein, was recently identified as an epithelial cell receptor for measles virus (Mühlebach et al., 2011; Noyce et al., 2011). Some proteins were first identified as viral receptors and subsequently shown to be components or possible regulators of tight junctions, including CAR (Cohen et al., 2001) and the receptor for human hepatitis A virus, respectively (Martin et al., 2011). Why viruses use tight junction proteins as attachment or entry receptors is poorly understood (Bergelson, 2009). However, in the setting of the BBB, targeting of tight junctions may enable viral access to the brain parenchyma. For example, recently HCV RNA has been demonstrated to be present in brain tissues of infected individuals, and *in vitro* brain endothelial cell infection by HCV appears to be claudin-1-dependent (Fletcher

et al., 2011).

Despite use of tight junction components as receptors by a number of viruses few correlations have been made with junctional damage upon virus binding. However, there is ample evidence for disruption of tight junctions of non-neural vasculature or epithelia at mucosal surfaces as a direct or indirect result of viral infection. For example, HCV infection promotes expression of vascular endothelial growth factor, which alters tight junction integrity and polarity of hepatocytes (Mee et al., 2010). Hemorrhagic hantavirus infection of renal epithelial and endothelial cells results in redistribution and reduction in tight junction protein ZO-1 and reduced transepithelial electrical resistance (Krautkrämer et al., 2011). Dengue virus infection increases vascular permeability, particularly in severe dengue hemorrhagic fever and dengue shock syndrome. It does so at least in part by inducing macrophage migration inhibitory factor, which causes redistribution of the tight junction protein ZO-1 (Chuang et al., 2011). In cases of severe influenza, in which there is multi-organ failure with edema and high levels of cytokine production, there is increased vascular permeability that is associated with loss of ZO-1 (Wang et al., 2010). Given the variety of viruses that utilize tight junction and adherens junction proteins as attachment receptors or entry factors, and the known disruption of tight junctions outside the CNS by viruses, a fruitful area of study will be to investigate junctional damage that results in the BBB as a result of specific virus-host protein interactions.

Concluding remarks

The interplay between viruses and their hosts at the BBB is complex. From HIV-1, we have learned that specific viral genes affect (i) signaling pathways that lead to

oxidative stress, (ii) expression of enzymes such as MMPs that disrupt the structure of tight junctions, iii) cytokines that affect inflammation, and (iv) proteasomal degradation of tight junction proteins from within cells. The cumulative effects of these are BBB damage. Much less is known about other encephalitic viruses, but accumulating evidence demonstrates that they too use a variety of mechanisms to breach the BBB. Many viruses disrupt the actin cytoskeleton as part of their life cycle (Taylor et al., 2011), and since cytoskeletal integrity is essential for BBB function, these effects on the cytoskeleton likely play an underappreciated role in BBB disruption.

Much knowledge about BBB disruption by viruses has been gained by extending studies of non-viral CNS disease pathogenesis, including ischemic stroke and multiple sclerosis. Comparing and contrasting viral infections that alter tight junctions in the brain with those that do so in the respiratory, gastrointestinal, or genital tracts will also be informative in future research investigating both viral genes and host response involved in tight junction disruption. Similarly, we can also learn from studies of parasites that breach or damage the BBB, such as *Plasmodium* spp., *Toxoplasma gondii*, and trypanosomes, which alter permeability by modifying expression of tight junction proteins and MMPs (Kang and McGavern, 2010; Lacerda-Queiroz et al., 2011; Prato et al., 2011; Zougbédé et al., 2011).

The development of good *in vitro* models, such as immortalized endothelial cells that retain key endothelial properties (Weksler et al., 2005), holds promise for exciting new developments in the study of encephalitic viruses and how they disrupt the BBB (Box 1). Infections of small animals with viruses are important *in vivo* models that provide insight into virus-host interactions at the whole animal level. Moreover,

expanded use of genetically altered mice, particularly knockouts in innate immune system components such as TLRs and inflammasome components, will enable studies of the impact of the host response to BBB disruption that are not possible *in vitro*. The use of sensitive *in situ* zymography to detect active MMPs (Engelhardt and Sorokin, 2009), and live cell imaging, including intravital microscopy (McGavern and Kang, 2011), will extend the use of *in vivo* and *in vitro* models. Currently we have a basic knowledge of how viruses disrupt the BBB. Advances in understanding virus-host interactions are likely to be forthcoming as researchers apply powerful genetic, immunological, biochemical, and cell biology approaches to this inquiry.

Box 1. Outstanding questions

1. To what extent do virus-induced cytoskeletal changes in brain endothelial cells contribute to BBB disruption?

2. What is the sequence of events in BBB damage by encephalitic viruses, i.e., disruption from within the cell, or degradation of basal lamina or tight junction proteins from outside? How does this differ among viruses?

3. What viral gene products or host responses induce changes in tight junction protein expression in endothelial cells, leading to tight junction protein relocalization, altered phosphorylation, and/or degradation? What mechanisms are involved?

4. To what extent do viral interactions with non-endothelial cells of the NVU (e.g., astrocytes) contribute to BBB disruption?

5. What is the biological significance of viral CNS infection? What is the advantage to the virus of infecting this site?

Table 3.2. Glossary

Adherens junctions	Protein complexes located at cell-cell contacts in endothelium and epithelium. Adherens junctions are essential for formation of tight junctions and are anchored on actin cytoskeletons.
Astrocytes	Cells with long processes ('star' shaped) that comprise of the majority of neuroglial cells in the brain and spinal cord. Astrocytes are important for development and/or maintenance of BBB characteristics.
Blood-brain barrier (BBB)	The interface between the brain and peripheral circulation. It is composed of specialized capillaries and adjoining cells that function to strictly regulate substances entering the brain from the peripheral circulation.
Central nervous system (CNS)	The part of the nervous system that contains the brain and the spinal cord. Responsible for the control and coordination of the entire body.
Claudins	A family of small transmembrane proteins important for tight junction formation.
Endothelial cells	Cells forming the main structural component of blood vessels.
Junctional adhesion molecules (JAMs)	Members of the immunoglobulin family involved in cell-cell adhesion.
Lymphocytes	A subset of white blood cells of the immune system that includes T cells, B cells and NK cells.
Neurovascular unit (NVU)	An association of endothelium, extracellular matrix, astrocytes, pericytes, microglia, and neurons that contributes structurally and functionally to permeability of the microvasculature.
Matrix metalloproteinases (MMPs)	Zinc-dependent endopeptidases that are involved in a variety of processes including tissue repair, angiogenesis, cell division, apoptosis and host immunity. These proteins can be soluble, matrix-bound or cell-associated.
Microglia	Resident macrophages of the brain and spinal cord. They are the initial and main host immune system responders in the CNS.
Occludin	Transmembrane tight junction protein.
Paracellular transport	Transport of substances between or around cells
Reactive oxygen and nitrogen species (ROS, RNS)	Highly reactive molecules or free radicals that contain oxygen or nitrogen, respectively. These chemicals can mediate cellular damage by attacking biological molecules.

Tight junctions	Protein complexes that include transmembrane and cytoplasmic proteins. Tight junctions are located in intercellular clefts and form close associations that restrict the passage of molecules.
Tissue inhibitors of MMP (TIMPs)	Natural regulators of MMPs.
Transcellular transport	Transport of substances through a cell.
Zona (or zonula) occludens (ZO) proteins	A family of intracellular scaffolding proteins important for the structural integrity of intercellular tight junctions.

Notes

This work was reprinted with permission from Spindler, K.R., and T.-H. Hsu. Viral disruption of the blood-brain barrier. 2012. Trends Microbiol. doi:10.1016/j.tim.2012.03.009.

We apologize to authors whose work we did not have space to cite. We thank Jason Weinberg for comments on the manuscript. K.R.S. has been supported by NIH grants AI023762, AI068645, and AI091721. T.-H. Hsu has been supported by NIH National Research Service Award T32 GM07544, a University of Michigan (U-M) Rackham Graduate School fellowship and Rackham research grants, a U-M Frances Wang Chin Fellowship, and the U-M Endowment for the Development of Graduate Education.

References

Abbott, N.J., Patabendige, A.A., Dolman, D.E., Yusof, S.R., and Begley, D.J. (2010). Structure and function of the blood-brain barrier. *Neurobiol Dis* 37, 13-25.

Afonso, P.V., Ozden, S., Cumont, M.C., Seilhean, D., Cartier, L., Rezaie, P., Mason, S., Lambert, S., Huerre, M., Gessain, A., Couraud, P.O., Pique, C., Ceccaldi, P.E., and Romero, I.A. (2008). Alteration of blood-brain barrier integrity by retroviral infection. *PLoS Pathog.* 4, e1000205.

Andras, I.E., Pu, H., Tian, J., Deli, M.A., Nath, A., Hennig, B., and Toborek, M. (2005). Signaling mechanisms of HIV-1 Tat-induced alterations of claudin-5 expression in brain endothelial cells. *J. Cereb. Blood Flow Metab.* 25, 1159-1170.

Ashley, S.L., Welton, A.R., Harwood, K.M., Van Rooijen, N., and Spindler, K.R. (2009). Mouse adenovirus type 1 infection of macrophages. *Virology* 390, 307-314.

Avraham, H.K., Jiang, S., Lee, T.H., Prakash, O., and Avraham, S. (2004). HIV-1 Tat-mediated effects on focal adhesion assembly and permeability in brain microvascular endothelial cells. *J. Immunol.* 173, 6228-6233.

Barton, E.S., Forrest, J.C., Connolly, J.L., Chappell, J.D., Liu, Y., Schnell, F.J., Nusrat, A., Parkos, C.A., and Dermody, T.S. (2001). Junction adhesion molecule is a receptor for reovirus. *Cell* 104, 441-451.

Bergelson, J.M. (2009). Intercellular junctional proteins as receptors and barriers to virus infection and spread. *Cell Host Microbe* 5, 517-521.

Bojarski, C., Weiske, J., Schoneberg, T., Schroder, W., Mankertz, J., Schulzke, J.D., Florian, P., Fromm, M., Tauber, R., and Huber, O. (2004). The specific fates of tight junction proteins in apoptotic epithelial cells. *J. Cell Sci.* 117 (Pt10), 2097-2107.

Boven, L.A., Middel, J., Verhoef, J., De Groot, C.J., and Nottet, H.S. (2000). Monocyte infiltration is highly associated with loss of the tight junction protein zonula occludens in HIV-1-associated dementia. *Neuropathol. Appl. Neurobiol.* 26, 356-360.

Candelario-Jalil, E., Yang, Y., and Rosenberg, G.A. (2009). Diverse roles of matrix metalloproteinases and tissue inhibitors of metalloproteinases in neuroinflammation and cerebral ischemia. *Neuroscience* 158, 983-994.

Chuang, Y.C., Lei, H.Y., Liu, H.S., Lin, Y.S., Fu, T.F., and Yeh, T.M. (2011). Macrophage migration inhibitory factor induced by dengue virus infection increases vascular permeability. *Cytokine* 54, 222-231.

Cioni, C., and Annunziata, P. (2002). Circulating gp120 alters the blood-brain barrier permeability in HIV-1 gp120 transgenic mice. *Neurosci. Lett.* 330, 299-301.

Cohen, C.J., Shieh, J.T., Pickles, R.J., Okegawa, T., Hsieh, J.T., and Bergelson, J.M. (2001). The coxsackievirus and adenovirus receptor is a transmembrane component of the tight junction. *Proc. Natl. Acad. Sci. U S A* 98, 15191-15196.

Coyne, C.B., Shen, L., Turner, J.R., and Bergelson, J.M. (2007). Coxsackievirus entry across epithelial tight junctions requires occludin and the small GTPases Rab34 and Rab5. *Cell Host Microbe* 2, 181-192.

Dallasta, L.M., Pisarov, L.A., Esplen, J.E., Werley, J.V., Moses, A.V., Nelson, J.A., and Achim, C.L. (1999). Blood-brain barrier tight junction disruption in human immunodeficiency virus-1 encephalitis. *Am. J. Pathol.* 155, 1915-1927.

Engelhardt, B., and Coisne, C. (2011). Fluids and barriers of the CNS establish immune privilege by confining immune surveillance to a two-walled castle moat surrounding the CNS castle. *Fluids Barriers CNS* 8, 4.

Engelhardt, B., and Sorokin, L. (2009). The blood-brain and the blood-cerebrospinal fluid barriers: Function and dysfunction. *Semin. Immunopathol.* 31, 497-511.

Eugenin, E.A., Clements, J.E., Zink, M.C., and Berman, J.W. (2011). Human immunodeficiency virus infection of human astrocytes disrupts blood-brain barrier integrity by a gap junction-dependent mechanism. *J. Neurosci.* 31, 9456-9465.

Eugenin, E.A., Osiecki, K., Lopez, L., Goldstein, H., Calderon, T.M., and Berman, J.W. (2006). CCL2/monocyte chemoattractant protein-1 mediates enhanced transmigration of human immunodeficiency virus (HIV)-infected leukocytes across the blood-brain barrier: A potential mechanism of HIV-CNS invasion and NeuroAIDS. *J. Neurosci.* 26, 1098-1106.

Evans, M.J., von Hahn, T., Tscherne, D.M., Syder, A.J., Panis, M., Wolk, B., Hatziioannou, T., McKeating, J.A., Bieniasz, P.D., and Rice, C.M. (2007). Claudin-1 is a hepatitis C virus co-receptor required for a late step in entry. *Nature* 446, 801-805.

Feng, S., Cen, J., Huang, Y., Shen, H., Yao, L., Wang, Y., and Chen, Z. (2011). Matrix metalloproteinase-2 and -9 secreted by leukemic cells increase the permeability of blood-brain barrier by disrupting tight junction proteins. *PLoS One* 6, e20599.

Fletcher, N.F., Meeker, R.B., Hudson, L.C., and Callanan, J.J. (2011). The neuropathogenesis of feline immunodeficiency virus infection: barriers to overcome. *Vet. J.* 188, 260-269.

Francis, K., van Beek, J., Canova, C., Neal, J.W., and Gasque, P. (2003). Innate immunity and brain inflammation: The key role of complement. *Expert Rev. Mol. Med.* 5, 1-19.

Gandhi, N., Saiyed, Z.M., Napuri, J., Samikkannu, T., Reddy, P.V., Agudelo, M., Khatavkar, P., Saxena, S.K., and Nair, M.P. (2010). Interactive role of human immunodeficiency virus type 1 (HIV-1) clade-specific Tat protein and cocaine in blood-brain barrier dysfunction: implications for HIV-1-associated neurocognitive disorder. *J. Neurovirol.* 16, 294-305.

Giebel, S.J., Menicucci, G., McGuire, P.G., and Das, A. (2005). Matrix metalloproteinases in early diabetic retinopathy and their role in alteration of the blood-retinal barrier. *Lab. Invest.* 85, 597-607.

Gralinski, L.E., Ashley, S.L., Dixon, S.D., and Spindler, K.R. (2009). Mouse adenovirus type 1-induced breakdown of the blood-brain barrier. *J. Virol.* 83, 9398-9410.

Griffin, D.E. (2011). Viral encephalomyelitis. *PLoS Pathog.* 7, e1002004.

Guida, J.D., Fejer, G., Pirofski, L.-A., Brosnan, C.F., and Horwitz, M.S. (1995). Mouse adenovirus type 1 causes a fatal hemorrhagic encephalomyelitis in adult C57BL/6 but not BALB/c mice. *J. Virol.* 69, 7674-7681.

Gurney, K.J., Estrada, E.Y., and Rosenberg, G.A. (2006). Blood-brain barrier disruption by stromelysin-1 facilitates neutrophil infiltration in neuroinflammation. *Neurobiol. Dis.* 23, 87-96.

Haorah, J., Ramirez, S.H., Schall, K., Smith, D., Pandya, R., and Persidsky, Y. (2007). Oxidative stress activates protein tyrosine kinase and matrix metalloproteinases leading to blood-brain barrier dysfunction. *J. Neurochem.* 101, 566-576.

Hasebe, R., Suzuki, T., Makino, Y., Igarashi, M., Yamanouchi, S., Maeda, A., Horiuchi, M., Sawa, H., and Kimura, T. (2010). Transcellular transport of West Nile virus-like particles across human endothelial cells depends on residues 156 and 159 of envelope protein. *BMC Microbiol.* 10, 165.

Hawkins, B.T., and Davis, T.P. (2005). The blood-brain barrier/neurovascular unit in health and disease. *Pharmacol. Rev.* 57, 173-185.

Hicks, K., O'Neil, R.G., Dubinsky, W.S., and Brown, R.C. (2010). TRPC-mediated actin-myosin contraction is critical for BBB disruption following hypoxic stress. *Am. J. Physiol. Cell Physiol.* 298, C1583-1593.

Ivey, N.S., MacLean, A.G., and Lackner, A.A. (2009a). Acquired immunodeficiency syndrome and the blood-brain barrier. *J. Neurovirol.* 15, 111-122.

Ivey, N.S., Renner, N.A., Moroney-Rasmussen, T., Mohan, M., Redmann, R.K., Didier, P.J., Alvarez, X., Lackner, A.A., and Maclean, A.G. (2009b). Association of FAK activation with lentivirus-induced disruption of blood-brain barrier tight junction-associated ZO-1 protein organization. *J. Neurovirol.*, 1-12.

Ju, S.M., Song, H.Y., Lee, J.A., Lee, S.J., Choi, S.Y., and Park, J. (2009). Extracellular HIV-1 Tat up-regulates expression of matrix metalloproteinase-9 via a MAPK-NF-kappaB dependent pathway in human astrocytes. *Exp. Mol. Med.* 41, 86-93.

Kajon, A.E., Brown, C.C., and Spindler, K.R. (1998). Distribution of mouse adenovirus type 1 in intraperitoneally and intranasally infected adult outbred mice. *J. Virol.* 72, 1219-1223.

Kang, S.S., and McGavern, D.B. (2010). Microbial induction of vascular pathology in the CNS. *J. Neuroimmune Pharmacol.* 5, 370-386.

Kanmogne, G.D., Primeaux, C., and Grammas, P. (2005). HIV-1 gp120 proteins alter tight junction protein expression and brain endothelial cell permeability: Implications for the pathogenesis of HIV-associated dementia. *J. Neuropathol. Exp. Neurol.* 64, 498-505.

Kanmogne, G.D., Schall, K., Leibhart, J., Knipe, B., Gendelman, H.E., and Persidsky, Y. (2007). HIV-1 gp120 compromises blood-brain barrier integrity and enhances monocyte migration across blood-brain barrier: implication for viral neuropathogenesis. *J .Cereb. Blood Flow Metab.* 27, 123-134.

Knipe, D.M., and Howley, P.M., Eds. (2007). Fields Virology. 5th ed. Philadelphia: Wolters Kluwer Health/Lippincott Williams & Wilkins.

Kohleisen, B., Shumay, E., Sutter, G., Foerster, R., Brack-Werner, R., Nuesse, M., and Erfle, V. (1999). Stable expression of HIV-1 Nef induces changes in growth properties and activation state of human astrocytes. *AIDS* 13, 2331-2341.

Krautkrämer, E., Grouls, S., Stein, N., Reiser, J., and Zeier, M. (2011). Pathogenic old world hantaviruses infect renal glomerular and tubular cells and induce disassembling of cell-to-cell contacts. *J. Virol.* 85, 9811-9823.

Kring, S.C., King, C.S., and Spindler, K.R. (1995). Susceptibility and signs associated with mouse adenovirus type 1 infection of adult outbred Swiss mice. *J. Virol.* 69, 8084-8088.

Lacerda-Queiroz, N., Lima, O.C., Carneiro, C.M., Vilela, M.C., Teixeira, A.L., Teixeira-Carvalho, A., Araujo, M.S., Martins-Filho, O.A., Braga, E.M., and Carvalho-Tavares, J. (2011). Plasmodium berghei NK65 induces cerebral leukocyte recruitment in vivo: an intravital microscopic study. *Acta Trop.* 120, 31-39.

Lai, C.-H., Kuo, K.-H., and Leo, J.M. (2005). Critical role of actin in modulating BBB permeability. *Brain Res. Brain Res. Rev.* 50, 7-13.

Lehner, C., Gehwolf, R., Tempfer, H., Krizbai, I., Hennig, B., Bauer, H.C., and Bauer, H. (2011). Oxidative stress and blood-brain barrier dysfunction under particular consideration of matrix metalloproteinases. *Antioxid. Redox Signal.* 15, 1305-1323.

Lévêque, T., Le Pavec, G., Boutet, A., Tardieu, M., Dormont, D., and Gras, G. (2004). Differential regulation of gelatinase A and B and TIMP-1 and -2 by TNFα and HIV virions in astrocytes. *Microbes Infect.* 6, 157-163.

Liu, T.H., Liang, L.C., Wang, C.C., Liu, H.C., and Chen, W.J. (2008). The blood-brain barrier in the cerebrum is the initial site for the Japanese encephalitis virus entering the central nervous system. *J. Neurovirol.* 14, 514-521.

Liu, Z., Shi, C., Yang, J., Zhang, P., Ma, Y., Wang, F., and Qin, H. (2012). Molecular regulation of the intestinal epithelial barrier: implication in human diseases. *Front. Biosci.* 17, 2903-2909.

Louboutin, J.P., Agrawal, L., Reyes, B.A., Van Bockstaele, E.J., and Strayer, D.S. (2010). HIV-1 gp120-induced injury to the blood-brain barrier: role of metalloproteinases 2 and 9 and relationship to oxidative stress. *J. Neuropathol. Exp. Neurol.* 69, 801-816.

Mahajan, S.D., Aalinkeel, R., Sykes, D.E., Reynolds, J.L., Bindukumar, B., Fernandez, S.F., Chawda, R., Shanahan, T.C., and Schwartz, S.A. (2008). Tight junction regulation by morphine and HIV-1 tat modulates blood-brain barrier permeability. *J. Clin. Immunol.* 28, 528-541.

Makino, A., Shimojima, M., Miyazawa, T., Kato, K., Tohya, Y., and Akashi, H. (2006). Junctional adhesion molecule 1 is a functional receptor for feline calicivirus. *J. Virol.* 80, 4482-4490.

Martin, T.A., Harrison, G.M., Mason, M.D., and Jiang, W.G. (2011). HAVcR-1 reduces the integrity of human endothelial tight junctions. *Anticancer Res.* 31, 467-473.

Masanetz, S., and Lehmann, M.H. (2011). HIV-1 Nef increases astrocyte sensitivity towards exogenous hydrogen peroxide. *Virol. J.* 8, 35.

Matullo, C.M., O'Regan, K.J., Hensley, H., Curtis, M., and Rall, G.F. (2010). Lymphocytic choriomeningitis virus-induced mortality in mice is triggered by edema and brain herniation. *J. Virol.* 84, 312-320.

McGavern, D.B., and Kang, S.S. (2011). Illuminating viral infections in the nervous system. *Nat. Rev. Immunol.* 11, 318-329.

Mee, C.J., Farquhar, M.J., Harris, H.J., Hu, K., Ramma, W., Ahmed, A., Maurel, P., Bicknell, R., Balfe, P., and McKeating, J.A. (2010). Hepatitis C virus infection reduces hepatocellular polarity in a vascular endothelial growth factor-dependent manner. *Gastroenterology* 138, 1134-1142.

Moens, E., and Veldhoen, M. (2012). Epithelial barrier biology: good fences make good neighbours. *Immunology* 135, 1-8.

Morrey, J.D., Olsen, A.L., Siddharthan, V., Motter, N.E., Wang, H., Taro, B.S., Chen, D., Ruffner, D., and Hall, J.O. (2008). Increased blood-brain barrier permeability is not a primary determinant for lethality of West Nile virus infection in rodents. *J. Gen. Virol.* 89, 467-473.

Mühlebach, M.D., Mateo, M., Sinn, P.L., Prüfer, S., Uhlig, K.M., Leonard, V.H., Navaratnarajah, C.K., Frenzke, M., Wong, X.X., Sawatsky, B., Ramachandran, S., McCray, P.B., Jr., Cichutek, K., von Messling, V., Lopez, M., and Cattaneo, R. (2011). Adherens junction protein nectin-4 is the epithelial receptor for measles virus. *Nature* 480, 530-583.

Nakamuta, S., Endo, H., Higashi, Y., Kousaka, A., Yamada, H., Yano, M., and Kido, H. (2008). Human immunodeficiency virus type 1 gp120-mediated disruption of tight junction proteins by induction of proteasome-mediated degradation of zonula occludens-1 and -2 in human brain microvascular endothelial cells. *J. Neurovirol.* 14, 186-195.

Nitta, T., Hata, M., Gotoh, S., Seo, Y., Sasaki, H., Hashimoto, N., Furuse, M., and Tsukita, S. (2003). Size-selective loosening of the blood-brain barrier in claudin-5-deficient mice. *J. Cell Biol.* 161, 653-660.

Noyce, R.S., Bondre, D.G., Ha, M.N., Lin, L.T., Sisson, G., Tsao, M.S., and Richardson, C.D. (2011). Tumor cell marker PVRL4 (nectin 4) is an epithelial cell receptor for measles virus. *PLoS Pathog.* 7, e1002240.

Phares, T.W., Fabis, M.J., Brimer, C.M., Kean, R.B., and Hooper, D.C. (2007). A peroxynitrite-dependent pathway is responsible for blood-brain barrier permeability changes during a central nervous system inflammatory response: TNF-alpha is neither necessary nor sufficient. *J. Immunol.* 178, 7334-7343.

Phares, T.W., Kean, R.B., Mikheeva, T., and Hooper, D.C. (2006). Regional differences in blood-brain barrier permeability changes and inflammation in the apathogenic clearance of virus from the central nervous system. *J. Immunol.* 176, 7666-7675.

Ploss, A., Evans, M.J., Gaysinskaya, V.A., Panis, M., You, H., de Jong, Y.P., and Rice, C.M. (2009). Human occludin is a hepatitis C virus entry factor required for infection of mouse cells. *Nature* 457, 882-886.

Prato, M., D'Alessandro, S., Van den Steen, P.E., Opdenakker, G., Arese, P., Taramelli, D., and Basilico, N. (2011). Natural haemozoin modulates matrix metalloproteinases and induces morphological changes in human microvascular endothelium. *Cell. Microbiol.* 13, 1275-1285.

Ranki, A., Nyberg, M., Ovod, V., Haltia, M., Elovaara, I., Raininko, R., Haapasalo, H., and Krohn, K. (1995). Abundant expression of HIV Nef and Rev proteins in brain astrocytes in vivo is associated with dementia. *AIDS* 9, 1001-1008.

Reijerkerk, A., Kooij, G., van der Pol, S.M., Khazen, S., Dijkstra, C.D., and de Vries, H.E. (2006). Diapedesis of monocytes is associated with MMP-mediated occludin disappearance in brain endothelial cells. *FASEB J.* 20, 2550-2552.

Roy, A., and Hooper, D.C. (2007). Lethal silver-haired bat rabies virus infection can be prevented by opening the blood-brain barrier. *J. Virol.* 81, 7993-7998.

Salinas, S., Schiavo, G., and Kremer, E.J. (2010). A hitchhiker's guide to the nervous system: the complex journey of viruses and toxins. *Nat. Rev. Microbiol.* 8, 645-655.

Schreibelt, G., Kooij, G., Reijerkerk, A., van Doorn, R., Gringhuis, S.I., van der Pol, S., Weksler, B.B., Romero, I.A., Couraud, P.O., Piontek, J., Blasig, I.E., Dijkstra, C.D., Ronken, E., and de Vries, H.E. (2007). Reactive oxygen species alter brain endothelial tight junction dynamics via RhoA, PI3 kinase, and PKB signaling. *FASEB J.* 21, 3666-3676.

Sellner, J., Simon, F., Meyding-Lamade, U., and Leib, S.L. (2006). Herpes-simplex virus encephalitis is characterized by an early MMP-9 increase and collagen type IV degradation. *Brain Res.* 1125, 155-162.

Stamatovic, S.M., Keep, R.F., and Andjelkovic, A.V. (2008). Brain endothelial cell-cell junctions: How to "open" the blood brain barrier. *Curr Neuropharmacol* 6, 179-192.

Stamatovic, S.M., Keep, R.F., Kunkel, S.L., and Andjelkovic, A.V. (2003). Potential role of MCP-1 in endothelial cell tight junction 'opening' signaling via Rho and Rho kinase. *J. Cell Sci.* 116, 4615-4628.

Strazza, M., Pirrone, V., Wigdahl, B., and Nonnemacher, M.R. (2011). Breaking down the barrier: the effects of HIV-1 on the blood-brain barrier. *Brain Res.* 1399, 96-115.

Suidan, G.L., McDole, J.R., Chen, Y., Pirko, I., and Johnson, A.J. (2008). Induction of blood brain barrier tight junction protein alterations by CD8 T cells. *PLoS One* 3, e3037.

Taylor, M.P., Koyuncu, O.O., and Enquist, L.W. (2011). Subversion of the actin cytoskeleton during viral infection. *Nat. Rev. Microbiol.* 9, 427-439.

Toneatto, S., Finco, O., van der Putten, H., Abrignani, S., and Annunziata, P. (1999). Evidence of blood-brain barrier alteration and activation in HIV-1 gp120 transgenic mice. *AIDS* 13, 2343-2348.

Tung, W.H., Tsai, H.W., Lee, I.T., Hsieh, H.L., Chen, W.J., Chen, Y.L., and Yang, C.M. (2010). Japanese encephalitis virus induces matrix metalloproteinase-9 in rat brain astrocytes via NF-kappaB signalling dependent on MAPKs and reactive oxygen species. *Br. J. Pharmacol.* 161, 1566-1583.

Valyi-Nagy, T., and Dermody, T.S. (2005). Role of oxidative damage in the pathogenesis of viral infections of the nervous system. *Histol. Histopathol.* 20, 957-967.

Verma, S., Kumar, M., Gurjav, U., Lum, S., and Nerurkar, V.R. (2010). Reversal of West Nile virus-induced blood-brain barrier disruption and tight junction proteins degradation by matrix metalloproteinases inhibitor. *Virology* 397, 130-138.

Verma, S., Lo, Y., Chapagain, M., Lum, S., Kumar, M., Gurjav, U., Luo, H., Nakatsuka, A., and Nerurkar, V.R. (2009). West Nile virus infection modulates human brain microvascular endothelial cells tight junction proteins and cell adhesion molecules: Transmigration across the in vitro blood-brain barrier. *Virology* 385, 425-433.

Wakisaka, Y., Chu, Y., Miller, J.D., Rosenberg, G.A., and Heistad, D.D. (2010). Spontaneous intracerebral hemorrhage during acute and chronic hypertension in mice. *J Cereb Blood Flow Metab* 30, 56-69.

Wang, P., Dai, J., Bai, F., Kong, K.F., Wong, S.J., Montgomery, R.R., Madri, J.A., and Fikrig, E. (2008). Matrix metalloproteinase 9 facilitates West Nile virus entry into the brain. *J. Virol.* 82, 8978-8985.

Wang, S., Le, T.Q., Kurihara, N., Chida, J., Cisse, Y., Yano, M., and Kido, H. (2010). Influenza virus-cytokine-protease cycle in the pathogenesis of vascular hyperpermeability in severe influenza. *J. Infect. Dis.* 202, 991-1001.

Wang, T., Town, T., Alexopoulou, L., Anderson, J.F., Fikrig, E., and Flavell, R.A. (2004). Toll-like receptor 3 mediates West Nile virus entry into the brain causing lethal encephalitis. *Nat. Med.* 10, 1366-1373.

Weksler, B.B., Subileau, E.A., Perriere, N., Charneau, P., Holloway, K., Leveque, M., Tricoire-Leignel, H., Nicotra, A., Bourdoulous, S., Turowski, P., Male, D.K., Roux, F., Greenwood, J., Romero, I.A., and Couraud, P.O. (2005). Blood-brain barrier-specific properties of a human adult brain endothelial cell line. *FASEB J.* 19, 1872-1874.

Wonderlich, E.R., Leonard, J.A., and Collins, K.L. (2011). HIV immune evasion disruption of antigen presentation by the HIV Nef protein. *Adv. Virus Res.* 80, 103-127.

Xu, R., Feng, X., Xie, X., Zhang, J., Wu, D., and Xu, L. (2011). HIV-1 Tat protein increases the permeability of brain endothelial cells by both inhibiting occludin expression and cleaving occludin via matrix metalloproteinase-9. *Brain Res.* 1436, 13-19.

Yang, Y., Estrada, E.Y., Thompson, J.F., Liu, W., and Rosenberg, G.A. (2007). Matrix metalloproteinase-mediated disruption of tight junction proteins in cerebral vessels is reversed by synthetic matrix metalloproteinase inhibitor in focal ischemia in rat. *J. Cereb. Blood Flow Metab.* 27, 697-709.

Yang, Y., Hill, J.W., and Rosenberg, G.A. (2011). Multiple roles of metalloproteinases in neurological disorders. *Prog. Mol. Biol. Transl. Sci.* 99, 241-263.

Zhong, Y., Smart, E.J., Weksler, B., Couraud, P.O., Hennig, B., and Toborek, M. (2008). Caveolin-1 regulates human immunodeficiency virus-1 Tat-induced alterations of tight junction protein expression via modulation of the Ras signaling. *J. Neurosci.* 28, 7788-7796.

Zougbédé, S., Miller, F., Ravassard, P., Rebollo, A., Cicéron, L., Couraud, P.O., Mazier, D., and Moreno, A. (2011). Metabolic acidosis induced by Plasmodium falciparum intraerythrocytic stages alters blood-brain barrier integrity. *J. Cereb. Blood Flow Metab.* 31, 514-526.

Chapter IV

Contribution of a Single Host Genetic Locus to Mouse Adenovirus Type 1 Infection and Encephalitis

ABSTRACT

Susceptibility to mouse adenovirus type 1 (MAV-1) is mouse-strain dependent; susceptible mice die from hemorrhagic encephalomyelitis. The MAV-1 susceptibility quantitative trait locus *Msq1* accounts for ~40% of the phenotypic (brain viral load) variance that occurs between resistant BALB/c and susceptible SJL mice after MAV-1 infection. Using an interval-specific congenic mouse strain (C.SJL-Msq1^{SJL}), in which the SJL-derived allele *Msq1*^{SJL} is present in a BALB/c background, we demonstrate that *Msq1*^{SJL} controls the development of high brain viral titers in response to MAV-1 infection, yet does not account for the total extent of brain pathology or mortality in SJL mice. C.SJL-Msq1^{SJL} mice had disruption of the blood-brain barrier and increased brain water content after MAV-1 infection, but these effects occurred later or were not as severe, respectively, as those noted in infected SJL mice. As expected, BALB/c mice showed minimal pathology in these assays. Infection of SJL- and C.SJL-Msq1^{SJL}-derived primary mouse brain endothelial cells resulted in loss of barrier properties, whereas BALB/c-derived cells retained their barrier properties despite being equally capable of supporting MAV-1 infection. Finally, we provide evidence that organ pathology and inflammatory cell recruitment to the brain following MAV-1 infection were both

influenced by *Msq1*. These results validate *Msq1* as an important host factor in MAV-1 infection, and refine the major role of the locus in development of MAV-1 encephalitis. They further suggest that additional host factors or gene interactions are involved in the mechanism of pathogenesis in MAV-1-infected SJL mice.

IMPORTANCE

A successful viral infection requires both host and viral factors; identification of host components involved in viral replication and pathogenesis is important for development of therapeutic interventions. A genetic locus (*Msq1*) controlling mouse adenovirus type 1 (MAV-1) brain infection was previously identified. Genes in *Msq1* belong to the same family of genes associated with susceptibility to other encephalitic viruses, HIV-1 and West Nile virus. We constructed an interval-specific congenic mouse strain to examine the contribution of *Msq1* to MAV-1 susceptibility and brain morbidity. We compared infected resistant, susceptible and congenic mice regarding known MAV-1 disease manifestations in the brain (survival, viral loads, blood-brain barrier disruption, edema, mouse brain endothelial cell barrier properties, pathology and inflammatory cell recruitment) to determine the extent to which *Msq1* influences MAV-1 infection outcome. Our results showed that *Msq1* is a critical host genetic factor that controls many aspects of MAV-1 infection.

INTRODUCTION

Viruses from at least eleven different virus families can cause encephalitis (Fields et al., 2007). These include DNA viruses, RNA viruses and retroviruses. The mechanisms

of pathogenesis by encephalitic viruses are not well understood and likely multifactorial (Chaturvedi et al., 1991; Dallasta et al., 1999; Getts et al., 2008; Gralinski et al., 2009; Ivey et al., 2009; Verma et al., 2010). However, many encephalitic viral infections share certain common features, including recruitment of inflammatory cells, altered production of cytokines and chemokines, and modulation of tight junction protein and cell adhesion molecule expressions leading to blood-brain barrier (BBB) disruption (Chaturvedi et al., 1991; Dallasta et al., 1999; Getts et al., 2008; Gralinski et al., 2009; Ivey et al., 2009; Verma et al., 2010).

The BBB is composed of a specialized layer of microvascular endothelial cells joined by complex tight cell-cell junctions, a basement membrane, and the foot processes of perivascular astrocytes (Abbott et al., 2010; Coisne and Engelhardt, 2011; Hawkins and Davis, 2005). It is a highly regulated physical, transport, and biochemical interface that functions to maintain and protect normal brain activity by controlling the passage of ions, macromolecules, and other solutes from the peripheral circulation to the central nervous system (CNS). The BBB also strictly restricts infiltration of immune cells into the CNS; consequently, accumulation of leukocytes in the CNS is usually a sign of pathologic inflammatory processes.

Viral infection and inflammation of the CNS can lead to perturbations in function of the BBB, compromising its ability to exclude harmful substances and immune cells from the brain parenchyma. Changes in BBB permeability can also have significant effects on CNS tissue homeostasis, including changes in intracellular and extracellular water content that may lead to electrolyte imbalance (Klatzo, 1987). In some instances of CNS viral infection, these disruptions have devastating outcomes, including acute

neuroinflammation and neurodegeneration (Getts et al., 2008; Kanmogne et al., 2005; Lee et al., 2006; Major et al., 1992).

Human adenoviruses can infect the CNS of immunocompromised individuals who suffer from disseminated infections (Carrigan, 1997; Echavarria, 2008; Tebruegge and Curtis, 2010). However, the study of human adenovirus brain pathogenesis has been limited by the species-specificity of adenoviruses and inherent difficulties in collecting samples from ongoing human CNS infections. In contrast, mouse adenovirus type 1 (MAV-1) is a well-characterized non-human adenovirus that enables *in vivo* study of a natural encephalitic viral infection in a convenient small animal model. MAV-1 infection causes fatal hemorrhagic encephalomyelitis with BBB disruption in susceptible mouse strains (Gralinski et al., 2009; Guida et al., 1995; Kring et al., 1995). The MAV-1/mouse model enables comparison of mouse strains to identify host factors that play a role in MAV-1 infection and encephalitis. Knowledge of the role that host factors play in viral encephalitis will inform future design of therapeutic strategies. Antiviral drugs that interfere with host factors essential for viral replication are under development for several viruses. For example, inhibitors that interfere with cyclophilins are being developed to counter hepatitis C virus (HCV) infection. A cyclophilin A inhibitor, currently in Phase III studies, has potent anti-viral activity with low incidence of adverse effects (Flisiak et al., 2008). Another example of host-targeting drugs in development are CCR5 antagonists, which have been shown to be effective at decreasing HIV's entry into host cells (Gilliam et al., 2011). Thus, identifying host cell pathways that are important for viral replication is important for treatment of viral diseases.

Susceptibility to MAV-1 is mouse strain-dependent and is inherited as a dominant trait (Charles et al., 1998; Guida et al., 1995; Kring et al., 1995; Spindler et al., 2001; Welton et al., 2005); SJL mice are highly susceptible to MAV-1 infection, while BALB/c mice are resistant (Spindler et al., 2001). Using a positional cloning approach to identify host genes that contribute to MAV-1 infection and encephalitis, we identified a 0.75 Mb locus on mouse chromosome 15 that is strongly linked to brain viral loads, *mouse adenovirus type 1 susceptibility quantitative trait locus 1* (*Msq1*) (Spindler et al., 2001; Spindler et al., 2010; Welton et al., 2005). This locus contributes ~40% of the variation in brain viral loads of (BALB/c×SJL)F_1×BALB/c backcross mice and is the single most significant determinant of susceptibility between resistant BALB/c and susceptible SJL mice.

In this study, we tested the genetic contribution of *Msq1* to the outcome of MAV-1 infection using an interval-specific congenic strain. We show that *Msq1* controls MAV-1 brain infection and contributes significantly to strain susceptibility. These findings corroborate our positional cloning results identifying *Msq1* as a major genetic host factor for MAV-1 infection. We also compared BALB/c, SJL and C.SJL-Msq1^{SJL} mice, and primary mouse brain endothelial cells derived from these strains, for a number of parameters following MAV-1 infection, including BBB exclusion of small and large molecule dyes from the CNS, edema, transendothelial electrical resistance (TEER), brain pathology, and leukocyte recruitment. Our data demonstrate that *Msq1* is an important factor for a subset of physiological components of MAV-1-induced encephalitis. Additionally, differences between infected C.SJL-Msq1^{SJL} and SJL mice suggest that other host factors are involved in MAV-1-induced brain pathology.

RESULTS

Construction of the congenic mouse strain C.SJL-Msq1^{SJL}. To determine the *in vivo* contribution of *Msq1* to the outcome of MAV-1 infection, we bred a congenic mouse strain (C.SJL-Msq1^{SJL}) that contains the SJL-derived *Msq1* susceptibility locus on the BALB/c background. After 11 generations of backcrossing, >99.9% of the C.SJL-Msq1^{SJL} congenic mouse genome is of the recipient (BALB/c) genome, while the remaining <0.1% includes *Msq1^{SJL}* and other scattered loci from the donor (SJL) strain that may remain in the congenic background. Progeny homozygous for *Msq1* were used to initiate a homozygous congenic strain. Heterozygotes were also mated to produce littermates of the following genotypes: heterozygous for *Msq1* (C.SJL-Msq1$^{BALB/SJL}$), homozygous for BALB-derived *Msq1* (C.SJL-Msq1^{BALB}), and homozygous for SJL-derived *Msq1* (C.SJL-Msq1^{SJL}). Because *Msq1* is an important contributor to MAV-1-susceptibility, and susceptibility to MAV-1 is dominant, we expected both C.SJL-Msq1^{SJL} and C.SJL-Msq1$^{BALB/SJL}$ mice to be susceptible.

C.SJL-Msq1^{SJL} mice have brain viral loads comparable to those of SJL mice but increased survival rates. We performed infection experiments with the congenic mice to determine their susceptibility to MAV-1. Previous studies showed that susceptible mouse strains develop high brain viral loads at 8 days post infection (dpi) when infected at 10^2 PFU MAV-1; brain viral loads at this time point were used in our positional mapping studies to identify the *Msq1* locus (Spindler et al., 2001; Welton et al., 2005). We used the 10^2 PFU MAV-1 dose and assayed congenic mice and controls for brain virus loads 8 dpi.

MAV-1 infected C.SJL-Msq1^{SJL} mice had significantly higher brain viral titers than their C.SJL-Msq1^{BALB} littermates (Fig. 4.1A) ($P < 0.0001$). These data indicate that high viral loads seen in C.SJL-Msq1^{SJL} mice were due to the contribution of *Msq1* and not other minor scattered loci. C.SJL-Msq1^{BALB} mice had viral loads similar to resistant parental BALB/c mice. The brain viral loads of C.SJL-Msq1^{SJL} mice were comparable to those of SJL mice infected in parallel. SJL brain viral loads were consistent with levels assayed in previous experiments (Welton et al., 2005) and were also significantly higher ($P < 0.0001$) than those seen in C.SJL-Msq1^{BALB} mice. Congenic littermate mice heterozygous for *Msq1*, C.SJL-Msq1$^{BALB/SJL}$, had brain viral loads comparable to C.SJL-Msq1^{SJL} brain viral loads. This demonstrates that the *Msq1* locus acts as a dominant trait, and that a single copy of *Msq1* is sufficient to confer the brain viral load phenotype on an otherwise resistant mouse background. On the other hand, C.SJL-Msq1$^{BALB/SJL}$ brain viral loads were significantly different from SJL brain viral loads ($P = 0.0017$). Infrequently, MAV-1-infected SJL, C.SJL-Msq1^{SJL} and C.SJL-Msq1$^{BALB/SJL}$ mice had low brain viral titers. This is consistent with previous experimental results for MAV-1 infection of SJL and other MAV-1-susceptible mouse strains. Anomalous infections among these genetically uniform animals are likely due to variability in the infection process or environmental factors. Congenic mice that survived MAV-1 infection showed no clinical signs of disease, and virus was not detected in their brains at 21 dpi by capture ELISA (Fig. 4.1C).

We challenged C.SJL-Msq1^{SJL} and SJL mice with either 10^2 or 10^4 PFU to compare their survival over time (Fig. 4.1B). Survival of C.SJL-Msq1^{SJL} and SJL mice were significantly different at doses of both 10^2 and 10^4 PFU. At 10^4 PFU, all SJL mice

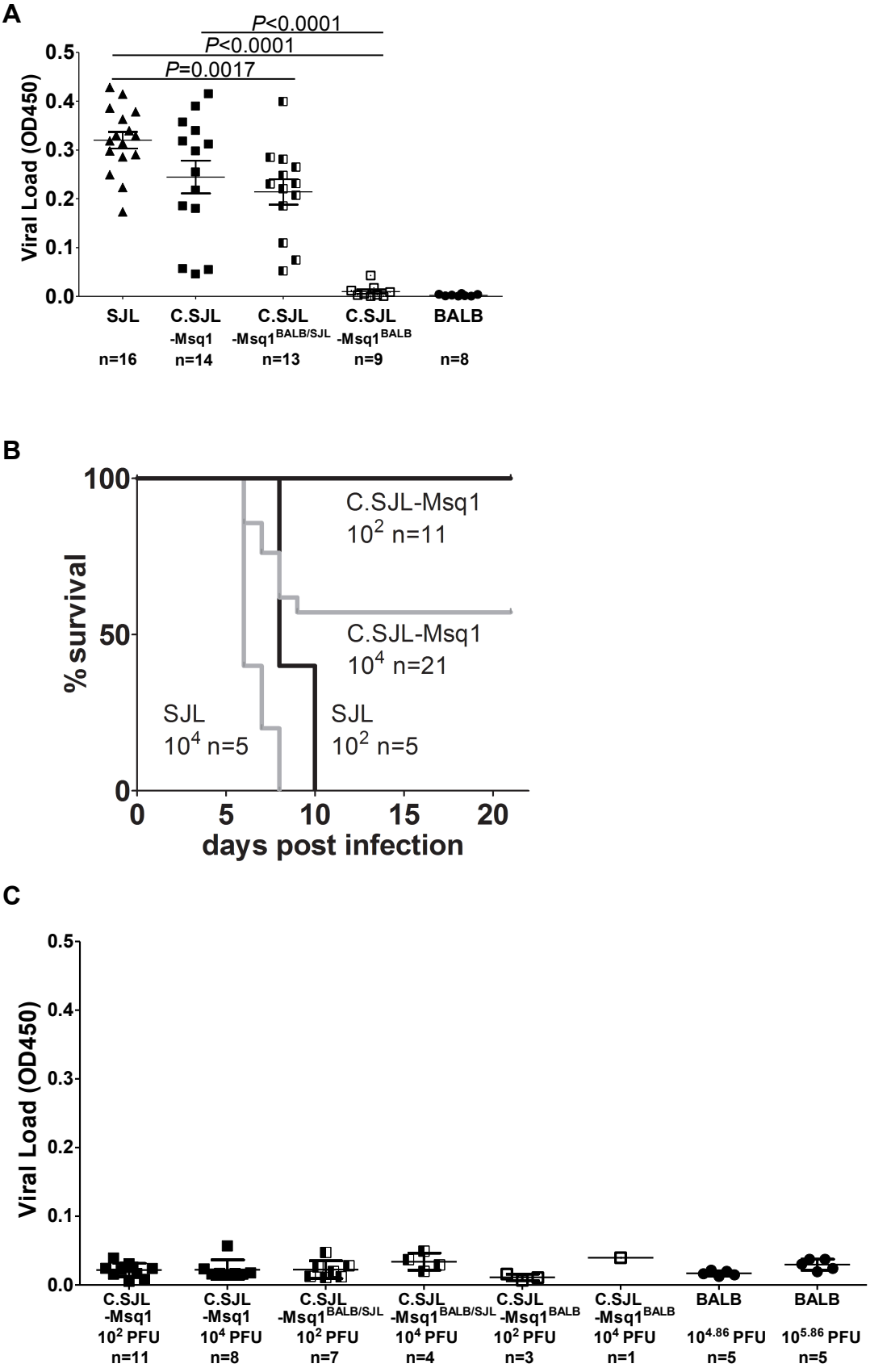
A
P<0.0001
P<0.0001
P=0.0017
Viral Load (OD450)
0.5
0.4
0.3
0.2
0.1
0.0
SJL
n=16
C.SJL -Msq1
n=14
C.SJL -Msq1BALB/SJL
n=13
C.SJL -Msq1BALB
n=9
BALB
n=8
B
100
50
0
% survival
C.SJL-Msq1
10^2 n=11
C.SJL-Msq1
10^4 n=21
SJL
10^4 n=5
SJL
10^2 n=5
0
5
10
15
20
days post infection
C
Viral Load (OD450)
0.5
0.4
0.3
0.2
0.1
0.0
C.SJL -Msq1
10^2 PFU
n=11
C.SJL -Msq1
10^4 PFU
n=8
C.SJL -Msq1BALB/SJL
10^2 PFU
n=7
C.SJL -Msq1BALB/SJL
10^4 PFU
n=4
C.SJL -Msq1BALB
10^2 PFU
n=3
C.SJL -Msq1BALB
10^4 PFU
n=1
BALB
10^4.86 PFU
n=5
BALB
10^5.86 PFU
n=5

Figure 4.1. Congenic mice are susceptible to MAV-1 infection. (A) Mice of the indicated strains were infected with 10^2 PFU MAV-1, and brains were harvested 8 dpi. Viral loads in brain homogenates were measured using capture ELISA. Each symbol represents the mean of three measurements per homogenate for an individual mouse; the number of mice is indicated below the axis. The mean and standard deviation (SD) are indicated. Statistical significance was calculated by two-tailed Mann-Whitney. OD450, optical density at 450 nm. (B) SJL and C.SJL-Msq1^{SJL} (designated C.SJL-Msq1 here and in subsequent figures) mice were infected with either 10^2 PFU or 10^4 PFU of virus. The numbers of mice in each group are indicated. For SJL mice infected at 10^2 PFU versus C.SJL-Msq1 infected at 10^2 PFU, P=0.0001; for SJL mice infected at 10^4 PFU versus C.SJL-Msq1 infected at 10^4 PFU, P=0.0022. Statistical significance for survival curves were calculated by the log-rank (Mantel-Cox) test. (C) C.SJL-Msq1^{SJL}, C.SJL-Msq1$^{BALB/SJL}$, and BALB/c mice were infected with the indicated viral doses, and brains were harvested at the end of the survival curve experiment (21 dpi). Brain viral loads were measured using capture ELISA. Each symbol represents the mean of three measurements per homogenate for an individual mouse; the number of mice is indicated below the axis. The mean and standard deviation (SD) are indicated.

died by 8 dpi, while more than half of C.SJL-Msq1^{SJL} mice survived. At 10^2 PFU, C.SJL-Msq1^{SJL} mice were resistant to MAV-1 infection up to 21 dpi, while all SJL mice died between 8 and 10 dpi.

C.SJL-Msq1 mice were then infected with MAV-1 doses ranging from 10^2 to 10^7 PFU to determine their 50% lethal dose (LD_{50}). The LD_{50} of C.SJL-Msq1^{SJL} mice was determined to be $10^{3.5}$ PFU; C.SJL-Msq1$^{BALB/SJL}$ mice, which have only a single copy of *Msq1*^{SJL}, had an LD_{50} of $10^{5.6}$ PFU. The time of death was dose-dependent for both strains of mice. C.SJL-Msq1^{SJL} and C.SJL-Msq1$^{BALB/SJL}$ mice given 10^7 PFU died by 3 to 4 dpi, while those that succumbed to lower doses died later, by 9 dpi. All of the C.SJL-Msq1^{SJL} mice and 7 of 8 C.SJL-Msq1$^{BALB/SJL}$ mice survived MAV-1 infection at the lowest dose tested (10^2 PFU). Congenic mice that survived MAV-1 infection showed no clinical signs of disease, and virus was not detected in their brains at 21 dpi by capture ELISA (Fig. 4.1C).

BALB/c mice were previously assayed to have an LD_{50} value of $>10^{4.4}$ PFU; we hypothesized that the actual LD_{50} value is likely higher; $10^{4.4}$ PFU was the maximum dose achievable at the time of the study (Spindler et al., 2001). In order to accurately determine the LD_{50} of BALB/c mice, we infected them with MAV-1 doses that exceed $10^{4.4}$ PFU (i.e., up to $10^{6.9}$ PFU). The LD_{50} of BALB/c was calculated to be $10^{6.4}$ PFU. With this new calculation of the BALB/c LD_{50}, we determined that the LD_{50} for C.SJL-Msq1^{SJL} mice was ~3 log units lower than that of BALB/c mice. These results confirm that *Msq1* is a major genetic determinant of brain viral loads and also of host susceptibility to MAV-1.

Increased BBB permeability in SJL and C.SJL-Msq1^{SJL} infected mice. MAV-1 causes encephalitis in susceptible mouse strains (Charles et al., 1998; Guida et al., 1995; Kring et al., 1995; Spindler et al., 2001). MAV-1 infection results in dose-dependent encephalomyelitis and breakdown of the BBB in susceptible C57BL/6 mice (Gralinski et al., 2009; Guida et al., 1995). Similarly, SJL mice infected with 10^2 PFU of virus at 8 dpi also show changes to the endothelial cell vasculature, including mild perivascular edema and inflammatory cell infiltration (Spindler et al., 2001). In addition, positive endothelial cell staining in both SJL and C3H/HeJ mice is seen using *in situ* hybridization with a MAV-1 early region 3 riboprobe (Spindler et al., 2001), indicating that MAV-1 replicates in the vascular endothelium of both susceptible and resistant mice. However, high brain viral loads and brain pathology following MAV-1 infection are seen only in susceptible mouse strains. We investigated the role of *Msq1* in MAV-1-induced BBB pathology since the locus contributes significantly to the brain viral load phenotype.

We infected BALB/c, C.SJL-Msq1^{BALB}, SJL, and C.SJL-Msq1^{SJL} mice to examine whether there was evidence of increased BBB permeability. BALB/c mice were included in this study to act as a negative control; these mice are resistant to MAV-1-induced encephalitis and BBB disruption (Guida et al., 1995). Sodium fluorescein was used as a small tracer molecule to probe the integrity of the BBB in SJL and C.SJL-Msq1^{SJL} mice after MAV-1 infection (Gralinski et al., 2009). A functional BBB would restrict entry of small molecules into the brain parenchyma, while a compromised BBB would result in sodium fluorescein dye leakage into the CNS.

Increased BBB permeability was seen in MAV-1-infected SJL and C.SJL-Msq1^{SJL} mice, but not infected BALB/c or C.SJL-Msq1^{BALB} mice at 6 dpi

(Fig. 4.2). The brains of infected SJL mice had a 3.9 (± 2.5)-fold increase over mock in the amount of brain sodium fluorescein, while infected C.SJL-Msq1^{SJL} mouse brains had a 2.7 (± 1.6)-fold increase over mock-infected mice. At that time point, the difference between SJL and C.SJL-Msq1^{SJL} mice was not significant (P = 0.17). The increase in BBB permeability was significantly higher in infected SJL and C.SJL-Msq1^{SJL} mice than in infected BALB/c mice and C.SJL-Msq1^{BALB} mice. Neither BALB/c nor C.SJL-Msq1^{BALB} infected littermate mice had increased BBB permeability that could be detected by this assay. These data corroborate prior studies that showed degenerative vascular changes and increased permeability in susceptible mice (Gralinski et al., 2009; Guida et al., 1995; Spindler et al., 2001).

BBB disruption is delayed in C.SJL-Msq1^{SJL} mice compared to SJL mice. To investigate when BBB disruption begins following MAV-1 infection and whether strain differences in timing and/or severity exist, we measured BBB permeability at 1-day intervals after infection. Brain viral loads of these mice were also measured in parallel. In the time course studies, Evans blue, which is a larger molecule compared to sodium fluorescein (M_r = 961 and 376, respectively), was used to evaluate the permeability of BBB to macromolecules (Patterson et al., 1992). In addition to its higher molecular weight, Evans blue has a high affinity for albumin in the serum and forms large dye-albumin complexes, which under normal circumstances would be excluded from the CNS (Rawson, 1943). Accordingly, the presence of Evans blue dye in the brain indicates substantial BBB disruption and is a better indicator of damage that could have biological relevance.

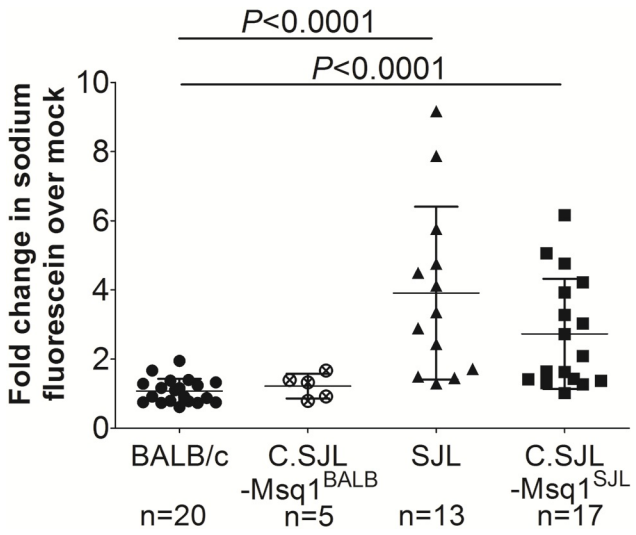

Figure 4.2. Increased BBB permeability seen in SJL and C.SJL-Msq1^{SJL} mice. BALB/c, C.SJL-Msq1^{BALB}, SJL, and C.SJL-Msq1^{SJL} mice were either mock infected or infected with 10^4 PFU of MAV-1, and brains were harvested 6 dpi. Sodium fluorescein in the brains and serum were measured in duplicate; the average amount of brain sodium fluorescein was normalized to average levels in serum for each mouse. After normalization, the amount of sodium fluorescein in brains of infected mice of the appropriate strain was determined and is represented as a ratio to the amount of dye in mock-infected brains. Each data point represents an individual mouse; numbers of mice in each group are indicated below the respective samples. For SJL versus C.SJL-Msq1^{BALB} mice, P=0.008; for C.SJL-Msq1^{SJL} versus C.SJL-Msq1^{BALB}, P=0.034. Means and SDs are indicated. Statistical significance was calculated by one-way analysis of variance (ANOVA) (Kruskal-Wallis) with Dunn's multiple comparison test.

We did not detect increased high viral loads or BBB permeability with Evans blue following MAV-1 infection in BALB/c mice from 3 to 6 dpi (Fig. 4.3). These results are consistent with our previous data using sodium fluorescein to measure BBB permeability (Fig. 4.2). Virus was detectable in SJL mouse brains at 3 dpi (Fig. 4.3A), and SJL mice had progressive BBB disruption beginning at 4 dpi (Fig. 4.3B); BBB permeability was significantly different between BALB/c and SJL mice by 4 dpi. In contrast, BBB disruption was seen one day later, at 5 dpi in infected C.SJL-Msq1^{SJL} mice. We do not show data for 6 dpi using this assay because when we attempted to measure BBB permeability in SJL mice at this time, 9 out of 10 SJL mice died or had to be euthanized following Evans blue injection. The deaths of these mice were not surprising given our survival data and previous findings (Fig. 4.1B, (Spindler et al., 2001)).

Despite the 1-day delay between SJL and C.SJL-Msq1^{SJL} mouse BBB results, the levels of BBB disruption reached were similar. The levels of increased BBB permeability seen in SJL mice (1.2 fold increase) at 4 dpi and C.SJL-Msq1^{SJL} mice at 5 dpi (1.7 fold increase) were not significantly different, nor was the difference between the levels of increased BBB permeability seen in SJL (1.7 fold increase) and C.SJL-Msq1^{SJL} mice at 5 dpi significant. These results indicate that this pathological change (BBB permeability to large macromolecules) is in part controlled by *Msq1* following MAV-1 infection.

Edema seen in MAV-1 infected SJL and C.SJL-Msq1^{SJL} mice. Significant alterations in vascular permeability can lead to cerebral edema. Edema occurs when there is an increase in brain water content due to accumulation of intracellular or extracellular fluid, leading to an increase in brain volume (Kempski, 2001; Klatzo, 1987). The healthy BBB strictly limits exchange of fluid between brain tissues and blood, providing an

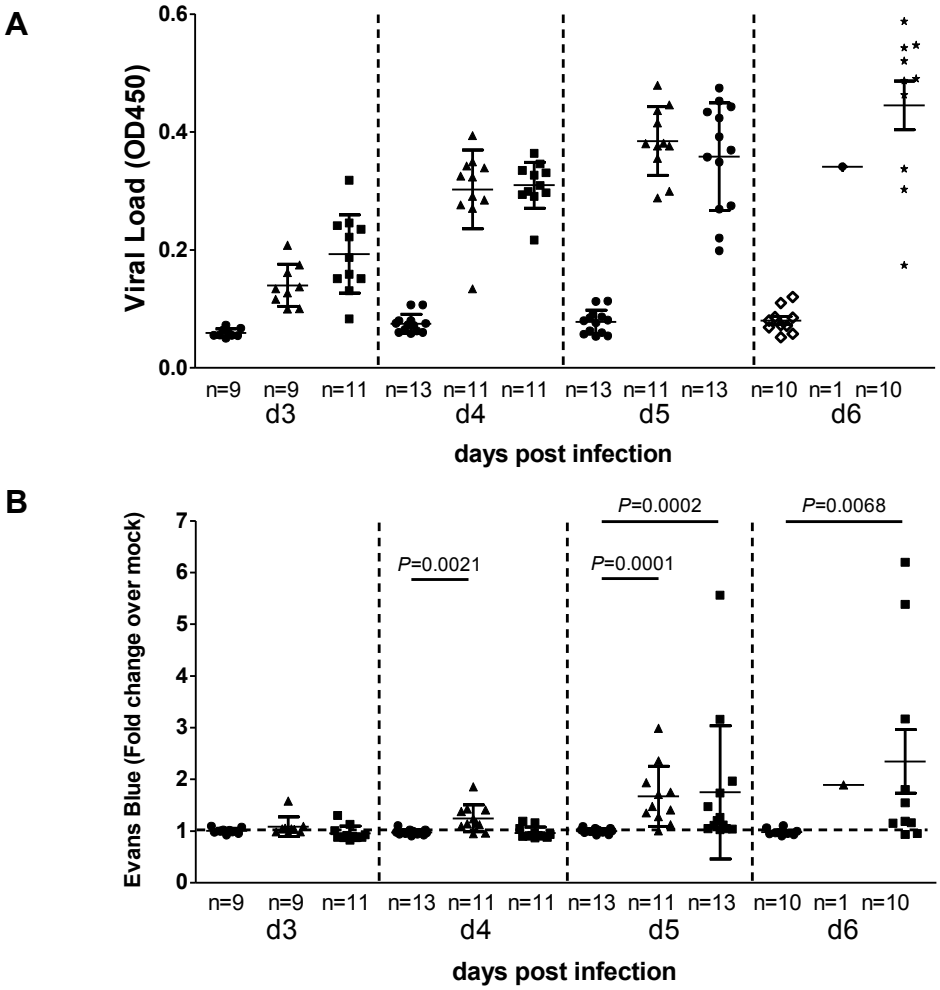

Figure 4.3. Onset of BBB disruption is delayed in C.SJL-Msq1^{SJL} mice. Mice were either mock infected or MAV-1 infected at 10^4 PFU and assayed for BBB disruption using Evans blue dye at 3, 4, 5 and 6 dpi. (A) Viral loads of individual infected mouse brains were measured by capture ELISA. Each symbol represents the mean of three measurements per homogenate. (B) The amount of Evans blue dye in infected mouse brains is represented as a ratio to the amount of dye found in mock-infected brains for each individual strain. Each symbol represents the average of duplicate measurements for an individual mouse; numbers of mice in each group are indicated. Means and SDs are indicated. Statistical significance was calculated by a two-tailed Mann-Whitney test.

optimal homeostatic environment for the brain. However, this regulation can be disrupted due to BBB damage during pathological conditions such as viral CNS infections. Since increased BBB permeability was seen in susceptible mice but not resistant mice, it is possible that the development of cerebral edema could contribute to differences in strain susceptibility. We tested whether the delay in onset of increased BBB permeability in C.SJL-Msq1^{SJL} mice compared to SJL mice resulted in reduced edema, thus helping to explain the observed susceptibility difference.

The brains of both SJL and C.SJL-Msq1^{SJL} mice infected with MAV-1 had significantly increased percentages of water content compared to mock-infected brains at 8 dpi, whereas infected BALB/c brains had no measurable change in water content (Fig. 4.4A). However, the increase in water content was significantly greater in SJL mice than C.SJL-Msq1^{SJL} mice. We also measured Na^+ and K^+ ion contents of these brains. Alteration of the levels and ratios of these major brain cations can be an important indicator of edema. In particular, leakage of high-sodium, low-potassium plasma contents into the brain following damage to the vasculature is commonly associated with vascular edema (Klatzo, 1987).

We observed significantly higher brain sodium levels in infected than mock-infected SJL mice (Fig. 4.4B, $P = 0.0004$). Conversely, no significant difference in sodium was measured for either C.SJL-Msq1^{SJL} or BALB/c mice upon infection. Potassium levels were essentially unchanged for all tested strains (Fig. 4.4C). These data are consistent with development of vascular edema following MAV-1 infection for SJL mice but not C.SJL-Msq1^{SJL} or BALB/c mice.

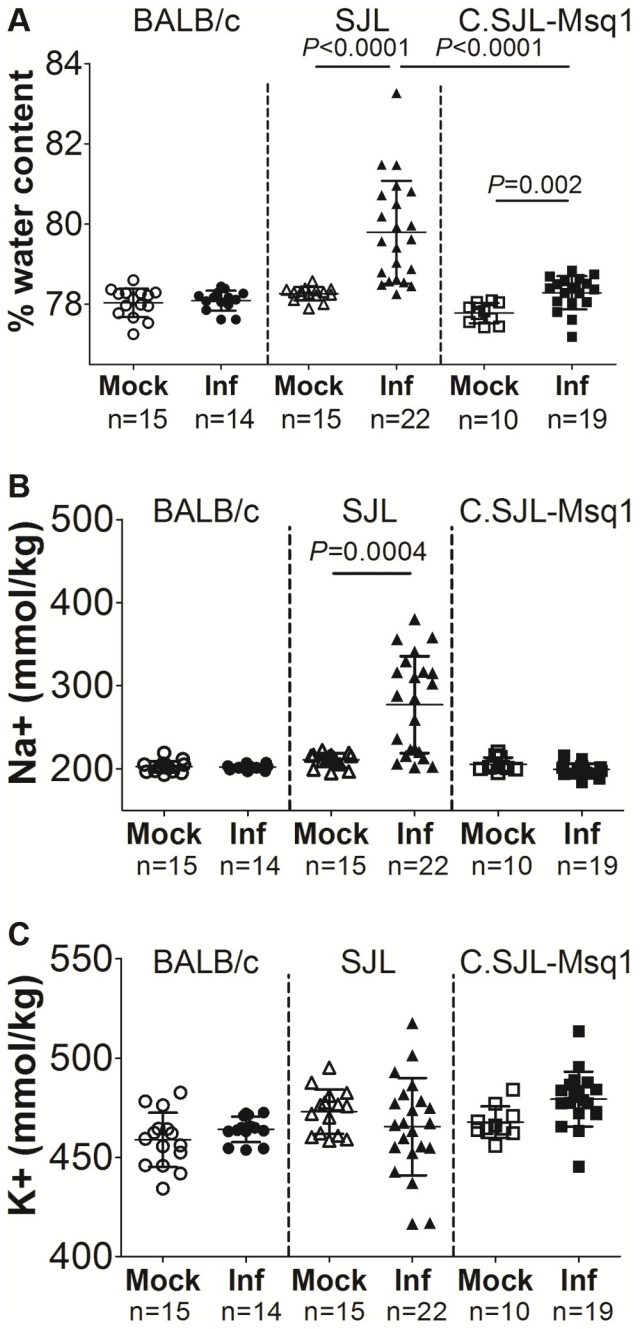

Figure 4.4. Edema in MAV-1 infected mouse strains. Mice of the indicated strains were either mock infected or MAV-1 infected (Inf) with 10^4 PFU MAV-1 and assayed 6 dpi. (A) Brain weights were determined prior to and after dehydration. Percentage water content was calculated as described in Materials and Methods. (B and C) Ion contents from the same brains shown in (A) were measured by flame photometry. Ion contents were then normalized to individual mouse brain weights. Each symbol is from a single mouse. Numbers of mice, means and SDs are indicated. Statistical significance was calculated by a two-tailed Mann-Whitney test.

MAV-1 infection of C.SJL-Msq1^{SJL}- and SJL-derived primary mouse brain endothelial cells (pmBECs) results in loss of barrier properties. Endothelial cells and the tight junctions they form are critical for BBB function (Abbott et al., 2010). MAV-1 infects endothelial cells (Guida et al., 1995; Kajon et al., 1998), and MAV-1 infection decreases barrier properties of C57BL/6 pmBECs by altering tight junction protein expression (Gralinski et al., 2009). To determine whether brain endothelial cells from resistant and susceptible mouse strains respond differently to MAV-1 infection, pmBECs were prepared from BALB/c, SJL and C.SJL-Msq1^{SJL} mice and cultured on transwells, allowed to form tight junctions, and infected with MAV-1. We used TEER values as a measure of tight junction integrity in the pmBECs; a monolayer of pmBECs with intact tight junctions has high TEER, while a compromised barrier has decreased TEER (Gaillard et al., 2001).

pmBECs from all tested strains were able to establish equally high TEER levels. By 2 dpi, there was a drop in TEER in both infected SJL- or C.SJL-Msq1-derived pmBECs (Fig. 4.5B, C). Infected BALB/c-derived pmBECs did not have a drop in TEER, indicating that tight junctions in the BALB/c wells remained intact up to 3 dpi (Fig. 4.5A). Mock-infected pmBECs derived from all the different strains maintained their TEER levels up to 3 dpi.

Increased MAV-1-associated pathology is not due to a difference in ability of virus to replicate in cells of different mouse strains. To determine whether the difference in abilities of pmBECs to maintain TEER was due to a difference in ability of

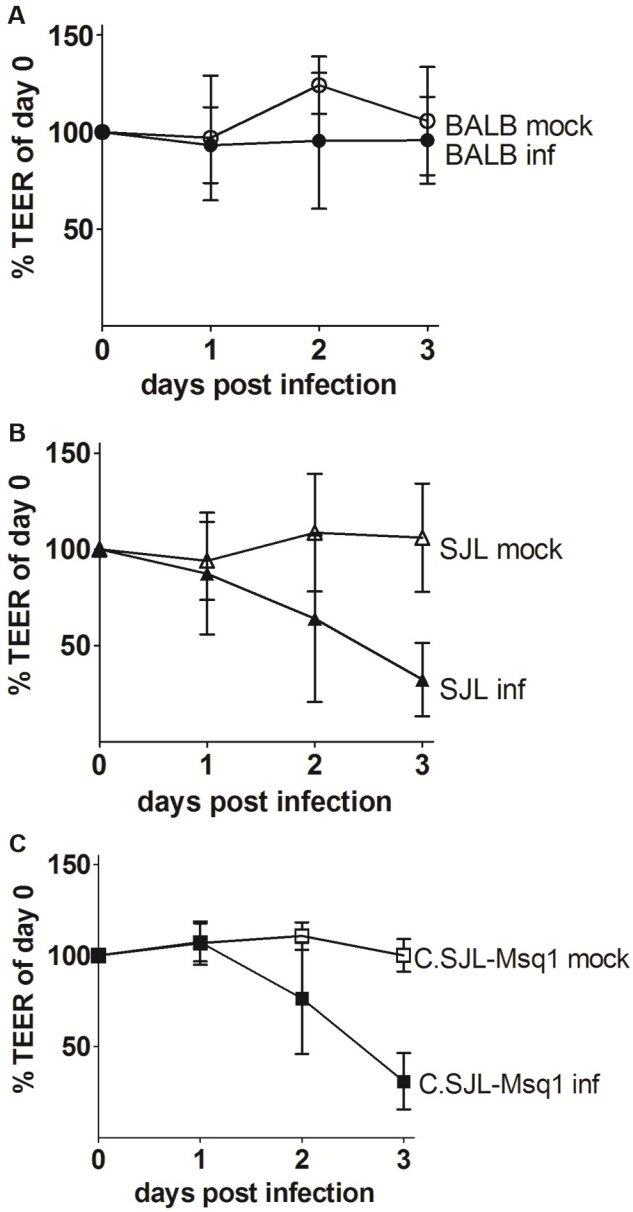

Figure 4.5. SJL- and C.SJL-Msq1-derived pmBECs lose BBB properties after MAV-1 infection. pmBECs from (A) BALB, (B) SJL or (C) C.SJL-Msq1 mice were isolated, grown to confluence and infected with MAV-1 at an MOI 5. TEER measured on the day of infection was normalized to 100%. After infection, measurements were taken at 24 h intervals in each sample well. Means and SDs at each time point are shown. Data for each graph are combined from 3 independent experiments.

the virus to grow in endothelial cells from different mouse strains, we isolated pmBECs and tested their capabilities to support MAV-1 growth. Differences in viral growth would suggest that there are strain differences at the cellular level in ability to support MAV-1 infection, such as expression levels of virus receptors or host factors involved in viral replication. MAV-1 replicated to similar levels in C.SJL-Msq1^{SJL}-, SJL- and BALB/c-derived pmBECs (Fig. 4.6). This suggests that cell-autonomous differences between strains in the ability to support replication do not account for the differences in susceptibility. These results are consistent with previous data suggesting that strain differences in susceptibility to MAV-1 are systemic (e.g., at the level of the tissue) rather than cellular (Spindler et al., 2001).

SJL brain lesions are more severe than in C.SJL-Msq1^{SJL} mice. We examined the pathology of MAV-1 infection in BALB/c, SJL and C.SJL-Msq1^{SJL} mice to investigate whether strain differences could be seen in the distribution or severity of lesions in different organs. We observed no significant lesions in BALB/c mice for any of the organs analyzed. The majority of lesions found in SJL and C.SJL-Msq1^{SJL} infected mice were in the brain. SJL and C.SJL-Msq1^{SJL} infected mice had similar brain lesions, consisting of lymphoid meningitis, vasculitis, scattered microhemorrhages and perivascular edema, which mostly affected the cerebellum. Molecular and granular layer capillaries were surrounded by scattered red blood cells and infrequent small numbers of neutrophils and mononuclear cells.

Although the types of lesions were similar, the extents and distributions of pathology seen in the brains of SJL mice were more severe than those seen in

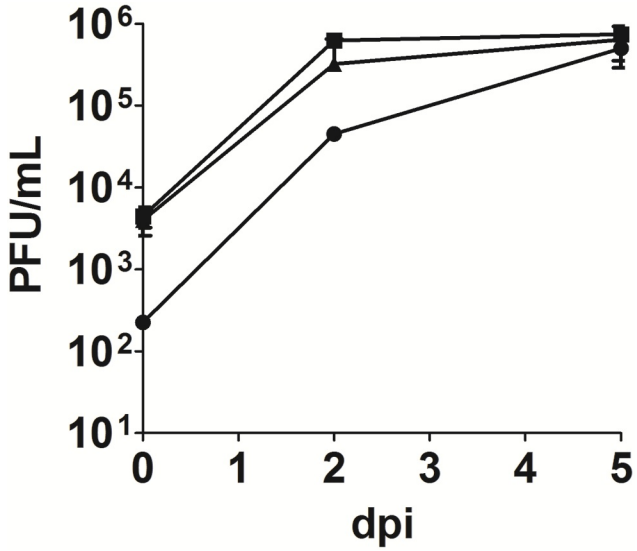

Figure 4.6. Growth curves of MAV-1 in SJL-, C.SJL-Msq1- and BALB/c-derived pmBECs. pmBECs from SJL, C.SJL-Msq1 or BALB/c mice were isolated and infected at a MOI 5. Cells were harvested at 0, 2 and 5 dpi and assayed for viral titers. Data are combined from at least 2 experiments. Virus yields were determined by plaque assays performed in triplicate. Means and SDs are shown.

C.SJL-Msq1^{SJL} mice (Fig. 4.7A). Only 2 of 5 infected SJL mice survived to 6 dpi. Both surviving mice had perivascular hemorrhages and edema. In one mouse, the vascular lesions were centered primarily in the cerebellum and brain stem. In the other, the vascular lesions were present throughout the brain. In contrast, 5 of 5 infected C.SJL-Msq1^{SJL} mice survived, and 3 of 5 had only mild lymphoid meningitis. The fourth mouse had multifocal vasculitis and microhemorrhages in all brain regions, and another had vasculitis with microhemorrhages in the cerebellum and brain stem. When brains were scored, SJL brains showed more severe signs of disease than C.SJL-Msq1^{SJL} brains. Because the number of mice per group used in these studies was low, we did not determine statistical significance.

Increased inflammatory cell recruitment to brains of SJL- and C.SJL-Msq1^{SJL}-infected mice. We used flow cytometry to identify and quantify immune cells whose recruitment to the brain in response to MAV-1 infection is directly or indirectly affected by the presence of *Msq1*. After MAV-1 infection, there was a large increase in the number of infiltrating leukocytes (CD45$^{(hi)}$) in SJL and C.SJL-Msq1^{SJL} mice, and low recruitment in BALB/c mice (Fig. 4.8). We further characterized the CD45$^{(hi)}$ cell population for cell-type-specific markers. There was an obvious increase in the total number of T cells (CD3^{+}), and both CD4^{+} (CD3^{+}, CD4^{+}) and CD8^{+} (CD3^{+}, CD8^{+}) T cells recruited to the brain of SJL mice following MAV-1 infection. There were also increases in the CD3^{+}, CD4^{+} and CD8^{+} T cell populations in infected C.SJL-Msq1^{SJL} mice and BALB/c mice, but to lesser extents. The same was true for neutrophils (CD11b^{+}, LY6G^{+}) and inflammatory monocytes (CD11b^{+}, LY6C$^{(hi)}$). However, for macrophages (F4/80^{+}),

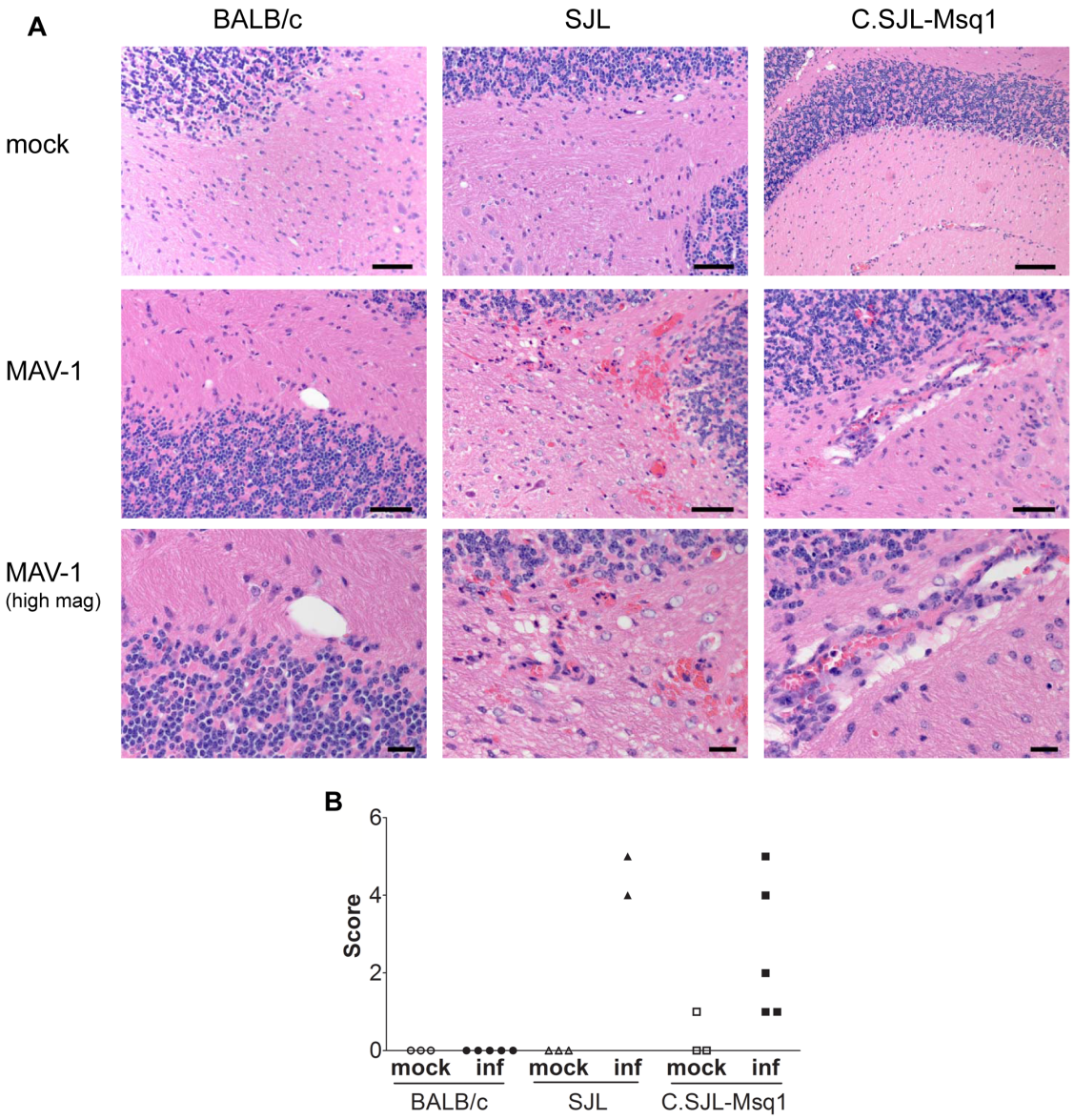

Figure 4.7. Increased pathology in brains of C.SJL-Msq1^{SJL} and SJL mice after MAV-1 infection. (A) Cerebellum sections from BALB/c, SJL and C.SJL-Msq1 mice infected with 10^4 PFU of virus at 6 dpi were stained with hematoxylin and eosin. Top panel, cerebellum from mock infected BALB, SJL and C.SJL-Msq1. Bars, 100 μm. Middle panel, cerebellum from virus infected BALB, SJL and C.SJL-Msq1. Bars, 50 μm. Bottom panel, high magnification of MAV-1-infected BALB, SJL and C.SJL-Msq1 showing vasculitis in the latter two images. Bars, 20 μm. (B) Histological changes were assigned scores and then totaled. Presence of vasculitis, microhemorrhages, perivascular edema, focal lesions, and meningeal lymphoid infiltrates each received a score of 1. Multifocal lesions received a score of 2. Each symbol represents the score of a single mouse. There were 5 mice per infected group, but 3 SJL mice died prior to analysis. Due to the small sample size, we did not determine whether differences between groups were statistically significant.

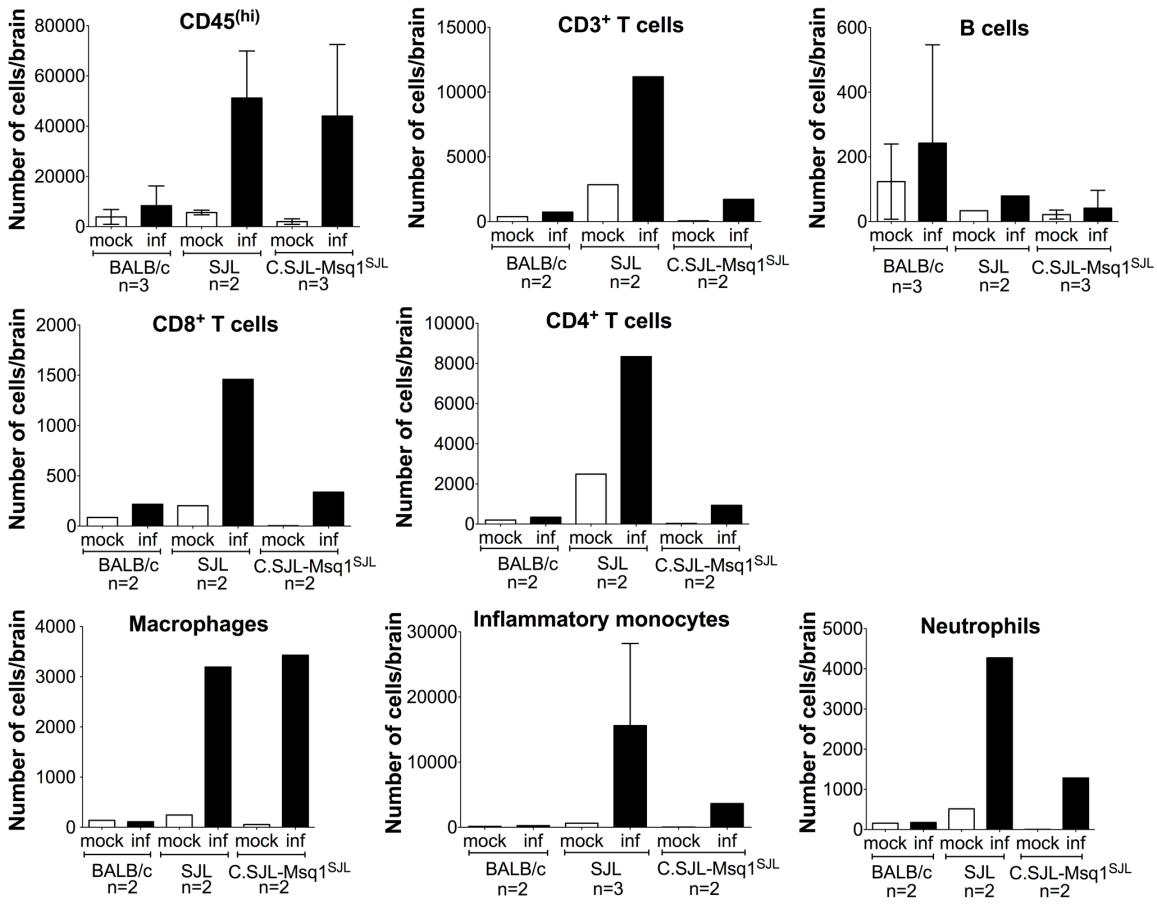

Figure 4.8. Increased inflammatory cell recruitment to brains of C.SJL-Msq1^{SJL} and SJL mice after MAV-1 infection. Mice from the indicated strains were infected with 10^2 PFU MAV-1, and mice were euthanized 8 dpi. Cells isolated from brains were isolated and pooled from either mock-infected or MAV-1 infected mice and stained with relevant antibodies. The numbers of experiments for each group are indicated on the graphs. For the CD45$^{(hi)}$ population, the numbers of cells were determined independently in at least 2 separate tubes per experiment.

the increased recruitment of cells following MAV-1 infection was similar between SJL and C.SJL-Msq1^{SJL} mice. No increase was seen in macrophage recruitment in brains of infected versus mock-infected BALB/c mice. No change in the numbers of brain B cells (major histocompatiability complex [MHC] class II^{+}, CD19^{+}) was seen for any of the mouse strains after MAV-1 infection.

DISCUSSION

We demonstrate here that *Msq1* is a major genetic determinant of susceptibility to MAV-1, confirming the localization of the quantitative trait locus. Not only do C.SJL-Msq1^{SJL} mice develop high brain viral loads after MAV-1 infection, but also the presence of *Msq1* alone on a resistant strain background is sufficient to confer a ~3 log unit decrease in LD_{50} compared to the parental BALB/c strain. However, *Msq1* does not account for the entire difference in susceptibility between the two strains, since the LD_{50}s for SJL and C.SJL-Msq1^{SJL} mice are different. This is consistent with previous results from genetic mapping studies, from which it was calculated that *Msq1* contributes to ~40% of the phenotypic variation between BALB/c and SJL mice (Welton et al., 2005). The data indicate that susceptibility to MAV-1 is a polygenic trait; there are additional quantitative trait loci for susceptibility that were identified in the mapping study. It is likely that a combination of genetic and environmental factors is needed to deliver the full susceptibility phenotype of SJL mice.

We observed that SJL and C.SJL-Msq1^{SJL} mice differ significantly in susceptibility (survival and LD_{50}), despite detection of similar levels of brain viral loads in the two strains. In previous studies, death and low LD_{50} values correlated well with

high viral loads in the brain for a number of mouse strains, making viral loads a good predictor of susceptibility (Spindler et al., 2001; Spindler et al., 2010; Welton et al., 2005). Strains with low LD_{50} values have high brain viral loads after 8 dpi with 10^2 PFU MAV-1; strains with high LD_{50} values have low brain viral loads. Mice that displayed signs of disease (including ruffled fur, lethargy, squinty eyes, hunched posture, and seizures), or those that were discovered dead also had high brain titers of MAV-1. Therefore, in our identification of *Msq1*, we used brain viral loads as a quantifiable measure of susceptibility (Spindler et al., 2010; Welton et al., 2005), because it is not possible to use LD_{50} assays to determine individual mouse susceptibility. Our data demonstrate that high brain viral titers are not sufficient to cause death. Thus it is likely that other host factors contribute to mortality. It is also possible that the capture enzyme-linked immunosorbent assay (ELISA) method used is not sensitive enough to distinguish modest differences in viral loads between SJL and C.SJL-$Msq1^{SJL}$ infected mouse brains that are crucial in determining survival. These possibilities are not mutually exclusive.

MAV-1 infection of susceptible C57BL/6 mice results in BBB disruption (Gralinski et al., 2009), and we found here that BBB permeability also occurred in infection of two other susceptible mouse strains, SJL and 129SvEv/S6 (Ashley and Spindler, unpublished data), but not in BALB/c mice. *Msq1* contributed critically to the breakdown of the BBB in the susceptible strains. BBB disruption in C.SJL-$Msq1^{SJL}$ mice as assayed by sodium fluorescein was similar to that seen in SJL mice at the peak of infection, either 6 dpi at 10^4 PFU or 8 dpi at 10^2 PFU (Fig. 4.9). Strain differences regarding the timing of the onset of BBB permeability to macromolecules were detected through time course experiments using Evans blue. We attempted to measure BBB

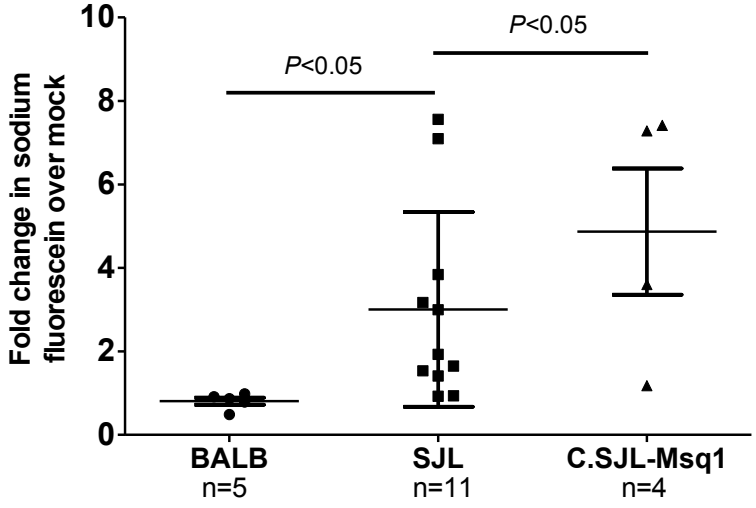

Figure 4.9. Increased BBB permeability seen in SJL and C.SJL-Msq1^{SJL} mice at 10^2 PFU. BALB/c, SJL, and C.SJL-Msq1^{SJL} mice were either mock infected or infected with 10^2 PFU of MAV-1, and brains were harvested 8 dpi. Sodium fluorescein in the brains and serum were measured in duplicate; the average amount of brain sodium fluorescein was normalized to average levels in serum for each mouse. After normalization, the amount of sodium fluorescein in brains of infected mice of the appropriate strain was determined and is represented as a ratio to the amount of dye in mock-infected brains. Each data point represents an individual mouse; numbers of mice in each group are indicated below the respective samples. Means and SDs are indicated. Statistical significance was calculated by one-way analysis of variance (ANOVA) (Kruskal-Wallis) with Dunn's multiple comparison test.

disruption using Evans blue at peak viral infection; however, at 6 dpi, 9 out of 10 SJL mice died or had to be euthanized after being injected with Evans blue. For both SJL and C.SJL-Msq1^{SJL} mice, there was a wide range of dye permeability and viral loads in response to MAV-1 infection. Phenotypic variability is also seen in other mouse models of virus-induced BBB damage (Matullo et al., 2010; Morrey et al., 2008) and may result from variability in biological response due to environmental causes. Comparable high levels of brain viral loads and BBB breakdown were seen in SJL and C.SJL-Msq1^{SJL} mice, and yet there were differences in MAV-1-induced mortality and edema between the strains. The correlation we see between brain viral loads and BBB disruption is consistent with previous published observations (Gralinski et al., 2009). However, there is not a clear connection of BBB disruption or viral loads with mortality.

It is possible that mortality following MAV-1 infection is associated with development of cerebral edema as a consequence of BBB disruption, since cerebral edema was observed in histopathological assessments of MAV-1-infected brains (Guida et al., 1995; Spindler et al., 2001). For another virus, lymphocytic choriomeningitis virus, data suggest that mortality in mice is caused by edema and ventricular failure rather than BBB damage (Matullo et al., 2010). We found evidence of vasogenic edema in the brains of MAV-1-infected SJL mice, but only a modest increase in brain water content of C.SJL-Msq1^{SJL} mice. Our observations also suggest that mice that are sicker have more severe edema; edema appeared to develop close to the time of death for SJL mice (Figs. 4.1B and 4.4). These results are significant, because SJL and C.SJL-Msq1^{SJL} had similar brain viral loads and BBB permeability at the time of assay. These data suggest that viral loads and the extent of BBB permeability at 6 dpi are insufficient in

C.SJL-Msq1^{SJL} mice to trigger the more severe increase in brain water content in SJL mice and that additional host factors outside the *Msq1* locus contribute to the development of vasogenic edema in SJL mice during MAV-1 infection. The data support the hypothesis that vasogenic edema correlates with mortality following MAV-1 infection.

MAV-1 infects endothelial cells, which are important structural components of the BBB (Charles et al., 1998; Spindler et al., 2001). We observed a loss of endothelial cell barrier integrity upon MAV-1 infection, as demonstrated by a drop in TEER in infected SJL- and C.SJL-Msq1-derived pmBECs. Loss of TEER during MAV-1 infection correlates with reduced tight junction protein mRNA and protein expression in pmBECs (Gralinski et al., 2009). *Msq1* includes 14 members of the *Ly6* gene-family (Spindler et al., 2010), which may play a role in MAV-1 BBB pathogenesis at the level of barrier structure. In *Drosophila*, members of the Ly6/CD49 family, Coiled and Boudin, mediate cell-cell adhesion by controlling structural organization of septate junction proteins in the BBB and the trachea, respectively (Hijazi et al., 2009). It is possible that MAV-1 causes a reorganization of tight junction proteins in C57BL/6-, SJL- and C.SJL-Msq1^{SJL}-derived pmBECs, leading to increased barrier permeability (Gralinski et al., 2009). The observed decrease in TEER in SJL- and C.SJL-Msq1-derived pmBECs upon infection is consistent with increases we observed in BBB permeability *in vivo*, but does not correlate with the marked alterations in vasogenic edema that we noted only in SJL mice. Identification of genetic loci that control vasogenic edema in MAV-1 infections and the molecular processes involved will require additional experiments and backcrosses.

Ly6 gene products are cell surface proteins, which makes them potential candidate viral receptors. We observed differences in the expression levels of two of three LY6 proteins that we examined on pmBECs from BALB/c and SJL mice (Fig. 4.10). Such expression variation might lead to differences in ability to support viral infection.

However, results from infecting endothelial cells *ex vivo* suggest that differences in susceptibility to MAV-1 seen *in vivo* are not attributable to LY6 protein expression in endothelial cells. Viral yields were similar between pmBECs derived from SJL, C.SJL-Msq1^{SJL}, and BALB/c mice. This is consistent with infection data of other cell types; MAV-1 infection of mouse embryonic fibroblasts and primary bone marrow macrophages (another target of MAV-1 infection *in vivo*) derived from resistant (C3H/HeJ) and susceptible (SJL) mouse strains also yield equivalent amounts of virus (Spindler et al., 2001). We cannot, however, rule out strain-specific differences in additional cell types we have not tested.

The difference in strain susceptibility to MAV-1 *in vivo* was not reflected in the ability of pmBECs to support virus growth *ex vivo*, leading us to investigate strain differences at the systemic level. We did not find differences between SJL and C.SJL-Msq1^{SJL} mice in the distribution of lesions in organs we collected, and in both strains of mice, the majority of lesions were found in the brain. In comparison, in infected BALB/c mice, no significant lesions were found in any of the organs collected. These data suggest that *Msq1* is responsible for the development and organ localization of MAV-1 pathology. However, we observed that the pathology found in the infected SJL brains was more severe than that found in C.SJL-Msq1^{SJL} brains, suggesting that other host factors likely contribute to the severity of MAV-1 brain pathology.

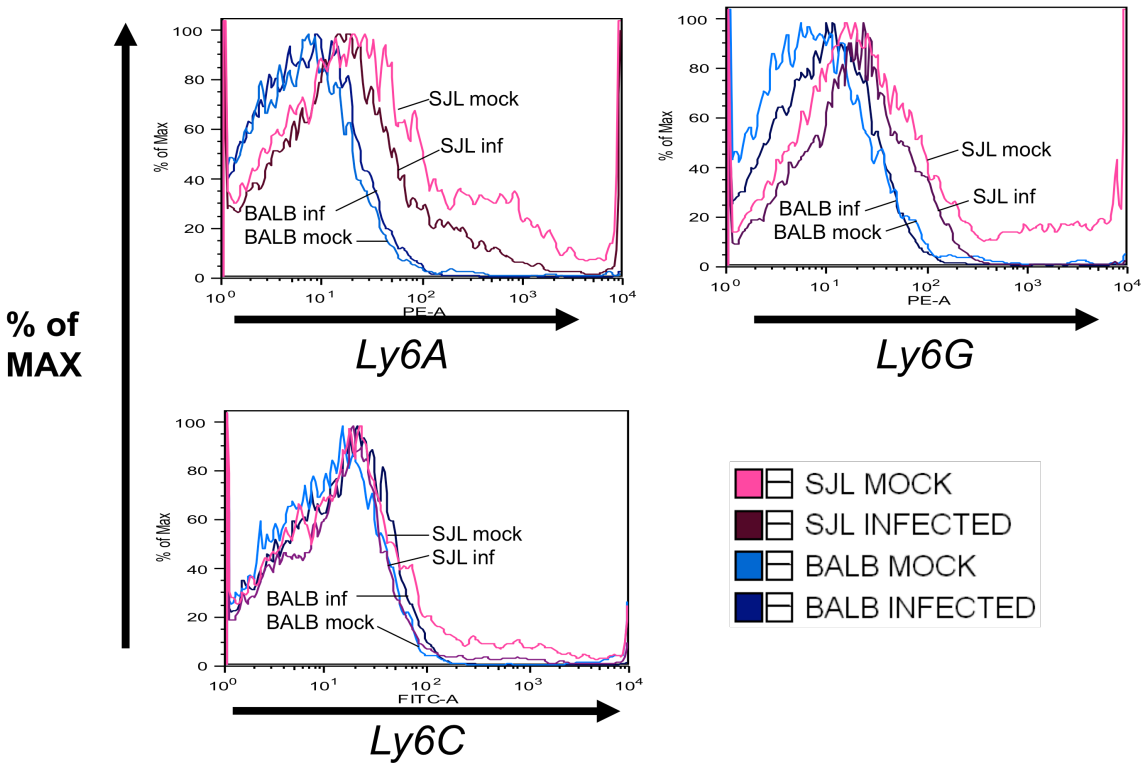

Figure 4.10. Higher *Ly6A* and *Ly6G* expression levels on SJL pmBECs. pmBECs from SJL and BALB/c mice were isolated and either mock infected or infected at a MOI of 5. Cells were harvested at 2 dpi and stained with the relevant antibodies. Ly6G (PE, clone 1A8), Ly6A/E (PE, clone D7), and Ly6C (FITC, clone AL21). Data are from one experiment.

Our studies revealed that SJL and C.SJL-Msq1^{SJL} mice had large increases in the numbers of infiltrating cells, whereas BALB/c mice had a comparatively smaller infiltrate of cells. LY6 proteins have known and putative immune functions; therefore it is likely that *Msq1* is involved in immune cell recruitment to the brain. LY6A and LY6C proteins affect lymphocyte development, activation, adhesion and homing (Bamezai et al., 1995; Cray et al., 1990; Flood et al., 1990; Hänninen et al., 1997). In addition, upregulation of LY6 proteins, in particular LY6C, is linked to increased chemokine secretion (Flanagan et al., 2008). Finally, a human LY6 antigen, E48 (highly homologous to mouse LY6D), regulates the release of chemoattractant factors from human umbilical vein endothelial cells that induce monocytes to migrate across an endothelial cell layer (Eshel et al., 2002).

MAV-1 infects cells of the monocytic lineage (Ashley et al., 2009; Kajon et al., 1998), which could lead to the hypothesis that these cells are involved in viral spread. We observed an increase in macrophage and inflammatory monocyte recruitment for both C.SJL-Msq1^{SJL} and SJL mice, but not BALB/c mice, after MAV-1 infection. However, clodronate-loaded liposome depletion of liver, spleen, lymph node and peritoneal macrophages does not affect brain viral titers in either SJL or BALB/c mice (Ashley et al., 2009). It is therefore unlikely that infected macrophages are responsible for dissemination of the virus to the brain. The depletion treatment also results in increased spleen viral loads in BALB/c mice, suggesting that macrophages have a role in controlling MAV-1 infection. However, despite the large numbers of recruited macrophages in SJL and C.SJL-Msq1^{SJL} mouse brains, viral loads were high. It is possible that the recruitment of macrophages was delayed in SJL and C.SJL-Msq1^{SJL}

mice and thus unable to control the infection. Alternatively, we hypothesize that the large increase in inflammatory monocytes at the BBB may result in increased secretion of chemokines or proteases, such as matrix metalloproteinases (Goetzl et al., 1996), resulting in opening of the BBB and leading to further cell recruitment. A systematic examination of the kinetics of cell recruitment after MAV-1 infection will be informative to explain strain differences in susceptibility.

Numbers of all analyzed cell types, with the exception of B cells, were increased in the brain following MAV-1 infection of all strains. B cells are crucial for survival from acute MAV-1 infection (Moore et al., 2004). Infected mice lacking Bruton's tyrosine kinase, and B cell-deficient mice on both C57BL/6 and BALB/c backgrounds suffer from disseminated infection with high brain and spleen viral loads and death. Our data suggest that B cells do not play a role in MAV-1-induced brain pathology in SJL mice, and that B cell recruitment is not influenced by *Msq1*. However, given the crucial role of B cells in controlling MAV-1 infection, it is likely that they influence the progression of MAV-1 infection of SJL mice in other organs or in the brain at different time points.

T cells are responsible for much of the acute pathology attributed to MAV-1 infection, and, they are important for survival, control of MAV-1 replication and clearance (Moore et al., 2003). Mice on a C57BL/6 background are intermediate in susceptibility between BALB and SJL mice (Guida et al., 1995; Spindler et al., 2001), and the T-cell immune-deficient mice we have previously examined are on this background. Mice that lack T cells do not develop encephalomyelitis, but have detectable brain viral loads following MAV-1 infection (Moore et al., 2003). Furthermore, MAV-1-infected T cell-deficient mice have little or no immunopathology, suggesting that the

acute histopathology is due to T cells. More T cells were recruited to the brains of SJL than C.SJL-Msq1^{SJL} MAV-1-infected mice, suggesting that the large number of recruited T cells in SJL mice causes irreparable damage, leading to higher mortality. The fact that we see higher numbers of recruited T cells after MAV-1 infection in SJL than C.SJL-Msq1^{SJL} mice, but similar high brain viral loads in both strains, is consistent with previous data that T cells do not control brain viral loads (Moore et al., 2003).

Although the total numbers of CD45$^{(hi)}$ cells were similar between SJL and C.SJL-Msq1^{SJL} mice, there were significant differences in the numbers of cells between strains in each of the immune cell subpopulations we examined. The numbers of cells were lower for all subpopulations except macrophages and B cells in C.SJL-Msq1^{SJL} mice than in SJL mice. As a result, the combined number of immune cells from the subpopulations that we looked at corresponded well with the total number of infiltrating cells (CD45$^{(hi)}$) in SJL but not C.SJL-Msq1^{SJL} mice. There appears to be a population(s) of missing cells that do not express any of the markers that we examined, such as NK cells, dendritic cells and mast cells, which we did not analyze.

In addition to our results here, *Ly6* gene family members have also been identified as important host factors influencing viral replication in several other viruses, some of which cause viral encephalitis (Kenzy et al., 1973; Mims, 1957; Turtle et al., 2012; Wiley et al., 1991). Chicken LY6E is a candidate for susceptibility to Marek's disease, an avian herpesvirus, and interacts with viral protein US10 in two-hybrid assays (Liu et al., 2003; Morgan et al., 2001). Four mouse *Ly6* genes are more highly upregulated during infection by highly neuroinvasive West Nile virus strains than by strains that are less neuroinvasive (Venter et al., 2005). More recently, human LY6E was shown to affect West Nile virus

infection in a small interfering RNA screen (Krishnan et al., 2008). In addition, human LY6E increases viral replication of another flavivirus, yellow fever virus, *in vitro* (Schoggins et al., 2011). Finally, the human *Ly6* locus, *Ly6* and *Ly6*-related genes were also implicated in two separate screens for HIV susceptibility factors (Brass et al., 2008; Loeuillet et al., 2008). These results indicate that *Ly6* genes are susceptibility factors for diverse RNA and DNA viruses. Future studies of the function and interaction partners of LY6 proteins may lead to the identification and characterization of common pathways leading to vascular damage and/or mortality in encephalitis and may yield new therapeutic targets.

In summary, *Msq1* is an important genetic contributor to the pathogenesis of MAV-1 encephalitis, but does not account for the full susceptibility phenotype seen in SJL mice. Our data confirmed that *Msq1* regulated brain viral loads and that it contributed significantly to strain susceptibility. We demonstrated that the presence of $Msq1^{SJL}$ correlated with increased permeability of the BBB to both small and large tracer molecules, and differences in ability of infected pmBECs to maintain high TEER. *Msq1* also controlled the development of brain lesions caused by MAV-1 infection. The data reveal that other factors (environmental or genetic) likely contributed to the onset of increased BBB permeability and the development of vasogenic edema. We also show that *Msq1* mediated recruitment of certain subsets of inflammatory cells to the brain but not others. This difference in inflammatory cell infiltrate may help explain the difference we see in MAV-1 susceptibility and pathogenesis in SJL and C.SJL-$Msq1^{SJL}$ mice. Experiments are in progress to identify the major susceptibility gene(s) within *Msq1*.

MATERIALS AND METHODS

Generation of congenic strain. C.SJL-Msq1^{SJL} congenic mice were developed by backcrossing the SJL-derived *Msq1* locus onto a BALB/c background for 11 generations (N11). Progeny mice heterozygous for *Msq1* were then intercrossed to initiate a homozygous congenic strain. Genotyping was performed by polymerase chain reaction with tail DNA. Simple sequence length polymorphism markers were used to differentiate between SJL- and BALB/c-derived *Msq1* genomic interval. The flanking region loci genotyped were *D15Spn101* and *D15Spn54* (Spindler et al., 2001). PCR products were electrophoresed in 7% acrylamide gels and visualized by ethidium bromide staining.

Virus and mice. Wild type MAV-1 was obtained from S. Larsen (Ball et al., 1991). 3- to 4-week old and 4- to 5-week old BALB/c and SJL male mice were obtained from Jackson Laboratory and used for primary cell preparations and infection experiments, respectively. 3- to 4- week old and 3- to 8-week old male and female congenic mice were used for primary cell preparations and infection experiments, respectively. Mice were infected via intraperitoneal (i.p.) injection in volumes of 100 µl, with doses that ranged from 10^2 to 10^7 PFU of virus. Virus was diluted in 10-fold serial dilutions in endotoxin-free Dulbecco's phosphate-buffered saline (DPBS; Lonza). Mock-infected mice were injected with conditioned media similarly diluted in DPBS. Mice were monitored at least twice daily for signs of disease and were euthanized by CO_2 asphyxiation if moribund. The animal care and use complied with both federal and university guidelines. Food and water were provided to the mice *ad libitum*.

Determination of MAV-1 loads by capture ELISA. Whole brains were aseptically collected from euthanized mice. Brain homogenates were prepared as previously described (Welton et al., 2005) and assayed for MAV-1 viral load by capture ELISA (Welton and Spindler, 2007). In each assay, an undiluted MAV-1 virus stock, PBS, and conditioned media were included as controls. Quantification of virus particles by ELISA correlates with infectious virus levels measured by plaque assay (Welton et al., 2005).

Determination of LD_{50}. Experiments were carried out with 4- to 6-week-old C.SJL-Msq1^{SJL} mice. Serial dilutions of virus were prepared, and groups of five to twenty-one mice were infected with each dose; three or six doses were used in LD_{50} determination of BALB/c and C.SJL-Msq1 mice, respectively. LD_{50}s were determined using the Reed and Muench method (Reed and Muench, 1938). Mice were euthanized if moribund, or at the conclusion of the experiment.

Measurement of brain water and ion content. After euthanasia, brains were rapidly removed and weighed to obtain wet weight. Dry weight was determined after drying the brains for 24 h at 100˚C. Percentage water content was calculated as: [(wet weight-dry weight)/wet weight] × 100. Na^+ and K^+ contents were measured using a flame photometer (Model IL 943, Instrumentation Laboratory, Inc.) after reconstituting the dried brains in 0.1 M nitric acid for 72 to 144 hours at room temperature.

BBB permeability assay. Sodium fluorescein and Evans blue are small-molecule tracers used to assess permeability of the BBB. Mice were injected with either 200 µl of 2% Evans blue dye (Sigma-Aldrich) in DPBS 4 hours prior to euthanasia, or 100 µl of 10%

sodium fluorescein (Sigma) in DPS 10 minutes prior to euthanasia. Mice were euthanized by CO_2 asphyxiation. Cardiac blood was collected in heparinized syringes into tubes containing 50 µl 1 mg/ml heparin and placed on ice. Mice were immediately perfused transcardially with 30 ml of ice-cold PBS. Brains were collected and snap frozen until use.

Evans blue staining in brains was quantified as previously described (Matullo et al., 2010). Briefly, brains were thawed and photographed, then homogenized in N,N-Dimethylformamide (Sigma) at a concentration of 300 mg/ml and incubated at 50˚C for 48 hours. Samples were centrifuged (3000 × g, 10 min) and absorbance of the supernatant was measured on a multidetection microplate reader (Biotek Instruments) at 620 nm. The amount of Evans blue in the brain of each infected mouse is represented as a fold change from the average measurement in brains of mock-infected mice of the respective strain.

Sodium fluorescein in brain and plasma were determined as previously described (Gralinski et al., 2009; Phares et al., 2006). Fluorescence levels were measured on a multidetection microplate reader (Biotek) with 485-nm excitation and 530-nm emission. Standards were used to calculate the sodium fluorescein content of brain and plasma samples. Brain values were normalized to their respective plasma dye values to allow comparison among mice. The amount of sodium fluorescein in each infected mouse brain is represented as a fold change from the average uptake in brains of mock-infected mice of the respective strain.

pmBEC preparation. pmBECs were isolated similarly to methods previously described (Gralinski et al., 2009). For each primary cell preparation, we used 30 mouse brains from 3- to 4-week old BALB/c, SJL or C.SJL-Msq1^{SJL} mice. The cortexes were isolated and major blood vessels were removed based on visual inspection. Brains were minced and mechanically homogenized in Hanks' balanced salt solution (HBSS; Gibco Life Technologies) using a Dounce homogenizer. Cells were pelleted (205 × g, 5 min) and resuspended in 18% dextran solution (USB Products). The suspension was centrifuged (11,726 × g, 10 minutes, 4˚C) using the Sorvall SA-600 rotor. Myelin and liquid was aspirated, and erythrocytes and microvessels were resuspended in HBSS. The suspension was layered onto the top of pre-centrifuged (26,793 × g, 1 h, SW41 rotor, Sorvall ultracentrifuge) 46.5% Percoll (GE Healthcare) gradients and then centrifuged (1,800 × g, 10 min) in a Jouan benchtop centrifuge. Microvessels form a distinct red band in the density gradient and were carefully transferred to a 50-ml tube and washed with HBSS. Microvessels were repelleted (205 × g, 5 min). The pellet was resuspended in 1 mg/ml collagenase/dispase (Roche Diagnostics) and incubated at 37˚C for 20-40 minutes. The enzyme solution was then inactivated with the addition of 2 to 3 volumes of HBSS. Microvessels were repelleted (205 × g, 5 min). Supernatant was aspirated and the remaining cells were resuspended in growth media, which consists of DMEM (Gibco), pH 7.2 containing 10% fetal bovine serum, 10% newborn calf serum, 0.1 mg/ml endothelial cell growth supplement (BD Biosciences), 0.1 mg/ml heparin (Sigma), 2 mM glutamine, Pen/Strep (Gibco), antimycotic/antibiotic (Gibco), nonessential amino acids (Sigma) and 20 mM HEPES (Sigma). The cells were plated onto collagen IV-coated

plates (BD). 4 μg/ml of puromycin was added 24 hours post isolation for 48 hours total to inhibit growth of fibrocytes. Before use, cells were passed once at 1:2 or 1:3 with Accutase (EMD Millipore corporation) to release them from the plate.

Growth curve. pmBECs were isolated and plated in collagen IV-coated wells of a 12-well transwell plate (Corning Inc.) and infected at a multiplicity of infection (MOI) of 5. After 1 hour adsorption at 37˚C, the cells were washed 2 times with PBS before media was replenished. At 0, 2, and 4 or 5 dpi, supernatant, scraped cells and membrane were collected. Samples were freeze-thawed 3 times to release intracellular virus; infectious virus was quantified by plaque assay.

Measurement of TEER. After initial isolation, pmBECs were plated onto collagen IV-coated 12-well 0.4-μm pore transwells (Corning). Media was supplemented with 500 ng/ml hydrocortisone and 50-80% astrocyte-conditioned media to aid in the formation of tight junctions. Astrocyte-conditioned media was obtained from primary astrocytes prepared as described (Stamatovic et al., 2005). The percentage of astrocyte-conditioned media was gradually reduced to 20% once tight junctions had formed. TEER values ($\Omega \cdot cm^2$) were determined by subtraction of a blank well containing media alone and multiplying by the surface area of the transwell membrane. Cells were allowed to reach confluence over 7 to 10 days from time of plating, until TEER levels reached 20 to 50 $\Omega \cdot cm^2$. TEER was measured using an Endohm-12 electrical resistance apparatus (World Precision Instruments Inc). Cells were either mock infected or infected with MAV-1 at a multiplicity of infection (MOI) of 5. TEER was measured on the day of infection and at

24-h intervals thereafter. Data are presented as percentages of the initial (d0) TEER reading.

Histology. Mice were either mock infected or infected with MAV-1. Mice were perfused with PBS following euthanasia, and organs were collected for histopathology. Organs (thymus, lung, heart, brain, liver, kidney and spleen) were immersion-fixed in 10% neutral-buffered formalin for 24 h, embedded in paraffin, sectioned at 5 μm and stained with hematoxylin and eosin. Blinded and randomized samples were scored by a board-certified pathologist.

Isolation and staining of cells for flow cytometry. Mice were mock infected or infected with MAV-1 in groups of 5. On the day of harvest, mice were euthanized and immediately perfused with 30 ml of PBS prior to organ collection. Brains were pooled in DMEM (Gibco) containing 10% fetal bovine calf serum, and cells were mechanically isolated using a cell strainer. Cells were pelleted and resuspended in 70% isotonic Percoll (GE) in a final volume of 15 ml; 37% isotonic Percoll in DMEM and 30% isotonic Percoll in HBSS were sequentially overlaid on top of the cells (15 ml each) in a 50-ml conical tube. Samples were centrifuged for 20 min at 500 × g, and cells at the 37:70 interface were collected. Cells were stained with fluorescently labeled antibodies to CD45.1/CD45.2 (PerCP-Cy5.5, clones A20 and 104 for CD45.1 and CD45.2, respectively), CD3 (FITC, clone 145-2C11), CD8 (PE, clone 53-6.7), CD4 (biotin, clone GK1.5), CD44 (PE-Cy7, clone IM7), CD62L (APC, clone MEL-14), CD19 (APC, clone 1D3), MHC Class II (PE, clones M5/114.15.2 and OX-6 for BALB/c and SJL,

respectively), CD11b (FITC, clone M1/70), CD11c (PE-Cy7, clone N418), PDCA (biotin, clone eBio927), LY6G (PE, clone 1A8), LY6C (biotin, clone AL-21), F4/80 (APC, clone BM8), and biotinylated antibodies were detected with APC-eFluor 780 strepavidin. All antibodies were obtained from eBioSciences, except CD3, CD8, CD19, MHC Class II clone M5/114.15.2, LY6C and LYG were from BD; MHC Class II clone OX-6 was from Abcam and F4/80 was from Caltag Laboratories Invitrogen. Stained samples were analyzed using a FACSCanto^{TM} flow cytometer (BD) and Flowjo software (Tree Star, Inc.).

Statistical analysis. Statistical analysis was carried out using Microsoft Office Excel and Graph Pad Prism 5 software. Specific statistical tests are denoted in each figure legend.

Notes

This work was reprinted and modified with permission from Hsu, T.-H., Althaus, I. W., Foreman, O., & Spindler, K. R. (2012). Contribution of a Single Host Genetic Locus to Mouse Adenovirus Type 1 Infection and Encephalitis. mBio, 3(3), doi:10.1128/mBio.00131-12.

This work was supported by NIH R01 AI068645 to K.R.S. T.-H. Hsu has been supported by NIH National Research Service Award T32 GM07544, a University of Michigan (U-M) Rackham Graduate School Merit Fellowship and two Rackham graduate student research grants; a U-M Frances Wang Chin fellowship, and the U-M Endowment for the Development of Graduate Education award. The funders had no role in study design, data collection and analysis, decision to publish, or preparation of the manuscript.

We thank Amanda Welton, Shanna Ashley, and Jenny Imperiale for husbandry and genotyping of the early congenic mouse crosses. We thank Richard Keep for technical assistance, loan of equipment and advice regarding edema experiments. We are also grateful to Anuska Andjelkovic, Jason Weinberg and Yasmina Laouar for technical assistance. In addition, we thank David Burke, Michael Imperiale, David Miller and Bethany Moore for helpful discussion and comments on the manuscript.

References

Abbott, N.J., Patabendige, A.A., Dolman, D.E., Yusof, S.R., and Begley, D.J. (2010). Structure and function of the blood-brain barrier. *Neurobiol Dis* 37, 13-25.

Ashley, S.L., Welton, A.R., Harwood, K.M., Van Rooijen, N., and Spindler, K.R. (2009). Mouse adenovirus type 1 infection of macrophages. *Virology* 390, 307-314.

Ball, A.O., Beard, C.W., Villegas, P., and Spindler, K.R. (1991). Early region 4 sequence and biological comparison of two isolates of mouse adenovirus type 1. *Virology* 180, 257-265.

Bamezai, A., Palliser, D., Berezovskaya, A., McGrew, J., Higgins, K., Lacy, E., and Rock, K.L. (1995). Regulated expression of Ly-6A.2 is important for T cell development. *J Immunol* 154, 4233-4239.

Brass, A.L., Dykxhoorn, D.M., Benita, Y., Yan, N., Engelman, A., Xavier, R.J., Lieberman, J., and Elledge, S.J. (2008). Identification of host proteins required for HIV infection through a functional genomic screen. *Science* 319, 921-926.

Carrigan, D.R. (1997). Adenovirus infections in immunocompromised patients. *Am J Med* 102, 71-74.

Charles, P.C., Guida, J.D., Brosnan, C.F., and Horwitz, M.S. (1998). Mouse adenovirus type-1 replication is restricted to vascular endothelium in the CNS of susceptible strains of mice. *Virology* 245, 216-228.

Chaturvedi, U.C., Dhawan, R., Khanna, M., and Mathur, A. (1991). Breakdown of the blood-brain barrier during dengue virus infection of mice. *J Gen Virol* 72 (Pt 4), 859-866.

Coisne, C., and Engelhardt, B. (2011). Tight junctions in brain barriers during central nervous system inflammation. *Antioxid Redox Signal* 15, 1285-1303.

Cray, C., Keane, R.W., Malek, T.R., and Levy, R.B. (1990). Regulation and selective expression of Ly-6A/E, a lymphocyte activation molecule, in the central nervous system. *Brain Res Mol Brain Res* 8, 9-15.

Dallasta, L.M., Pisarov, L.A., Esplen, J.E., Werley, J.V., Moses, A.V., Nelson, J.A., and Achim, C.L. (1999). Blood-brain barrier tight junction disruption in human immunodeficiency virus-1 encephalitis. *Am J Pathol* 155, 1915-1927.

Echavarria, M. (2008). Adenoviruses in immunocompromised hosts. *Clin Microbiol Rev* 21, 704-715.

Eshel, R., Zanin, A., Kapon, D., Sagi-Assif, O., Brakenhoff, R., van Dongen, G., and Witz, I.P. (2002). Human Ly-6 antigen E48 (Ly-6D) regulates important

interaction parameters between endothelial cells and head-and-neck squamous carcinoma cells. *Int J Cancer* 98, 803-810.

Fields, B.N., Knipe, D.M., and Howley, P.M. (2007). "Fields Virology." 5th ed. Wolters Kluwer Health/Lippincott Williams & Wilkins, Philadelphia.

Flanagan, K., Modrusan, Z., Cornelius, J., Chavali, A., Kasman, I., Komuves, L., Mo, L., and Diehl, L. (2008). Intestinal epithelial cell up-regulation of LY6 molecules during colitis results in enhanced chemokine secretion. *J Immunol* 180, 3874-3881.

Flisiak, R., Horban, A., Gallay, P., Bobardt, M., Selvarajah, S., Wiercinska-Drapalo, A., Siwak, E., Cielniak, I., Higersberger, J., Kierkus, J., Aeschlimann, C., Grosgurin, P., Nicolas-Metral, V., Dumont, J.M., Porchet, H., Crabbe, R., and Scalfaro, P. (2008). The cyclophilin inhibitor Debio-025 shows potent anti-hepatitis C effect in patients coinfected with hepatitis C and human immunodeficiency virus. *Hepatology* 47, 817-826.

Flood, P.M., Dougherty, J.P., and Ron, Y. (1990). Inhibition of Ly-6A antigen expression prevents T cell activation. *J Exp Med* 172, 115-120.

Gaillard, P.J., Voorwinden, L.H., Nielsen, J.L., Ivanov, A., Atsumi, R., Engman, H., Ringbom, C., de Boer, A.G., and Breimer, D.D. (2001). Establishment and functional characterization of an in vitro model of the blood-brain barrier, comprising a co-culture of brain capillary endothelial cells and astrocytes. *Eur J Pharm Sci* 12, 215-222.

Getts, D.R., Terry, R.L., Getts, M.T., Muller, M., Rana, S., Shrestha, B., Radford, J., Van Rooijen, N., Campbell, I.L., and King, N.J. (2008). Ly6c+ "inflammatory monocytes" are microglial precursors recruited in a pathogenic manner in West Nile virus encephalitis. *J Exp Med* 205, 2319-2337.

Gilliam, B.L., Riedel, D.J., and Redfield, R.R. (2011). Clinical use of CCR5 inhibitors in HIV and beyond. *J Transl Med* 9 Suppl 1, S9.

Goetzl, E.J., Banda, M.J., and Leppert, D. (1996). Matrix metalloproteinases in immunity. *J Immunol* 156, 1-4.

Gralinski, L.E., Ashley, S.L., Dixon, S.D., and Spindler, K.R. (2009). Mouse adenovirus type 1-induced breakdown of the blood-brain barrier. *J Virol* 83, 9398-9410.

Guida, J.D., Fejer, G., Pirofski, L.A., Brosnan, C.F., and Horwitz, M.S. (1995). Mouse adenovirus type 1 causes a fatal hemorrhagic encephalomyelitis in adult C57BL/6 but not BALB/c mice. *J Virol* 69, 7674-7681.

Hänninen, A., Jaakkola, I., Salmi, M., Simell, O., and Jalkanen, S. (1997). Ly-6C regulates endothelial adhesion and homing of CD8(+) T cells by activating integrin-dependent adhesion pathways. *Proc Natl Acad Sci U S A* 94, 6898-6903.

Hawkins, B.T., and Davis, T.P. (2005). The blood-brain barrier/neurovascular unit in health and disease. *Pharmacol Rev* 57, 173-185.

Hijazi, A., Masson, W., Auge, B., Waltzer, L., Haenlin, M., and Roch, F. (2009). boudin is required for septate junction organisation in Drosophila and codes for a diffusible protein of the Ly6 superfamily. *Development* 136, 2199-2209.

Ivey, N.S., Renner, N.A., Moroney-Rasmussen, T., Mohan, M., Redmann, R.K., Didier, P.J., Alvarez, X., Lackner, A.A., and MacLean, A.G. (2009). Association of FAK activation with lentivirus-induced disruption of blood-brain barrier tight junction-associated ZO-1 protein organization. *J Neurovirol* 15, 312-323.

Kajon, A.E., Brown, C.C., and Spindler, K.R. (1998). Distribution of mouse adenovirus type 1 in intraperitoneally and intranasally infected adult outbred mice. *J Virol* 72, 1219-1223.

Kanmogne, G.D., Primeaux, C., and Grammas, P. (2005). HIV-1 gp120 proteins alter tight junction protein expression and brain endothelial cell permeability: implications for the pathogenesis of HIV-associated dementia. *J Neuropathol Exp Neurol* 64, 498-505.

Kempski, O. (2001). Cerebral edema. *Semin Nephrol* 21, 303-307.

Kenzy, S.G., Cho, B.R., and Kim, Y. (1973). Oncogenic Marek's disease herpesvirus in avian encephalitis (temporary paralysis). *J Natl Cancer Inst* 51, 977-982.

Klatzo, I. (1987). Pathophysiological aspects of brain edema. *Acta Neuropathol* 72, 236-239.

Kring, S.C., King, C.S., and Spindler, K.R. (1995). Susceptibility and signs associated with mouse adenovirus type 1 infection of adult outbred Swiss mice. *J Virol* 69, 8084-8088.

Krishnan, M.N., Ng, A., Sukumaran, B., Gilfoy, F.D., Uchil, P.D., Sultana, H., Brass, A.L., Adametz, R., Tsui, M., Qian, F., Montgomery, R.R., Lev, S., Mason, P.W., Koski, R.A., Elledge, S.J., Xavier, R.J., Agaisse, H., and Fikrig, E. (2008). RNA interference screen for human genes associated with West Nile virus infection. *Nature* 455, 242-245.

Lee, Y.R., Liu, M.T., Lei, H.Y., Liu, C.C., Wu, J.M., Tung, Y.C., Lin, Y.S., Yeh, T.M., Chen, S.H., and Liu, H.S. (2006). MCP-1, a highly expressed chemokine in dengue haemorrhagic fever/dengue shock syndrome patients, may cause permeability change, possibly through reduced tight junctions of vascular endothelium cells. *J Gen Virol* 87, 3623-3630.

Liu, H.C., Niikura, M., Fulton, J.E., and Cheng, H.H. (2003). Identification of chicken lymphocyte antigen 6 complex, locus E (LY6E, alias SCA2) as a putative Marek's

disease resistance gene via a virus-host protein interaction screen. *Cytogenet Genome Res* 102, 304-308.

Loeuillet, C., Deutsch, S., Ciuffi, A., Robyr, D., Taffe, P., Munoz, M., Beckmann, J.S., Antonarakis, S.E., and Telenti, A. (2008). In vitro whole-genome analysis identifies a susceptibility locus for HIV-1. *PLoS Biol* 6, e32.

Major, E.O., Amemiya, K., Tornatore, C.S., Houff, S.A., and Berger, J.R. (1992). Pathogenesis and molecular biology of progressive multifocal leukoencephalopathy, the JC virus-induced demyelinating disease of the human brain. *Clin Microbiol Rev* 5, 49-73.

Matullo, C.M., O'Regan, K.J., Hensley, H., Curtis, M., and Rall, G.F. (2010). Lymphocytic choriomeningitis virus-induced mortality in mice is triggered by edema and brain herniation. *J Virol* 84, 312-320.

Mims, C.A. (1957). The invasion of the brain by yellow fever virus present in the blood of mice. *Br J Exp Pathol* 38, 329-338.

Moore, M.L., Brown, C.C., and Spindler, K.R. (2003). T cells cause acute immunopathology and are required for long-term survival in mouse adenovirus type 1-induced encephalomyelitis. *J Virol* 77, 10060-10070.

Moore, M.L., McKissic, E.L., Brown, C.C., Wilkinson, J.E., and Spindler, K.R. (2004). Fatal disseminated mouse adenovirus type 1 infection in mice lacking B cells or Bruton's tyrosine kinase. *J Virol* 78, 5584-5590.

Morgan, R.W., Sofer, L., Anderson, A.S., Bernberg, E.L., Cui, J., and Burnside, J. (2001). Induction of host gene expression following infection of chicken embryo fibroblasts with oncogenic Marek's disease virus. *J Virol* 75, 533-539.

Morrey, J.D., Olsen, A.L., Siddharthan, V., Motter, N.E., Wang, H., Taro, B.S., Chen, D., Ruffner, D., and Hall, J.O. (2008). Increased blood-brain barrier permeability is not a primary determinant for lethality of West Nile virus infection in rodents. *J Gen Virol* 89, 467-473.

Patterson, C.E., Rhoades, R.A., and Garcia, J.G. (1992). Evans blue dye as a marker of albumin clearance in cultured endothelial monolayer and isolated lung. *Journal of Applied Physiology* 72, 865-873.

Phares, T.W., Kean, R.B., Mikheeva, T., and Hooper, D.C. (2006). Regional differences in blood-brain barrier permeability changes and inflammation in the apathogenic clearance of virus from the central nervous system. *J Immunol* 176, 7666-7675.

Rawson, R.A. (1943). The binding of T-1824 and structurally related diazo dyes by the plasma proteins. *American Journal of Physiology -- Legacy Content* 138, 708-717.

Reed, L.J., and Muench, H. (1938). A simple method of estimating fifty percent endpoints. *American Journal of Epidemiology* 27, 493-497.

Schoggins, J.W., Wilson, S.J., Panis, M., Murphy, M.Y., Jones, C.T., Bieniasz, P., and Rice, C.M. (2011). A diverse range of gene products are effectors of the type I interferon antiviral response. *Nature* 472, 481-485.

Spindler, K.R., Fang, L., Moore, M.L., Hirsch, G.N., Brown, C.C., and Kajon, A. (2001). SJL/J mice are highly susceptible to infection by mouse adenovirus type 1. *J Virol* 75, 12039-12046.

Spindler, K.R., Welton, A.R., Lim, E.S., Duvvuru, S., Althaus, I.W., Imperiale, J.E., Daoud, A.I., and Chesler, E.J. (2010). The Major Locus for Mouse Adenovirus Susceptibility Maps to Genes of the Hematopoietic Cell Surface-Expressed LY6 Family. *J Immunol* 184, 3055-3062.

Stamatovic, S.M., Shakui, P., Keep, R.F., Moore, B.B., Kunkel, S.L., Van Rooijen, N., and Andjelkovic, A.V. (2005). Monocyte chemoattractant protein-1 regulation of blood-brain barrier permeability. *J Cereb Blood Flow Metab* 25, 593-606.

Tebruegge, M., and Curtis, N. (2010). Adenovirus infection in the immunocompromised host. *Adv Exp Med Biol* 659, 153-174.

Turtle, L., Griffiths, M.J., and Solomon, T. (2012). Encephalitis caused by flaviviruses. *QJM* 105, 219-223.

Venter, M., Myers, T.G., Wilson, M.A., Kindt, T.J., Paweska, J.T., Burt, F.J., Leman, P.A., and Swanepoel, R. (2005). Gene expression in mice infected with West Nile virus strains of different neurovirulence. *Virology* 342, 119-140.

Verma, S., Kumar, M., Gurjav, U., Lum, S., and Nerurkar, V.R. (2010). Reversal of West Nile virus-induced blood-brain barrier disruption and tight junction proteins degradation by matrix metalloproteinases inhibitor. *Virology* 397, 130-138.

Welton, A.R., Chesler, E.J., Sturkie, C., Jackson, A.U., Hirsch, G.N., and Spindler, K.R. (2005). Identification of quantitative trait loci for susceptibility to mouse adenovirus type 1. *J Virol* 79, 11517-11522.

Welton, A.R., and Spindler, K.R. (2007). Capture ELISA quantitation of mouse adenovirus type 1 in infected organs. *Methods Mol Med* 130, 215-221.

Wiley, C.A., Schrier, R.D., Morey, M., Achim, C., Venable, J.C., and Nelson, J.A. (1991). Pathogenesis of HIV encephalitis. *Acta Pathol Jpn* 41, 192-196.

Chapter V

Narrowing of mouse adenovirus type 1 susceptibility quantitative trait locus 1 through use of BAC transgenesis

ABSTRACT

Susceptibility to mouse adenovirus type 1 (MAV-1) is controlled by a major quantitative trait locus, *Msq1*, on mouse chromosome 15 (Chr 15). *Msq1* contributes to ~40% of the brain viral load phenotype, which is a surrogate measure of susceptibility to MAV-1. The 0.75 Mb interval contains 15 predicted candidate genes, 14 of which belong to the *Ly6* gene superfamily. We used bacterial artificial chromosome (BAC) transgenesis to reduce the number of candidate genes by attempting to complement the susceptibility phenotype in resistant mice. Thus far none of the transgenic mice carrying any single one of seven different BAC constructs was susceptible to MAV-1, as measured by brain viral loads. One mouse strain containing both 1-F09 and 1-D09 BAC constructs was also not susceptible to MAV-1. Analysis of whether the inserted BAC constructs are intact and whether expression of transgenes can be detected is currently ongoing. Preliminary findings reveal that at least one of the BACs (1-F07) is not intact and that expression levels of transgenes in another BAC (1-F09) is different between the two established transgenic lines. Apart from their susceptibility phenotypes to MAV-1, obtaining this panel of transgenic mice will provide a useful future resource for functional studies of the *Ly6* gene superfamily and to examine their transcriptional regulation.

INTRODUCTION

The mouse adenovirus type 1 (MAV-1)/mouse experimental model is a convenient and powerful tool for *in vivo* dissection of genetic components that are responsible for the outcome of an encephalitic viral infection. Due to the lack of a known *in vitro* assay to determine susceptibility or resistance to MAV-1 infection, our group initiated genetic mapping using backcross and recombinant mice to identify markers that are most closely linked to a high brain viral load phenotype (Welton et al., 2005). For the genetic mapping, we used brain viral loads as a quantifiable surrogate measure of susceptibility, because it is not possible to assay LD_{50}s of individual mice. We determined that the ability of MAV-1 to replicate to high levels in the brain in susceptible mice is controlled in large part by a single 0.75 Mb locus on mouse Chr 15, designated mouse adenovirus type 1 susceptibility quantitative trait locus 1 (*Msq1*) (Spindler et al., 2010; Welton et al., 2005).

We previously introgressed the SJL-derived *Msq1* onto an otherwise resistant BALB/c background to create the C.SJL-$Msq1^{SJL}$ congenic mouse strain (Hsu et al., 2012). We used these interval-specific congenic mice to investigate the contribution of $Msq1^{SJL}$ to MAV-1 susceptibility. The presence of a single allele of $Msq1^{SJL}$ is sufficient to confer the high brain viral load phenotype in the absence of additional susceptibility loci. The presence of the susceptible allele of *Msq1* also contributes to the disruption of the blood-brain barrier *in vivo* and *ex vivo*, recruitment of certain leukocyte subsets to the brain, and brain pathology following MAV-1 infection. However, C.SJL-$Msq1^{SJL}$ mice are not as susceptible to MAV-1 infection. In summary, although $Msq1^{SJL}$ cannot account for the entire susceptibility phenotype and brain pathology of MAV-1 infection in SJL

mice (indicating that susceptibility to MAV-1 is likely under multigenic control and/or influenced by environmental factors), it contributes significantly to key aspects of MAV-1 pathogenesis.

Msq1 includes 14 members of the *Ly6* gene superfamily (Spindler et al., 2010). The *Ly6* gene complex has two known haplotypes, which correspond to two lymphocyte specificities, Ly6.1 and Ly6.2 (Potter et al., 1980). Ly6.2 mouse strains correspond to strains susceptible to MAV-1 infection, while Ly6.1 mouse strains correspond to MAV-1-resistant strains (Spindler et al., 2010). *Ly6* genes are highly homologous and are thought to have arisen through gene duplication (Bamezai, 2004; Gumley et al., 1995). *Ly6* gene products are cysteine-rich glycosylphosphatidylinositol (GPI)-anchored proteins which share similarities in structure and the position of conserved cysteine residues. However, despite structural similarities, LY6 proteins are involved in a myriad of diverse functions. Each LY6 protein is thought to bind a unique ligand.

Members of the *Ly6* gene family have a role in susceptibility to other DNA and RNA viruses. Susceptibility to an oncogenic avian herpesvirus, Marek's disease virus, maps to the *Ly6* locus, and there have been efforts to elucidate the role of *Ly6E* as a putative resistance gene to Marek's disease virus (Liu et al., 2003; Morgan et al., 2001). In addition, four mouse *Ly6* genes, *Ly6C*, *Ly6E*, *Ly6F*, and *Ly6A* are more highly upregulated following infection by highly neuroinvasive West Nile virus strains than during infection by less neuroinvasive strains (Venter et al., 2005). Human LY6E protein was shown to contribute to West Nile virus infection in a small interfering RNA screen (Krishnan et al., 2008). Human LY6E also increases *in vitro* viral replication of yellow fever virus (Schoggins et al., 2011). Finally, the human *Ly6* locus was identified as a HIV

susceptibility factor through genetic and siRNA dependency factor analyses (Brass et al., 2008; Loeuillet et al., 2008).

To reduce the 0.75 Mb *Msq1* interval, we generated transgenic mice using bacterial artificial chromosomes (BACs) from a 129S6/SvEv BAC library, with the goal of complementing the susceptibility phenotype in a resistant mouse background. Susceptibility to MAV-1 in 129S6/SvEvTac mice maps to the same interval on Chr 15 as susceptibility to SJL mice (Spindler et al., 2010). $Msq1^{129S6/SvEvTac}$ accounts for 54% of the brain viral load phenotype. This allowed us to use a readily available BAC library generated from the spleen of a 129S6/SvEvTac female mouse.

The BACs contain 150 to 200 kb genomic inserts derived from $Msq1^{129S6/SvEv}$ on a bacterial F′ plasmid vector. Because BACs are relatively large molecules, they are thought to include the necessary regulatory elements needed for the expression of transgenes at endogenous levels (Giraldo and Montoliu, 2001). In addition, BACs have high clonal stability and a low rate of chimerism (Shizuya et al., 1992). Finally, BAC contigs were developed for a variety of organisms for the purpose of whole genome sequencing, including humans and mice (Hoskins et al., 2000; McPherson et al., 2001; Mozo et al., 1999; Osoegawa et al., 2000).

BAC transgenesis is an important tool for study of *in vivo* gene regulation and function. BAC transgenesis was used to demonstrate functional *in vivo* complementation of mouse cytomegalovirus (MCMV) susceptibility (Lee et al., 2003). Genetic transfer of BAC clones generated from the locus controlling MCMV resistance conferred resistance to mice on a MCMV susceptible background. BAC transgenic mice will also provide us with the opportunity to investigate questions regarding the *Ly6* gene family during

MAV-1 infection, including which aspects of MAV-1 pathology individual *Ly6* genes participate in and whether the entire family of genes needs to be present for proper gene regulation and expression.

METHODS

Animals. All mice were purchased from The Jackson Laboratory and subsequently maintained at the animal facility at the University of Michigan. Animal care and use complied with both federal and university guidelines. Food and water were provided to the mice *ad libitum*. BALB/c male and female mice were used as egg donors and stud males to make founders for the 1-F07 and 1-F09 transgenic strains. For the remaining transgenic strains, BALB/cByJ females were used as egg donors and (BALB/cJ×A/J)F_1 mice were used as stud males.

Generation of the 129S6/SvEv BAC library. BAC DNA was generated from spleens of female 129S6/SvEvTac (Taconic) mice and cloned into a pBACe3.6 vector (Frengen et al., 1999). These BAC-containing plasmids were transfected into DH10B electrocompetent cells (Osoegawa et al., 2000). The BAC library (RPCI-22 129S6/SvEvTac mouse BAC library; Children's Hospital Oakland Research Institute [CHORI]) contains over 18,000 distinct mouse BAC clones arrayed in 384-well microtiter plates and gridded onto nylon filters for probe hybridization screening (http://bacpac.chori.org). To select for BAC clones specific to our region, 40 bp oligonucleotide synthetic probes were designed to span 72,893,719 Mb to 75,593,718 Mb on Chr15. The probes were made radioactive by filling in overhangs of two overlapping

sequences using radiolabelled ^{32}P-dATP, ^{32}P-dCTP and Klenow polymerase (McPherson et al., 2001). Colony filters containing relevant BAC clones were hybridized overnight with target region-specific probes. Following a wash to remove unspecific probes, filters were exposed to phosphor screens for 24-48 hours. The screens were scanned for positive-probe hybridization signals (Storm 860; Array Vision software with High density colony hybridization attachment). Probe-positive BACs were selected and plated onto 96-well plates. Bacterial clones positive for the Chr 15 region were received as Luria broth (LB) stab cultures containing 12.5 µg/mL of chloramphenicol (CAM). A subset of BAC clones spanning the region were chosen for further analysis based on their genome location determined from the end sequencing of probe-positive BAC clones (Agencourt Bioscience). These clones spanned mouse Chr 15: 72.85 – 75.43 Mb; mm9, build 37 of July 2007 UCSC Genome Browser.

Isolation of BACs. BAC clones were streaked to single colonies on an LB agar plate containing 12.5 µg/mL CAM. Single colonies were used to inoculate 500 mL LB cultures containing 12.5 µg/mL CAM and grown up for ~20 h at 37˚C. High purity BAC DNA was isolated using the Marligen PowerPrep™ HP plasmid purification system (Origene). Briefly, *E.coli* were spun down, then resuspended and lysed, DNA was bound to a column, washed, and eluted from the column. BAC DNA was precipitated using isopropanol, followed by a 70% ethanol wash, and resuspended in TE buffer (10 mM Tris, 1 mM EDTA, pH 8.0) containing 30 µM spermine and 70 µM spermidine. BAC DNA concentration was measured at 260 nm absorbance using a spectrophotometer

(NanoDrop; Thermo Scientific), and DNA was stored at 4˚C. Integrity of isolated BACs was verified on a pulsed-field gel, as described below.

Generation of BAC transgenic mice. Purified BAC DNA was microinjected into fertilized eggs by the University of Michigan Transgenic Animal Model Core. Pronuclear microinjection was performed as described (Nagy, 2003).

Pulse-field gel electrophoresis. BAC DNA was digested with NotI, XhoI, SalI or SbfI (New England Biolabs) for 2 hours at 37˚C and subjected to pulse-field gel electrophoresis (CHEF-DR III; BioRad) on a 1% agarose gel, under the following conditions: 6 V/cm, 120˚ angle with 1-25 s switch times, at 4˚C for 16 h. A Lambda ladder (Promega) prepared by concatemerization of λ phage DNA was used for size markers. Gels were stained after electrophoresis with ethidium bromide for analysis.

Identification of transgenic founders via PCR. Mouse tail DNA was used in PCR reactions. Approximately 2 mm of tail was incubated with 200 µl buffer (10 mM Tris pH8.3, 2.5 mM MgCl2, 50 mM KCl, 0.1 mg gelatin, 0.45% Tween 20, 0.45% Igepal, 0.05 mg/ml proteinase K) overnight at 55°C with gentle shaking. The samples were pelleted at 16,000 x g for 5 min. Fifty µl of supernatant was immediately removed and mixed with an equal volume of water and immediately used or frozen at -20°C. Four µl DNA was used in a 20 µl PCR reaction. Crude DNAs were amplified from both the T7-end of the BAC vector-insert junction, or from the KBr/TJ end of the BAC vector-insert junctions (Table 5.1). PCR amplification of a randomly-chosen endogenous genomic

Table 5.1 BAC primers.

Primer	Sequence
T7[a]	TAATACGACTCACTATAGGG
KBr/TJ[a]	CTGGCCGTCGACATTTAGG
SNP 19[b]	TTGGGTGTTTAGGGAGTGTTG
SNP 20[b]	ACCTTCCTAAGCGCAGAAGC

BAC clone	Primer sequence (T7-end)[c]	Primer sequence (with KBr/TJ-end)[c]
1-F09	CTGGATCCCTTTGTCTGCAT	GGTTGCTCCTGCTCTTTCAC
1-F07	CCCACCTACAATCCCACAAG	GCCATTCTGACTGGTGTGAGATGGAAT
1-D09	GAAGACAAGGATGACGAGGA	CATTGTACCCTCCTGCCACT
1-D10	AGGCATGCACATCCATACAA	GGGGTCTCTCTCAGCTTCCT
1-A01	TGCAGACATTGCTGTGATGA	CCTGTGGCCTACACACACAC
1-C10	GGCTCAAGTGGGCATTGTTA	CAGCATCCCAGGGAACTAAA
1-H01	GGGTGTTCCCAAGACAGAAA	AGTGAGGTTATGGGGCAGTG
1-E09	ATCCAGCCCCATGAGTACAG	CCAAGCCTATTCCCCTTCTC

[a]These primers are specific to the pBACe3.6 vector and were used for end sequencing.
[b]These primers amplify an endogenous gene and were used to check DNA integrity.
[c]These primers are specific to BAC sequence and were used with the appropriate pBACe3.6 T7 or KBr/TJ primer to amplify the BAC ends.

region of the recipient mouse background was also performed in parallel to control for the quality of isolated tail DNA. We used primer set SNP19/SNP20 (Table 5.1), which was previously used to amplify SNP rs3662946 (Spindler et al., 2010), to check for DNA quality. PCR products were electrophoresed in 7% acrylamide gels and visualized by ethidium bromide staining.

Infections. 3- to 8-week old mice were used for infection experiments. Mice were infected with 10^2 PFU of virus via intraperitoneal (i.p.) injection in volumes of 100 µl. Virus was diluted in 10-fold serial dilutions in endotoxin-free Dulbecco's phosphate-buffered saline (DPBS; Lonza). Mock-infected mice were injected with conditioned media similarly diluted in DPBS. Mice were monitored at least twice daily for signs of disease and were euthanized by CO_2 asphyxiation if moribund. Mice were euthanized by CO_2 asphyxiation at the indicated experimental endpoints.

Determination of MAV-1 loads by capture ELISA. Whole brains were aseptically collected from euthanized mice. Brain homogenates were prepared as previously described (Welton et al., 2005) and assayed for MAV-1 viral load by capture ELISA (Welton and Spindler, 2007). In each assay, an undiluted MAV-1 virus stock, PBS, and conditioned media were included as controls. Quantification of virus particles by ELISA correlates with infectious virus levels measured by plaque assay (Welton et al., 2005).

Sequencing

PCR products were purified using the QIAGEN QIAquick PCR purification kit, quantified at 260 nm absorbance using a spectrophotometer (NanoDrop; Thermo Scientific), and submitted to the University of Michigan DNA Sequencing Core. A BLAT search of the sequences against the mouse genome was performed to confirm product identity (http://genome.ucsc.edu/) and chromatograms were analyzed (FinchTV; Geospiza). Sequence alignment was performed using ClustalW and analyzed using DNASTAR Lasergene.

RNA isolation

RNA was isolated from brains using TriReagent (Molecular Research Center, Inc., Cincinnati, OH). 1 mL TriReagent was added per 100 mg brain tissue and the mixture was homogenized in a BioSpec bead-beater. Subsequent RNA isolation steps were in accordance with the manufacturer's instructions. RNA pellets were resuspended in ddH_2O and the concentrations were measured using a spectrophotometer (NanoDrop; Thermo Scientific).

cDNA synthesis and PCR amplification.

RNA was treated with RQ1 RNase-Free DNase (Promega) according to the manufacturer's instructions. cDNA was synthesized from 5 µg brain RNA using random hexamers and Moloney murine leukemia virus reverse transcriptase (RT) (Invitrogen). cDNA was PCR amplified using previously published PCR primers and conditions for PCR amplification of *Ly6* genes from cDNA(Stier and Spindler, 2011). PCR products

were purified using the QIAGEN QIAquick PCR purification kit and quantified at 260 nm absorbance using a spectrophotometer (NanoDrop; Thermo Scientific).

Ligation-PCR detection assay (Fig. 5.1).

Purified PCR product was added to the ligation mixture, containing APB buffer, ddH2O, ligase, and oligo mix. Oligo mix consisted of the following primers Ly6c1 L1, Ly6c1 L2.BALB, and Ly6c1 L2.129S6 (Table 5.2). These primers are designed to detect a SNP at 74,878,906 bp on Chr 15 in *Ly6C1* (Stier and Spindler, 2011) that is polymorphic between BALB/c and 129S6/SvEv mice (Stier and Spindler, unpublished). Alu size markers were generated from mouse genomic DNA using PCR amplification with ALUP1 and ALU P2 (Table 5.2), and ligation reactions were performed with Alu-specific primers (ALU 50 L1, ALU 50 L2, ALU 114L1, and ALU 114L2) in the presence of ligase. Ligation reaction products were ethanol precipitated and resuspended in ddH_2O. ALU size markers were added to the *Ly6C1* ligation products. Ligation mixtures were separated by capillary electrophoresis on a MegaBACE 1000 Sequencer. 6-FAM and HEX fluorescence intensity was measured and analyzed on chromatograms. ALU size markers generate peaks at 50 bp and 114 bp. BALB/c ligation products are 54 bp; 129S6/SvEvTac ligation products are 58 bp.

Statistical analysis. Statistical analysis was carried out using Microsoft Office Excel and Graph Pad Prism 5 software. Specific statistical tests are denoted in each figure legend.

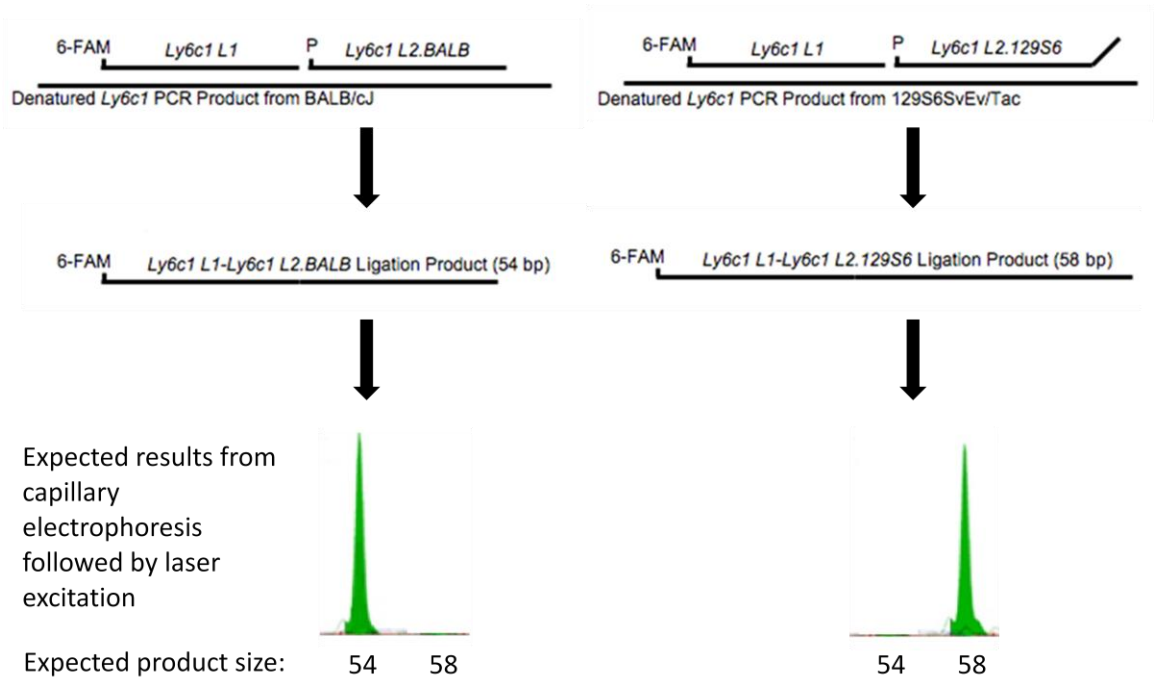

Figure 5.1 Ligation-PCR detection assay. The site of a single nucleotide polymorphism (SNP) in the *Ly6c1* PCR product is where the ligation reaction occurs. The SNP detected by these oligos is at 74,878,906 bp on Chr 15 (Stier and Spindler, 2011). *Ly6c1 L1* is a probe common to both BALB/c and 129S6/SvEv DNA that is modified with a 6-FAM fluorescent label. *Ly6c1 L2.BALB* and *Ly6c1 L2.129S6* are strain-specific primers that were used to detect the SNP in BALB/cJ and 129S6SvEv/Tac DNA, respectively (Table 5.2). *Ly6c1 L2.BALB* and *Ly6c1 L2.129S6* have identical sequences except at the 5' end (nucleotide complementary to desired SNP) and the 3' end, where *Ly6c1 L2.129S6* has an additional 4 non-specific terminal base pairs. The ligation products will therefore have a size difference of 4 bp. P: phosphorylation at the 5′ end of genotype-specific primers; SNP is at this location. There is no gap between the oligos; the 3' nucleotide of *Ly6c1 L1* is immediately adjacent to the 5' nucleotide of *Ly6c1 L2.BALB* or *Ly6c1 L2.129S6*. Size markers were not included in this figure for the sake of simplicity (Figure modified from Stier, 2011).

Table 5.2 Ligation primers.

Oligo	Sequence[a]	Modifications
Ly6c1 L1	ACACAGTAGGGCCACAAGAAGAAT	5'-6-FAM
Ly6c1 L2.BALB[b]	CAGCACACAGGACTTTGTAGTGTGAGAAAT	5'-P
Ly6c1 L2.129S6[c]	GAGCACACAGGACTTTGTAGTGTGAGAAAT[ACGT]	5'-P
ALU P1	GGAGCACGCTATCCCGTTAGACCCAGGAGTTCTGGGCTG TAG	none
ALU P2	CGCTGCCAACTACCGCACATGTGGAGTGCAGTGGCTATT CA	none
ALU 50 L1	AGGTCACCATATTGATGCCGAAC	5'-HEX
ALU 50 L2	TTAGTGCGGACACCCGATCG[ATGCTCA]	5'-P
ALU 114 L1	CCCACTACTGATCAGCACGGGAGTT	5'-HEX
ALU 114 L2	TTGACCTGCTCCGTTTCCGA[ATGCTCAGACACAATTAGC GCGACCCTTAATCCTTAGGTAATGCTCAGACACAATTAG CGCGACCCTTA]	5'-P

[a] [ ] enclose non-specific sequences added to differentiate the size of the ligation products

[b]detects BALB/cJ-specific single nucleotide polymorphism

[c]detects 129S6SvEv/Tac-specific single nucleotide polymorphism

RESULTS

Construction of BAC transgenic strains. We obtained BACs clones belonging to the RPCI-22 BAC library, which was derived from a mouse strain susceptible to MAV-1, 129S6/SvEvTac (Spindler et al., 2010). The BAC clones span the entire *Msq1*$^{129S6/SvEv}$ interval. From these, we selected 8 BACs to generate transgenic mice (Fig. 5.2). We expected progeny mice that have the susceptibility transgene, but not their non-transgenic littermates, to be susceptible to MAV-1. BAC transgenic mice were created by microinjection into the male pronuclei of fertilized eggs. Transgenic founder animals were identified through PCR amplification with primers specific for the vector-BAC junction ends (Table 5.1).

BALB/c females and males were used for establishing transgenic mouse lines for BAC constructs 1-F07 and 1-F09. However, our success rate of obtaining transgenic founders was very low, 1.5% and 2.5% for the 1-F07 and 1-F09 BAC constructs, respectively (Table 5.3). We decided to attempt to improve our transgenic success rate by changing our mating strategy and switching from using mice of the BALB/c background to strains with higher rates of superovulation and increased sperm counts. Mouse strains that produce large litters increase the likelihood of obtaining transgenic founders. BALB/cJ female mice produce 14 oocytes (on average), while BALB/cByJ females produce 34 oocytes (on average) (Byers et al., 2006). Therefore, to increase our chances of obtaining transgenic founders, we switched to using BALB/cByJ females as egg donors. Like BALB/c mice, BALB/cByJ and A/J mice are also resistant to MAV-1 infection (Fig. 5.3 and Spindler et al., 2001). (BALB/cJ X A/J)F_1 males were used as stud males because F_1 males have hybrid vigor and their sperm counts should be higher

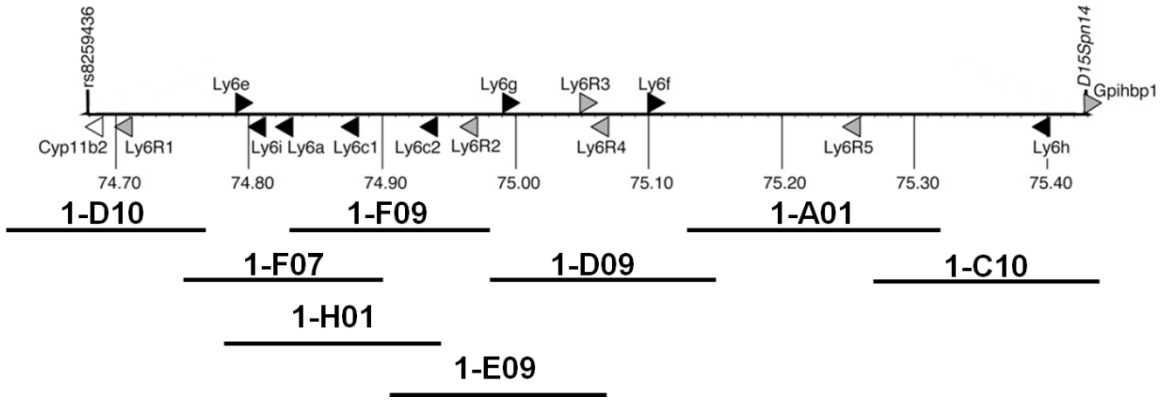

Figure 5.2. Physical map of *Msq1* and location of BACs. This is a representation of the critical interval with the candidate genes. Physical map positions are indicated in Mb (NCBI build 37). D15Spn14 is a genomic short sequence length polymorphism and rs8259436 is a single nucleotide polymorphism; together they define the ends of *Msq1*. *Ly6* genes are represented by black triangles, *Ly6*-related genes by gray triangles, and the gene encoding a cytochrome is indicated by a white triangle. BACs used to generate transgenic mice are shown below (Figure modified from Spindler et al., 2010).

Table 5.3 Transgenic mouse strains.

Construct	# tested for transgene	# of founders	% success	Phenotype	BAC integrity	Expression
1-F09	80	2	2.5	Resistant	Intact in both strains	Low expression
1-F07	66	1	1.5	Resistant	Not intact	No expression
1-D09	38	3	7.9	Resistant	Intact (1) Not intact (1)	-
1-D10	180	2	1.1	Resistant	-	-
1-A01	51	3	5.9	Resistant	-	-
1-C10	81	3	3.7	Resistant	-	-
1-H01	131	1	0.8	In progress	-	-
1-E09[a]	-	-	-	Not tested	-	-

[a]This BAC was submitted to the transgenic animal model core, but pups have not been born yet.

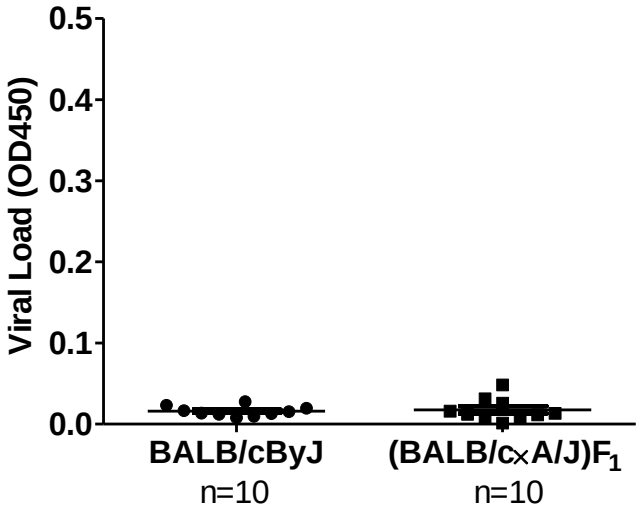

Figure 5.3. BALB/cByJ and (BALB/c×A/J)F_1 mice are resistant to MAV-1 infection. Mice of the indicated strains were infected with 10^2 PFU MAV-1, and brains were harvested 8 dpi. Brain viral loads were measured using capture ELISA. Each symbol represents the mean of three replicate measurements for each mouse. The number of mice is indicated.

compared to inbred males. When (BALB/c×A/J)F_1 mice were infected with MAV-1, they had low brain viral loads (Fig. 5.3), demonstrating that they would be a suitable MAV-1 resistant background strain for the BAC transgenesis approach.

Therefore, BALB/cByJ females and (BALB/c×A/J)F_1 stud males were used to establish transgenic mouse lines for BAC constructs 1-D09, 1-D10, 1-C10, 1-A01, 1-H01, 1-E09. The success rate of obtaining transgenic mice for these BACs ranged from 0.8% to 7.9% and was on average higher than that of using BALB/c mice as the egg donors and stud males.

Seven of the eight BAC transgenes do not complement the MAV-1 susceptibility phenotype. Tail biopsies were obtained and tail DNA used for detection of the integration of relevant BAC transgenes. Mice that were positive for the presence of the BAC transgene were identified, weaned and bred to non-transgenic littermate mice. We established a separate transgenic line for each transgenic founder mouse. The N_1 offspring were then tested for the presence of the transgene. N_1 male and female transgenic offspring from the same transgenic line were then mated in attempt to produce mice that were homozygous for the transgene. These intercrosses produced mice that were homozygous for the transgene, heterozygous transgenic mice, and non-transgenic littermates. If transgenic mice belonging to only one sex were available, mating pairs were set up with non-transgenic littermates to produce progeny that were heterozygous for the transgene and non-transgenic littermates. Subsequent matings were then set up with the goal of eventually generating a homozygous transgenic line for each founder mouse. Any additional mice that were not used for mating were phenotyped for their

susceptibility to MAV-1. These included mice of all three possible genotypes; in reporting the phenotypic data, we did not differentiate between transgenic mice that were homozygous or heterozygous for the transgene because we did not observe any differences in phenotype.

Homozygous and heterozygous progeny for the various transgenic strains were infected with MAV-1 and evaluated for their susceptibility to MAV-1. Brain viral loads were used as a surrogate measure for susceptibility. We expected to see high viral loads if the transgene contains the susceptibility gene(s). However, the mice of 7 different BAC transgene strains did not have high brain viral loads upon MAV-1 infection (Fig. 5.4). In contrast, control mice (either 129S6/SvEvTac or C.SJL-Msq1^{SJL} mice) that are susceptible had high brain viral loads after MAV-1 infection. Our results suggest that none of the transgenes were capable of conferring susceptibility, since none of the mice had high brain viral loads following MAV-1 infection.

The resistant phenotype of the transgenic mice could be a result of the following possibilities. First, the resistant phenotype could be a real result; i.e., none of the BACs are able to confer the susceptibility phenotype. This could be because genes on more than one BAC are necessary to confer the susceptibility phenotype; we may not have the right combination of susceptibility genes on any individual BAC. It is also possible that the entire 0.75 Mb region of *Msq1* is required for susceptibility. Second, it is possible that the transgenes are not being expressed. We will need to ensure that the BACs in the transgenic lines are intact and have not fragmented. Lack of expression could also be due to the absence of the necessary cis-regulatory regions. It is also possible that the

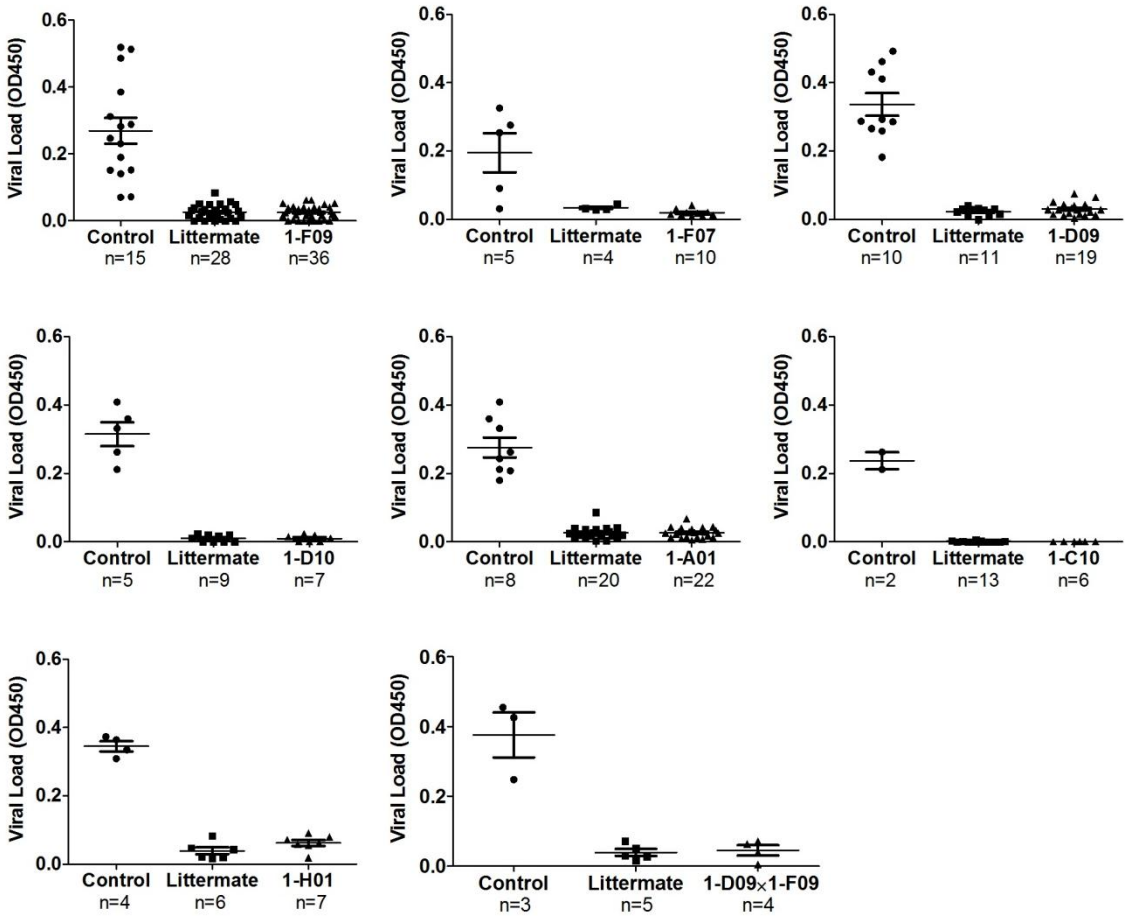

Figure 5.4 All tested transgenic mice were resistant to MAV-1. Mice of the indicated strains were infected with 10^2 PFU MAV-1, and brains were harvested 8 dpi. Controls were mice that are susceptible to MAV-1; littermates are non-transgenic progeny from the transgenic strains. Viral loads in brain homogenates were measured using capture ELISA. Each symbol represents the mean of three measurements per homogenate for an individual mouse; the number of mice is indicated below the axis. The mean and SD are indicated.

expression of transgenes is dependent on the BAC transgene integration site in the mouse chromosome.

The 1-F07 transgenic mouse strain may not have the entire BAC sequence. Our identification of transgenic founder mice included the assessment of whether the ends of each BAC were present, but not whether the middle of the BAC was also present. To determine whether the BAC transgenes are present in their entirety in the transgenic strains, we PCR amplified and sequenced DNA from the founder mice and F_2 transgenic progeny for single nucleotide polymorphisms (SNPs) between 129S6/SvEvTac and the background strain (either BALB/c or BALB/cByJ×(BALB/c×A/J)F_1) (Stier and Spindler, unpublished).

We screened the 1-F07 founder mouse and 1-F07 F_2 mice for SNPs in three genes (*Ly6A*, *Ly6E*, and *Ly6C1*) that are contained within the 1-F07 BAC (Stier and Spindler, 2011). We examined these SNPs by amplifying and sequencing genomic DNAs. In the founder mouse, we were able to detect a small peak corresponding to the *Ly6C1* transgene-specific SNP, but we were unable to detect either the *Ly6A* or *Ly6E* transgene-specific SNPs. In 1-F07 F_2 mice, we were unable to detect any of the 3 transgene-specific SNPs. These data suggest that the 1-F07 transgenic line lacks a significant portion of the BAC. The resistant phenotype of 1-F07 transgenic mice may be the result of the lack of transgene expression due to the large missing region in the integrated BAC.

Two transgenic founder lines were established for the 1-F09 BAC. We screened 1-F09 founders and F_2 mice from the two lines for the presence of the transgene-specific SNP in *Ly6c1*, which is located in the central region of the 1-F09 BAC. Both 1-F09

founders and their F_2 mice had the *Ly6C1* transgenic SNP (Stier and Spindler, unpublished), indicating that the middle of the 1-F09 BAC is present in both lines.

Three transgenic founder lines were established for the 1-D09 BAC. However, only two of the lines generated transgenic progeny. We tested both 1-D09 founders and the F_2 mice from the two lines that produced progeny (1-D09-2 and 1-D09-3) for four SNPs in the following genes on 1-D09: *Ly6G*, *BC025466*, *Gm10238*, and *Ly6F* (data not shown). We detected transgene-specific SNPs in 1-D09-3 at all tested loci, indicating that the entire 1-D09 BAC is present in the 1-D09-3 transgenic line. For 1-D09-2, we were able to detect the two transgenic SNPs (in *Ly6G* and *Ly6F*) that are located near the ends of the BAC. However, the other two SNPs (in *BC025466* and *Gm10238*) located near the middle of the 1-D09 BAC were not detected. This suggests that a middle portion of the BAC is missing in 1-D09-2 mice.

1-F07 and 1-F09 BAC transgenes have either low expression or are not expressed in the transgenic strains. We also determined whether genes in the BAC transgenes were being expressed in transgenic mice. We used a ligation-PCR detection reaction to detect the relative expression of the BAC transgene in 1-F07 and 1-F09 F_2 progeny mice (Fig. 5.1). This reaction makes use of DNA ligase, which catalyzes the formation of the phosphodiester bond between nucleotides that bind to a target DNA sequence (Barany and Gelfand, 1991; Luo et al., 1996). DNA ligase is a highly specific enzyme and will only work if there is perfect complementarity between the nucleotide and the target DNA sequence. A single base mismatch is sufficient to inhibit ligation. Allele-specific primers were designed so that they differ by the SNP of interest at their 5'-end, and differ in

length by 4 nucleotides at their 3' end (Table 5.2). An additional primer, which is fluorescently labeled, common to both alleles is also used. Since the strain-specific primers were designed to be of different length, the detected products corresponding to transgene mRNA and the endogenous (background strain) mRNA can be distinguished according to length.

For both 1-F07 and 1-F09 F_2 transgenic progeny, we examined the relative expression of the *Ly6C1* BAC-derived transgene. We used primers specific for the SNP on either the BALB/c or 129S6/SvEvTac transcript (Table 5.2). As expected, we were able to detect the BALB/c transcript in all of the transgenic mice (Stier and Spindler, unpublished). The 129S6/SvEvTac *Ly6C1* transcript was detected in low levels in the 1-F09-2 transgenic strain F_2 progeny mice. However, the transgene-derived transcript was not detected in either 1-F07 or 1-F09-1 F_2 transgenic progeny. These data suggest that the transgenes were not expressed. The interpretation of the phenotyping results thus cannot be attributed to expression of the transgenes.

Mice containing both 1-F09 and 1-D09 BAC transgene constructs are resistant to MAV-1. Another possibility is that the entire *Ly6* supergene locus encompassed by *Msq1*, or a larger region than is encoded in any single BAC, is needed to confer the susceptibility phenotype. Susceptibility to MAV-1 is under multigenic control; C.SJL-Msq1 mice are less susceptible than inbred SJL mice (Hsu et al., 2012). We are currently developing mouse strains that contain more than one BAC, by mating mice from different transgenic strains. From this mating strategy, we have obtained transgenic mice that have both 1-F09 and 1-D09 transgene constructs. However, when these mice

were infected, they did not exhibit high brain viral loads (Fig. 5.4). Efforts to establish additional “double” and “triple” transgenic strains (containing 2 or 3 BACs, respectively) are underway. In addition, we will test whether we can detect transgene expression in all the strains we generate.

DISCUSSION

The BAC transgenic approach holds promise in identifying the gene(s) responsible for the susceptibility phenotype, if the phenotype corresponding to the introduced BAC is obtained. Negative results, in this case, resistant phenotypes for the BAC transgenic progeny, are more problematic. Our data demonstrate that it is necessary to interpret the resistant phenotypes of transgenic progeny mice with caution. From our data, we demonstrate in the 1-F07 transgenic line that the BAC construct is not intact. We also demonstrate in 1-F09 transgenic lines that insertion of the BAC construct does not guarantee expression of the transgenes. Transgenic mice will thus need to be carefully characterized for both the integrity of the inserted BAC and also the expression of the individual transgenes.

Both 1-F09 transgenic lines have intact 1-F09 BAC constructs. However, we were only able to detect the *Ly6C1* transcript in one. It is also possible this was result of where the BACs had integrated in the genome. Differences in the integration site of a transgene can lead to variable gene expression (Weis et al., 1991), which may be an obstacle to the study of gene function in our locus. Position effects can manifest in several different ways, including unintended sites of expression, no transgene expression, decreasing

transgene expression over generations, and expression of the transgene in only a subset of cells.

It is also possible that the difference we see between the two 1-F09 transgenic lines is a result of having different copy numbers of 1-F09 BAC integrate into the mouse genomes. In addition, homologous recombination between BACs can occur prior to integration events to form a tandem array (Rulicke and Hubscher, 2000). High copy numbers of integration can cause repeat-mediated gene silencing. Phenotype analysis can also be complicated if the transgene integration event disrupts endogenous gene expression (Meisler, 1992). It is therefore important to establish more than one transgenic line for a transgene to determine that the phenotypes can be attributed to the introduction of the transgene and not other integration site effects.

Circular BAC DNA was used in the microinjection because the additional steps to free the linear DNA from the cloning vector require manipulations of the BAC DNA that may contribute to DNA shearing and lower BAC yields (Van Keuren et al., 2009). There is also no evidence that there is an advantage for use of linear over circular BACs, since they generate approximately the same transgenesis efficiency and expression outcome. However, it is possible that injection of circularized DNA could result in random breaks within the BAC, resulting in interruption of genes or cis-regulatory regions.

Expression of a BAC transgene can also be affected by whether all transcription regulatory elements are present in the BAC (Huber et al., 1994). Cis-regulatory elements (enhancers, insulators and locus control regions) cooperate with each other. For the chicken lysozyme gene locus, the concerted action of all cis-regulatory elements is necessary for integration site-independent expression, regardless of copy number of

integrated transgenes (Huber et al., 1994). It is therefore possible that the absence of a complete genetic context in our transgenic mice could have affected BAC transgene expression levels, and accordingly, the tested phenotype. Selection of future BACs should include as much of the sequence leading up to the gene of interest as possible.

It is possible to modify BAC DNA using homologous recombination, without causing additional rearrangements or deletions in the modified BAC (Court et al., 2002; Yang et al., 1997). This method can be useful in adding genotyping markers and introducing deletions, mutations and insertions into BACs. Addition of genotyping markers can aid verification that the integrated BAC is intact. Also, a reporter gene such as *lacZ* or GFP can facilitate determination of whether genes are being properly expressed in the relevant tissues. Because we are interested in more than one candidate gene within each BAC, it would be necessary to insert more than one reporter gene into the BAC construct at different positions in order to ensure that transgenes throughout the BAC are expressed. Insertions of cell type-specific promoters can also direct transgene expression in defined organs, tissues or cells.

A limitation to extrapolating data obtained from inbred mouse models to human disease is that humans experience greater genetic heterogeneity, and this inevitably complicates the assessment of the contribution of a particular QTL. A single gene, *Nramp1* (annotated *Slc11a1*), is responsible for the susceptibility difference between specific inbred mouse strains to *Mycobacterium bovis*, the causative agent of tuberculosis in cattle, and a number of additional bacterial species (Bradley, 1977; Plant and Glynn, 1976; Skamene et al., 1982; Skamene et al., 1984; Vidal et al., 1993). The contribution of this gene to susceptibility in humans was less dramatic; the modest contribution of

Slc11a1 in humans was in contrast to the major effect the gene had in mice (Remus et al., 2003). To determine the role of *Msq1* in the presence or absence of other potentially contributing loci, complementation of the susceptibility phenotype can be attempted on different mouse strain backgrounds

Notes

Matt Stier performed the sequencing experiments that examined BAC integrity in 1-D09, 1-F09 and 1-F07 transgenic mice, and he also performed the ligation detection experiments which examined *Ly6C1* expression levels in 1-F09 and 1-F07 mice. Figure 5.1 and Table 5.2 were modified from his University of Michigan undergraduate honors thesis. We are grateful for Dave Burke and his lab members for their assistance in experimental design and loan of equipment for the ligation-detection experiments.

We acknowledge Wanda Filipiak and Maggie van Keuren for preparation of transgenic mice, Thom Saunders for advice on BAC transgenesis, and the Transgenic Animal Model Core of the University of Michigan's Biomedical Research Core Facilities. Core support was provided by the University of Michigan Cancer Center, NIH grant number CA46592 and the University of Michigan Multipurpose Arthritis Center, NIH grant number AR20557. We thank Tyson Luoma for bioinformatics analysis of the CHORI BAC library sequencing data. We are also grateful to Brad Harlan, Kaveri Rajula, Michelle Passater, and Samantha Sayers for husbandry and genotyping of the transgenic mouse strains.

This work was supported by NIH R01 AI068645 to K.R.S. T.-H. Hsu has been supported by NIH National Research Service Award T32 GM07544, a University of

Michigan (U-M) Rackham Graduate School Merit Fellowship and two Rackham graduate student research grants; a U-M Frances Wang Chin fellowship, and the U-M Endowment for the Development of Graduate Education award. The funders had no role in study design, data collection and analysis, decision to publish, or preparation of the manuscript.

References

Bamezai, A. (2004). Mouse Ly-6 proteins and their extended family: markers of cell differentiation and regulators of cell signaling. *Arch Immunol Ther Exp (Warsz)* 52, 255-266.

Barany, F., and Gelfand, D.H. (1991). Cloning, overexpression and nucleotide sequence of a thermostable DNA ligase-encoding gene. *Gene* 109, 1-11.

Bradley, D.J. (1977). Regulation of Leishmania populations within the host. II. genetic control of acute susceptibility of mice to Leishmania donovani infection. *Clin Exp Immunol* 30, 130-140.

Brass, A.L., Dykxhoorn, D.M., Benita, Y., Yan, N., Engelman, A., Xavier, R.J., Lieberman, J., and Elledge, S.J. (2008). Identification of host proteins required for HIV infection through a functional genomic screen. *Science* 319, 921-926.

Byers, S.L., Payson, S.J., and Taft, R.A. (2006). Performance of ten inbred mouse strains following assisted reproductive technologies (ARTs). *Theriogenology* 65, 1716-1726.

Court, D.L., Sawitzke, J.A., and Thomason, L.C. (2002). Genetic engineering using homologous recombination. *Annu Rev Genet* 36, 361-388.

Frengen, E., Weichenhan, D., Zhao, B., Osoegawa, K., van Geel, M., and de Jong, P.J. (1999). A modular, positive selection bacterial artificial chromosome vector with multiple cloning sites. *Genomics* 58, 250-253.

Giraldo, P., and Montoliu, L. (2001). Size matters: use of YACs, BACs and PACs in transgenic animals. *Transgenic Res* 10, 83-103.

Gumley, T.P., McKenzie, I.F., and Sandrin, M.S. (1995). Tissue expression, structure and function of the murine Ly-6 family of molecules. *Immunol Cell Biol* 73, 277-296.

Hoskins, R.A., et al. (2000). A BAC-based physical map of the major autosomes of Drosophila melanogaster. *Science* 287, 2271-2274.

Hsu, T.H., Althaus, I.W., Foreman, O., and Spindler, K.R. (2012). Contribution of a single host genetic locus to mouse adenovirus type 1 infection and encephalitis. *MBio* 3(3), e00131–12–e00131–12. doi:10.1128/mBio.00131-12.

Huber, M.C., Bosch, F.X., Sippel, A.E., and Bonifer, C. (1994). Chromosomal position effects in chicken lysozyme gene transgenic mice are correlated with suppression of DNase I hypersensitive site formation. *Nucleic Acids Res* 22, 4195-4201.

Krishnan, M.N., Ng, A., Sukumaran, B., Gilfoy, F.D., Uchil, P.D., Sultana, H., Brass, A.L., Adametz, R., Tsui, M., Qian, F., Montgomery, R.R., Lev, S., Mason, P.W., Koski, R.A., Elledge, S.J., Xavier, R.J., Agaisse, H., and Fikrig, E. (2008). RNA

interference screen for human genes associated with West Nile virus infection. *Nature* 455, 242-245.

Lee, S.H., Zafer, A., de Repentigny, Y., Kothary, R., Tremblay, M.L., Gros, P., Duplay, P., Webb, J.R., and Vidal, S.M. (2003). Transgenic expression of the activating natural killer receptor Ly49H confers resistance to cytomegalovirus in genetically susceptible mice. *J Exp Med* 197, 515-526.

Liu, H.C., Niikura, M., Fulton, J.E., and Cheng, H.H. (2003). Identification of chicken lymphocyte antigen 6 complex, locus E (LY6E, alias SCA2) as a putative Marek's disease resistance gene via a virus-host protein interaction screen. *Cytogenet Genome Res* 102, 304-308.

Loeuillet, C., Deutsch, S., Ciuffi, A., Robyr, D., Taffe, P., Munoz, M., Beckmann, J.S., Antonarakis, S.E., and Telenti, A. (2008). In vitro whole-genome analysis identifies a susceptibility locus for HIV-1. *PLoS Biol* 6, e32.

Luo, J., Bergstrom, D.E., and Barany, F. (1996). Improving the fidelity of Thermus thermophilus DNA ligase. *Nucleic Acids Res* 24, 3071-3078.

McPherson, J.D., et al. (2001). A physical map of the human genome. *Nature* 409, 934-941.

Meisler, M.H. (1992). Insertional mutation of 'classical' and novel genes in transgenic mice. *Trends Genet* 8, 341-344.

Morgan, R.W., Sofer, L., Anderson, A.S., Bernberg, E.L., Cui, J., and Burnside, J. (2001). Induction of host gene expression following infection of chicken embryo fibroblasts with oncogenic Marek's disease virus. *J Virol* 75, 533-539.

Mozo, T., Dewar, K., Dunn, P., Ecker, J.R., Fischer, S., Kloska, S., Lehrach, H., Marra, M., Martienssen, R., Meier-Ewert, S., and Altmann, T. (1999). A complete BAC-based physical map of the Arabidopsis thaliana genome. *Nat Genet* 22, 271-275.

Nagy, A. (2003). "Manipulating the mouse embryo : a laboratory manual." 3rd ed. Cold Spring Harbor Laboratory Press, Cold Spring Harbor, N.Y.

Osoegawa, K., Tateno, M., Woon, P.Y., Frengen, E., Mammoser, A.G., Catanese, J.J., Hayashizaki, Y., and de Jong, P.J. (2000). Bacterial artificial chromosome libraries for mouse sequencing and functional analysis. *Genome Res* 10, 116-128.

Plant, J., and Glynn, A.A. (1976). Genetics of resistance to infection with Salmonella typhimurium in mice. *J Infect Dis* 133, 72-78.

Potter, T.A., McKenzie, I.F., Morgan, G.M., and Cherry, M. (1980). Murine lymphocyte alloantigens. I. The Ly-6 locus. *J Immunol* 125, 541-545.

Remus, N., Alcais, A., and Abel, L. (2003). Human genetics of common mycobacterial infections. *Immunol Res* 28, 109-129.

Rulicke, T., and Hubscher, U. (2000). Germ line transformation of mammals by pronuclear microinjection. *Exp Physiol* 85, 589-601.

Schoggins, J.W., Wilson, S.J., Panis, M., Murphy, M.Y., Jones, C.T., Bieniasz, P., and Rice, C.M. (2011). A diverse range of gene products are effectors of the type I interferon antiviral response. *Nature* 472, 481-485.

Shizuya, H., Birren, B., Kim, U.J., Mancino, V., Slepak, T., Tachiiri, Y., and Simon, M. (1992). Cloning and stable maintenance of 300-kilobase-pair fragments of human DNA in Escherichia coli using an F-factor-based vector. *Proc Natl Acad Sci U S A* 89, 8794-8797.

Skamene, E., Gros, P., Forget, A., Kongshavn, P.A., St Charles, C., and Taylor, B.A. (1982). Genetic regulation of resistance to intracellular pathogens. *Nature* 297, 506-509.

Skamene, E., Gros, P., Forget, A., Patel, P.J., and Nesbitt, M.N. (1984). Regulation of resistance to leprosy by chromosome 1 locus in the mouse. *Immunogenetics* 19, 117-124.

Spindler, K.R., Fang, L., Moore, M.L., Hirsch, G.N., Brown, C.C., and Kajon, A. (2001). SJL/J mice are highly susceptible to infection by mouse adenovirus type 1. *J Virol* 75, 12039-12046.

Spindler, K.R., Welton, A.R., Lim, E.S., Duvvuru, S., Althaus, I.W., Imperiale, J.E., Daoud, A.I., and Chesler, E.J. (2010). The major locus for mouse adenovirus susceptibility maps to genes of the hematopoietic cell surface-expressed LY6 family. *J Immunol* 184, 3055-3062.

Stier, M.T. (2011). Undergraduate honors program. University of Michigan, Ann Arbor.

Stier, M.T., and Spindler, K.R. (2011). Polymorphisms in Ly6 genes in Msq1 encoding susceptibility to mouse adenovirus type 1. *Mamm Genome*.

Van Keuren, M.L., Gavrilina, G.B., Filipiak, W.E., Zeidler, M.G., and Saunders, T.L. (2009). Generating transgenic mice from bacterial artificial chromosomes: transgenesis efficiency, integration and expression outcomes. *Transgenic Res* 18, 769-785.

Venter, M., Myers, T.G., Wilson, M.A., Kindt, T.J., Paweska, J.T., Burt, F.J., Leman, P.A., and Swanepoel, R. (2005). Gene expression in mice infected with West Nile virus strains of different neurovirulence. *Virology* 342, 119-140.

Vidal, S.M., Malo, D., Vogan, K., Skamene, E., and Gros, P. (1993). Natural-resistance to infection with intracellular parasites - isolation of a candidate for Bcg. *Cell* 73, 469-485.

Weis, J., Fine, S.M., David, C., Savarirayan, S., and Sanes, J.R. (1991). Integration site-dependent expression of a transgene reveals specialized features of cells associated with neuromuscular junctions. *J Cell Biol* 113, 1385-1397.

Welton, A.R., Chesler, E.J., Sturkie, C., Jackson, A.U., Hirsch, G.N., and Spindler, K.R. (2005). Identification of quantitative trait loci for susceptibility to mouse adenovirus type 1. *J Virol* 79, 11517-11522.

Welton, A.R., and Spindler, K.R. (2007). Capture ELISA quantitation of mouse adenovirus type 1 in infected organs. *Methods Mol Med* 130, 215-221.

Yang, X.W., Model, P., and Heintz, N. (1997). Homologous recombination based modification in Escherichia coli and germline transmission in transgenic mice of a bacterial artificial chromosome. *Nat Biotechnol* 15, 859-865.

Chapter VI

Discussion

Chapter summary

Susceptible mouse strains develop dose-dependent hemorrhagic encephalitis following mouse adenovirus type 1 (MAV-1) infection (Guida et al. 1995; Kring et al. 1995; Charles et al. 1998; Kajon et al. 1998; Spindler et al. 2001; Spindler et al. 2007). In the work described here, we examined the contribution of MAV-1 susceptibility quantitative trait locus (*Msq1*) to MAV-1-induced pathogenesis and encephalitis. We also attempted to uncover the identity of the susceptibility gene(s) within *Msq1* through a bacterial artificial chromosome (BAC) transgenesis approach.

In Chapter VI, we characterized the role of *Msq1*, a 0.75 Mb quantitative trait locus (QTL) strongly linked to the high brain viral load phenotype in MAV-1-infected mice (Welton et al. 2005; Spindler et al. 2010). Through comparison studies using resistant BALB/c mice, susceptible SJL mice, and mice congenic for $Msq1^{SJL}$ on a BALB/c background (C.SJL-Msq1), we determined that *Msq1* is a key determinant of the outcome of MAV-1 infection. *Msq1* controls in large part the ability of the virus to replicate in brains of mice, the development of blood-brain barrier (BBB) permeability during MAV-1 infection, brain pathology, the recruitment of specific subsets of immune cells, and the ability to maintain barrier function in *ex vivo* infection. However, the locus does not account for the full extent of susceptibility in SJL mice; C.SJL-Msq1 mice are less susceptible than SJL mice. In addition, *Msq1* does not control the development of

cerebral vascular edema following MAV-1 infection. These data are consistent with our previous findings that susceptibility to MAV-1 is under multigenic control.

In Chapter V, we attempted to reduce the size of the critical interval for susceptibility to MAV-1 using a BAC transgenesis approach by introducing BACs generated from a susceptible strain as transgenes onto a resistant strain background. Because susceptibility is semi-dominant (Welton et al. 2005), we expected that the introduction of a transgene containing the susceptibility gene(s) would cause the transgenic mouse to be susceptible to MAV-1 infection. However, to date, introduction of BACs from the *Msq1* interval has not resulted in susceptible mice. Current efforts to assess BAC integrity and determine whether the transgenes within the BACs are being expressed within the transgenic strains have revealed additional difficulties we will need to overcome.

One transgenic mouse strain (1-F07) did not carry an intact BAC. Two 1-F09 transgenic lines both had the entire BAC sequence; but they had different expression levels of the *Ly6C1* transgene. In one, expression of the transgene was low, while in the other, we were unable to detect expression of *Ly6C1*. Unsurprisingly, we also could not detect *Ly6C1* expression in 1-F07 mice that do not have the complete BAC construct. We will continue to determine whether our transgenic strains contain intact BAC constructs, and if the transgenes within those constructs are being expressed. Without this information, we are unable to evaluate the relative phenotypic contribution of the different transgenes.

Defining the congenic interval

The C.SJL-Msq1 interval-specific congenic strain was constructed using an initial BALB/c and SJL cross, with subsequent repeated backcrosses to BALB/c mice (Hsu et al. 2012). Following each cross, progeny positive for *Msq1*^{SJL} were selected for the next breeding pair using two single nucleotide polymorphism (SNP) markers that flank the boundaries based on fine mapping of *Msq1* (Spindler et al. 2010; Hsu et al. 2012). The current *Msq1* interval spans from 74.68 to 75.43 Mb on mouse chromosome 15 (Chr 15). At the N_{11} generation, congenic mice have a genome that is 99.9% BALB/c-derived. The 0.1% SJL contribution includes *Msq1*, loci immediately adjacent to *Msq1* that got carried forward due to their proximity to the selected locus, and any additional scattered SJL-derived remnant passenger loci throughout the genome. To rule out the possibility that genes outside of *Msq1* are responsible for the phenotypes we have observed in our congenic mouse strain, we will need to identify any additional loci outside of *Msq1* in our C.SJL-Msq1 strain.

To determine the extent of the congenic interval, i.e., the amount of genome sequence outside of the region defined by the two SNP markers, we are using the JAX mouse diversity genotyping array. We submitted a single tail of a C.SJL-Msq1^{SJL} mouse from the N_{11} generation to the Jackson Laboratory for the diversity array analysis, from which high quality DNA was prepared and genome-wide profiling of SNPs was performed. This array uses genome-wide profiling of densely spaced SNPs that are present among mouse strains to determine the BALB/c and SJL strain contributions across the entire genome of our congenic mouse strain. Over 625,000 SNPs were assayed and the results have been provided to us, and await bioinformatics analysis.

We will compare the SNP identity of the congenic mouse strain to that of C57BL/6 mice. The bioinformatics report for our data will allow us to determine whether each SNP site is in one of the following categories: (i) identical to C57BL/6, (ii) identical to the next most common genotype not associated with C57BL/6, (iii) heterozygous, or (iv) a missing call (none of the above). We will only be able to identify strain contributions for any given SNP site if the BALB/c and SJL genotypes are in different categories from one another. There is a possibility that in many regions, we will be unable to determine if the specific SNP is BALB/c- or SJL-derived, for example, if both SJL and BALB/c SNPs are identical to the C57BL/6 SNP. However, the SNPs used in the array are on average 4.3 kb apart on the C57BL/6 mouse background, which should be dense enough to determine the approximate size of the *Msq1* interval and flanking SJL-derived sequence. Specifically, we would like to rule out the possibility that APOBEC3 (Chr 15, ~79.9 Mb) plays a role in susceptibility. Members of the human *APOBEC3* gene family play roles in *in vivo* cellular immune function against several different viruses, including HIV, hepatitis B and human papillomavirus, through genetic editing of single-stranded DNA (Zhang et al. 2003; Suspene et al. 2005; Vartanian et al. 2008; Malim 2009).

Genetic loci outside of *Msq1* also contribute to the susceptibility phenotype

Use of C.SJL-Msq1 mice allowed us to examine the genetic contribution of $Msq1^{SJL}$ in the absence of any additional SJL genes from other loci that may act in an additive manner with regard to susceptibility. *Msq1* accounts for 40% of the variance in the viral brain load phenotype between SJL and BALB/c mice (Welton et al. 2005),

which is a substantial contribution by a single genetic locus. Accordingly, MAV-1-infected C.SJL-Msq1 mice have comparable brain viral loads to similarly infected SJL mice. However, C.SJL-Msq1 mice are not as susceptible as SJL mice to MAV-1 infection, based on survival and LD_{50} (Hsu et al. 2012). C.SJL-Msq1 mice also do not have the severe vasogenic edema seen in SJL mice (Hsu et al. 2012). This was surprising, because C.SJL-Msq1 and SJL mice have similar levels of BBB disruption as measured by sodium fluorescein and Evans blue dye uptake into brain tissues.

It is possible that at the BBB, passage of water molecules is regulated differently from the movement of sodium fluorescein and Evans blue molecules across the barrier. In addition, opening of the blood-brain barrier may be either transient or prolonged, resulting in differences in the amount of water that is able to pass through the BBB or the ability of the strains to control brain water content. The data suggest that occurrence of edema correlates well with death, while high brain viral loads and increased BBB permeability do not necessitate death. These data are consistent with findings for lymphocytic choriomeningitis virus infection, where edema and brain herniation due to increased intracranial pressure are the causes of death, not BBB disruption (Matullo et al. 2010). While we cannot rule out the contribution of BBB disruption to MAV-1 disease, from our current data, it appears that edema is a more significant factor in MAV-1 mortality.

The data also indicate that there are additional genes outside of *Msq1* that contribute to MAV-1 susceptibility. These could be additional genes that are involved in conferring susceptibility independent of *Msq1*, or genes that have additive effect in conjunction with *Msq1* to produce the full susceptibility phenotype. In support of the

hypothesis that susceptibility to MAV-1 is multigenic, we previously identified a minor QTL on mouse Chr5 during our mapping analysis that has additive effect on the brain viral load phenotype (Welton et al. 2005). Together, *Msq1* and the Chr5 locus account for 41.7% of the trait variance. We could test whether the Chr5 QTL could be involved in the increased edema seen in SJL mice, thus contributing to the susceptibility phenotype. We would do so by introgressing the Chr5 interval onto the C.SJL-Msq1 background, thus creating a congenic strain specific for both $Msq1^{SJL}$ and the SJL-derived Chr 5 interval.

Msq1 is introgressed onto a resistant strain background, which may have genes that counteract the susceptibility phenotype of *Msq1*. Therefore, it may be useful to construct an interval-specific congenic strain with $Msq1^{BALB}$ on a SJL background (SJL.C-Msq1). We would expect mice of this genotype to have low brain viral loads and thus be phenotypically resistant to MAV-1 infection. If the SJL.C-Msq1 congenic strain is more susceptible than BALB/c mice in survival assays, the difference could be attributed to (SJL) genes outside of *Msq1*. However, it is also possible that susceptibility requires the additive effect of multiple genetic loci, such that in the absence of the major susceptibility QTL $Msq1^{SJL}$, the mice may still be resistant to MAV-1 infection.

Role of CNS infiltrating inflammatory cells during MAV-1 infection

The host immune response is important for effective control and clearance of viral infections. Following MAV-1 infection, there are differences among the number of immune cells that are recruited to the brains of C.SJL-Msq1, BALB/c and SJL mice (Hsu et al. 2012). In the brains of BALB/c mice, in which viral loads are low, there is no significant increase in any of the immune cell subsets that we examined upon MAV-1

infection. In both SJL and C.SJL-Msq1 mice upon infection, there is a significant increase in the total number of cells infiltrating into the brain. For SJL mice, there is a large CNS infiltration of the following cell populations: $CD4^+$ and $CD8^+$ T cells, macrophages, inflammatory monocytes and neutrophils. For C.SJL-Msq1 mice, there is an equally large increase for macrophages as in SJL mice. However, the increase for the other cellular subsets (T cells, inflammatory monocytes and neutrophils) is modest compared to SJL mice. Finally, in mice of all three strains, the number of B cells in brains of mice following MAV-1 infection does not change significantly. These strain differences in CNS infiltrate suggest that immune cells are involved in MAV-1-induced pathology and mortality. We discuss potential contributions of monocytic cells, neutrophils, T cells and B cells in the following sections.

Monocytic cells and MAV-1 infection

Cells of the monocyte lineage can be productively infected at low levels with MAV-1, which suggests that they may be involved in dissemination of virus (Kajon et al. 1998; Ashley et al. 2009). Macrophages are recruited in large numbers to the brains of infected SJL, C.SJL-Msq1 and C57BL/6 mice; however, macrophages were not recruited to the brain in BALB/c mice (Gralinski et al. 2009; Hsu et al. 2012). These data are consistent with previous findings that MAV-1-infected CCR2-/- mice (on a BALB/c background), which are defective in macrophage recruitment, show no differences in survival or brain and spleen viral loads compared to wt BALB/c mice. Brain and spleen viral loads in both strains were low. It is possible that the presence of resident macrophages in the peritoneum is sufficient to protect against viral replication, since

CCR2-/- mice are only deficient in macrophage recruitment, and the levels of macrophages in the peritoneum of wild type (wt) and CCR2-/- mice are similar. However, it is also likely that macrophages simply do not get recruited to the brain in infected BALB/c mice.

Macrophage precursors, inflammatory monocytes, are also present in increased numbers in the brains of MAV-1-infected SJL mice. Inflammatory monocytes can be differentiated from circulating monocytes based on their differential expression of LY6C (Gordon and Taylor 2005). During West Nile virus infection, $LY6C^{(hi)}$ inflammatory monocytes that migrate into the CNS can differentiate into microglia (Getts et al. 2008). This is significant because although immunohistochemical staining of MAV-1 infected CNS tissues from susceptible C57BL/6 mice showed presence of virus primarily in the vascular endothelium, weak staining (corresponding to the presence of virus) was also seen in microglial cells (Charles et al. 1998). The authors attributed the staining seen in microglial cells to be a result of the phagocytosis of cell debris from infected cells that were lysed. However, the West Nile virus data suggest an alternative hypothesis that inflammatory monocytes migrate to the MAV-1-infected CNS and differentiate into microglia or macrophages. It is possible that this is how MAV-1 is able to access the brain. It may be informative to sort the recruited inflammatory monocyte cells from SJL and C.SJL-Msq1 mice by flow cytometry and determine whether they have been infected with MAV-1. We can also infect mice with GFP-labeled MAV-1, isolate brain leukocytes, gate on $Ly6C^{(hi)}CD11b^{+}$ cells and determine whether they are positive for GFP.

Because monocytic cells are key effector cells of the innate immune system, it is also probable that macrophages are responsible for controlling MAV-1 infection. BALB/c mice that are depleted of spleen, liver, lymph node and peritoneal macrophages via treatment with clodronate-loaded liposomes have high spleen viral loads following MAV-1 infection, but brain viral loads are low (Van Rooijen 1989; Ashley et al. 2009). This is in contrast to untreated BALB/c mice (with normal macrophage levels), in which spleen and brain viral loads are low. These data suggest that macrophages serve a protective function in controlling viral replication in the spleens of BALB/c mice. To explain the low viral loads observed in the brains of BALB/c clodronate-treated mice, it is feasible that the presence of resident macrophages may be sufficient to control viral replication, since clodronate-loaded liposomes are unable to deplete brain macrophages (Van Rooijen 1989). Alternatively, perhaps viral infection is effectively controlled in the spleen, even in macrophage-depleted BALB/c mice, and thus does not disseminate to the brain. Finally, it is also possible that macrophages are not recruited to the brain in BALB/c mice.

High viral loads are seen in the brains and spleens in both wt and clodronate-loaded liposome treated SJL mice (Ashley et al. 2009; Hsu et al. 2012). These data suggest that the macrophage response is neither protective against nor effective at controlling the dissemination of MAV-1 infection in SJL mice. In addition, since virus is able to reach the brain of SJL mice even in the absence of macrophages, it suggests that another cell type is also involved in MAV-1 dissemination to the brain.

Neutrophils and MAV-1 infection

After MAV-1 infection, there is a large neutrophil infiltrate in SJL mice, an intermediate increase in neutrophil number in C.SJL-Msq1 mice, and no change in BALB/c mice. Neutrophils contribute to the loss of BBB permeability during mouse hepatitis virus infection (Zhou et al. 2003). We have not formally tested the role of neutrophils in MAV-1 brain pathogenesis. However, similar levels of BBB disruption are seen between C57BL/6 mice infected with a MAV-1 virus that is null for an early region 3 (E3) protein and mice infected with wild-type MAV-1, despite the former having reduced CNS infiltation of $CD8^+$ T cells and B cells, but equivalent numbers of $CD4^+$ T cells, macrophages and neutrophils. It is therefore possible that neutrophils are involved in BBB disruption during MAV-1 infection. Contribution of these immune cells can be better studied by antibody depletion of neutrophils.

T and B cells and MAV-1 infection

The functions played by T and B cells during MAV-1 infection have been examined in various immune-deficient mouse strains. RAG-$1^{-/-}$ mice, which lack both T and B cells, are more susceptible to MAV-1 infection than control C57BL/6 mice (Moore et al. 2003). SCID mice, also T and B cell deficient, are also more susceptible to MAV-1 (Pirofski et al. 1991). In addition, mice lacking α/β T cells eventually succumb to MAV-1 infection (Moore et al. 2003). These mice have high brain and spleen viral loads and are unable to clear virus, in contrast to control C57BL/6 mice in which virus is undetectable by 12 days post infection (dpi). Surprisingly, the presence of either $CD4^+$ or $CD8^+$ effector T cells is sufficient for T cell-mediated clearance of MAV-1. However, cytotoxic

$CD8^+$ T cells cause acute pathology, and contribute to MAV-1-induced encephalomyelitis (Moore et al. 2003).

Consistent with these data, the increased number of cytotoxic T cells seen during acute infection of SJL mice may contribute to extensive brain pathology and lead to mortality (Hsu et al. 2012). C57BL/6 mice, which have an intermediate susceptibility to MAV-1, also have a large increase in the number of $CD8^+$ T cells in their brains during acute infection (Gralinski et al. 2009). On the other hand, C.SJL-Msq1 mice have a more modest increase in the number of recruited $CD8^+$ T cells than SJL mice, but significant brain pathology and leakage of the blood-brain barrier (comparable to that seen in SJL mice) is also observed following infection. Depletion of T cell subsets using monoclonal antibodies may help dissect the role of $CD4^+$ and $CD8^+$ T cells in encephalomyelitis and long-term viral clearance.

Because LY6 proteins have been shown to have roles in T cell adherence and homing, it will be interesting to determine whether the differences seen in $CD8^+$ T cell migration to the brain during MAV-1 infection can be attributed to differences in LY6 protein expression levels among mouse strains. Treatment with a LY6C antibody decreases *in vivo* homing of $CD8^+$ T cells to lymph nodes in mice, and *in vitro* $CD8^+$ T cell endothelial adhesion (Hänninen et al. 1997). LY6 molecules may also be involved in activating additional adhesion molecules; crosslinking of LY6C molecules prevents homotypic aggregation of CD8+ T cells (Hänninen et al. 1997). LY6A also mediates cell-cell adhesion in thymocytes (Bamezai and Rock 1995).

T cell adherence is an important step toward generation of effector T cells and a cellular immune response. We have been examining whether there are strain differences

in the ability of T cells to adhere to primary mouse brain endothelial cells in BALB/c, SJL and C.SJL-Msq1 mice (Edewaard, Hsu, and Spindler, unpublished). Since LY6 proteins are expressed on both T cells (Shevach and Korty 1989; Walunas et al. 1995) and pmBECs (Chapter IV, Fig. 4.10), we will subsequently determine whether LY6 proteins on either cell type mediate the T cell adhesion differences, using an antibody blocking approach.

B cells are necessary for survival of acute MAV-1 infection (Moore et al. 2004). μMT mice, which lack B cells, are more susceptible to MAV-1 than C57BL/6 mice, dying early (7 to 10 dpi) with high brain and spleen viral loads. Bruton's tyrosine kinase (Btk)-deficient mice also succumb to MAV-1 infection, demonstrating that an antibody response is necessary for protection against MAV-1. We do not see a difference between resistant BALB/c and susceptible SJL and C.SJL-Msq1 mouse strains with regard to B cell recruitment to the brain after infection with 10^2 PFU of MAV-1. However, when C57BL/6 mice are infected at a higher dose (10^3 PFU), there is an increase in the number of B cells in the CNS at 8 dpi (Gralinski et al. 2009). This may be a result of having a 10-fold increase in MAV-1 inoculum delivered to mice, therefore altering the kinetics of MAV-1 infection. In Chapter VI we looked at inflammatory cell recruitment at only one time point, 8 dpi. It is possible that B cells are involved at earlier or later time points. The difference in results between the Gralinski et al. study and the results in Chapter IV here could have also arisen through differences in the isolation methods for brain leukocytes, as well as differences in selecting positive populations when analyzing flow cytometry charts. With the C57BL/6 data, the total number of leukocytes was determined by

number of cells that strain positively for CD45. In contrast, in Chapter IV, we gated on the $CD45^{(hi)}$ population, which corresponds to the infiltrating leukocyte population.

Examining different immune cell subsets at a single time point and a single infection dose provides merely a snapshot of what is occurring during infection. Different cells are recruited to the brain at different rates and times post infection, and thus we likely have not detected all strain differences in immune cell recruitment in studies performed thus far. Sampling brains of infected mice from multiple time points would give us a more complete picture of the relative contributions of different immune cells. In addition, the combined number of immune cells from the subpopulations that we looked at correspond well with the total number of infiltrating cells ($CD45^{(hi)}$) in SJL but not C.SJL-$Msq1^{SJL}$ mice. There appears to be a population(s) of unaccounted for cells in C.SJL-$Msq1^{SJL}$ mice that do not express any of the markers that we examined. Cell populations we did not analyze include NK cells, dendritic cells, and mast cells. We will examine these additional cell populations in the future.

Antibody depletions of different cell types (T cells, neutrophils and B cells) may better inform our understanding of the roles immune cells play during MAV-1 infection. In another approach, we can also perform adoptive transfer of immune cells from (resistant) BALB/c mice to (susceptible) (BALB/c×SJL)F_1 mice. Using F_1 progeny instead of susceptible SJL mice should decrease the chances of immune rejection of the transferred cells by the recipient mouse. We can then determine whether adoptive transfer of different immune cell subsets has an effect on overall viral loads in susceptible mice.

Matrix metalloproteinases and MAV-1 infection

Matrix metalloproteinases (MMPs) are endopeptidases that can be upregulated during pathological conditions, including viral infections, to cause BBB disruption through degradation of tight junction proteins and the extracellular matrix (Reijerkerk et al. 2006; Chen et al. 2009; Engelhardt and Sorokin 2009; Spindler and Hsu 2012). MMP9 production during West Nile virus infection leads to BBB disruption and virus entry into the CNS (Wang et al. 2008). HIV infection also increases MMP2 and 9 activities *in vitro* (Eugenin et al. 2006). Likewise, MMP2 and MMP9 are both upregulated in the brains of MAV-1-infected SJL and C.SJL-Msq1 mice, but not in brains of BALB/c mice (data not shown).

Many cell types in and around the BBB can produce MMPs (Candelario-Jalil et al. 2009). To identify cells that produce MMPs in response to MAV-1 infection, we will need to isolate these cells and determine the effect of MAV-1 infection on their MMP production. We have preliminary data that shows MMP activity changes (as measured by gelatin zymography) following MAV-1 infection *in vitro* of different cells isolated from the CNS (Ashley, Domanski, Hsu, Stier and Spindler, unpublished). We can subsequently use an *in vitro* co-culture model of primary mouse brain endothelial cells (pmBECs) with different CNS cell types (e.g., astrocytes or microglia), to determine their relative contribution and the effect of MMPs on pmBEC barrier integrity (measured by transendothelial electrical resistance [TEER]) during MAV-1 infection.

Members of the *Ly6* superfamily as candidate susceptibility genes for MAV-1

Msq1 is currently 0.75 Mb in length and contains 15 genes, 14 of which are *Ly6* or *Ly6*-related genes (Spindler et al. 2010). *Ly6* gene products are glycosyl phosphatidylinositol (GPI)-anchored molecules that were first identified on mouse lymphocytes (McKenzie et al. 1977). Due to their unique expression patterns during differentiation, LY6 proteins have been used as cell subtype-specific markers for defining immune cell subsets. They can also be expressed on a number of non-hematopoietic cells.

Ly6 genes are strong candidate genes for susceptibility to MAV-1-infection because they are involved in the outcomes of other viral infections, including HIV, West Nile and Marek's disease virus (Morgan et al. 2001; Liu et al. 2003; Venter et al. 2005; Brass et al. 2008; Krishnan et al. 2008; Loeuillet et al. 2008). In addition, expression of *Ly6* genes can be upregulated by type I and II interferons (Bamezai 2004). The functions of *Ly6* genes have not been well characterized, but some are thought to be involved in cell signaling events and adhesion (Rock et al. 1989; Hänninen et al. 1997; Bamezai 2004).

Ly6 gene homologs have been found in other rodents, invertebrates, and in humans, suggesting that their gene products have important biological functions (Bamezai 2004; Holmes and Stanford 2007; Hijazi et al. 2011). Human *Ly6* genes on chromosome 8 (8q24.3) are orthologs of *Ly6* genes found on mouse chromosome 15. However, 9 genes in the murine *Ly6* locus do not have homologs in either the rat or the human chromosome (Holmes and Stanford 2007). Genes between *Ly6E* and *Ly6H* on mouse chromosome 15 are not present in the corresponding region on human chromosome 8 (Fig 6.1). In particular, humans do not have orthologs for *Ly6C* and *Ly6A*.

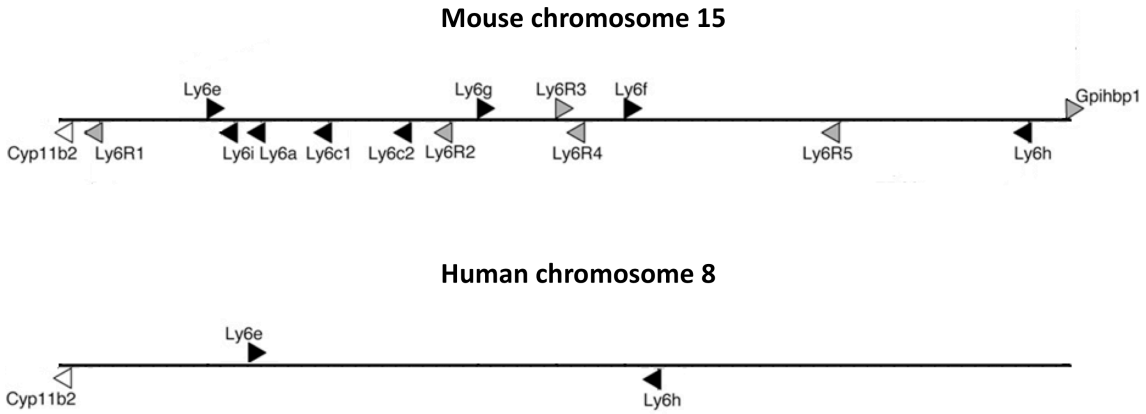

Figure 6.1. Mouse and human *Ly6* genes. Humans do not have orthologs for mouse genes that lie between *Ly6E* and *Ly6H*. *Ly6* genes are indicated by black triangles, *Ly6*-related genes by gray triangles, and the other gene by a white triangle. Genes transcribed from the top (+) strand point to the right and genes transcribed from the bottom (−) strand point to the left (Figure modified from Spindler et al. 2010).

However, other human *Ly6* genes may function as paralogs of these genes. In both organisms *Ly6* superfamily genes are also found at other chromosomal locations.

LY6 proteins can directly affect viral infection *in vitro*, either positively or negatively. Upregulation of human LY6E during yellow fever virus infection in a cell-based screen increases virus yields (Schoggins et al. 2011). In contrast, human LY6E inhibits growth of vesicular stomatitis virus, identified via a similar large-scale *in vitro* screen (Liu et al. 2012). In addition, chicken LY6E expression is upregulated during highly pathogenic avian influenza virus infection in chicken kidney cells (Zhang et al. 2008). *Ly6C*, *Ly6E*, *Ly6F*, and *Ly6A* are also upregulated following infection of mice by a highly neuroinvasive West Nile virus strain (Venter et al. 2005). In addition, susceptibility to Marek's disease virus and HIV have been mapped to the chicken *Ly6E* and the human *Ly6* locus, respectively (Liu et al. 2003; Loeuillet et al. 2008). The mechanisms by which LY6E affects the outcomes of these infections are not known, but these data suggest an underappreciated role of LY6 proteins in viral infections at the cellular level.

MAV-1 replicates and reaches equally high titers in BALB/c, SJL and C.SJL-Msq1 pmBECs by 5 dpi (Hsu et al. 2012). However, there is a slight lag in viral yield in BALB/c pmBECs up to 2 dpi. We also examined MAV-1 yields at 3 dpi in SJL and BALB/c pmBECs (when we see the decrease in tight junction integrity in SJL and C.SJL-Msq1 pmBECs measured by TEER), but there was no difference between the two mouse strains (Fig. 6.2). These data reveal that the loss of TEER occurs independently of viral yield and suggests that there are strain-specific differences at the cellular level that

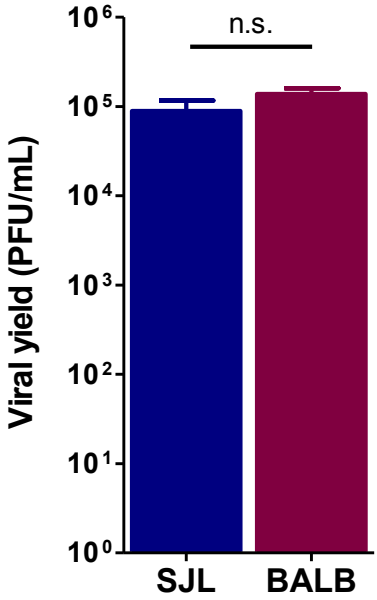

Figure 6.2. Viral yields are similar between SJL and BALB/c pmBECs at 3 dpi. pmBECs from SJL and BALB/c mice were isolated, grown to confluence and infected at a MOI of 5. Cells were harvested at 3 dpi and viral titers were assayed by plaque assay performed in triplicate. Data are from three replicates in a single experiment. Means and SDs are shown.

control barrier integrity during MAV-1 infection that are independent of how much virus is being produced.

LY6 proteins could also be important for the structural integrity of tight junctions in endothelial cells. Septate junctions that occur in invertebrates are thought to be functional analogs to the tight junctions found in vertebrates. They also function as paracellular barriers to regulate diffusion of solutes and migration of cells across the epithelium (Lewin 2007). In *Drosophila*, a LY6 protein encoded by the gene *boudin* is involved in septate junction organization in tracheal cells and in the embryonic peripheral nervous system (Hijazi et al. 2009). Another Drosophila gene, *coiled*, is also involved in septate junction organization; unlike *boudin*, it is required for the maintenance of the blood-brain barrier (Hijazi et al. 2011). However, another *Ly6* gene, *retroactive*, appears to be dispensable for the maintenance of septate junction integrity, but is involved in chitin filament assembly, a process that also involves septate junctions (Moussian et al. 2006). Thus, these LY6 proteins have related but non-redundant functions. LY6 proteins in mice may have similar structural functions in the tight junctions in the BBB, and MAV-1 infection may alter the distribution of LY6 proteins or downregulate their expression levels, leading to the loss of barrier integrity and disruption of the BBB. To test this, we can stain for the distribution of these proteins by immunofluorescence before and after MAV-1 infection to determine if their localization changes post-infection.

Mouse LY6A, LY6C and LY6G are expressed on pmBECs (Chapter IV, Fig. 4.10). Higher levels of LY6A and LY6G are expressed on SJL-derived pmBECs than BALB/c pmBECs, while LY6C expression levels appear to be comparable between the two strains. Brain endothelial cells from C57BL mice have also been reported to express

LY6C *in vivo* (Alliot et al. 1998). Studies also show that the cell-type distribution of LY6A expression in CNS tissues is mouse strain-dependent (Cray et al. 1990). We can examine whether LY6 is expressed on the same cells infected by MAV-1 *in vivo* or *in vitro* using LY6-specific antibodies and either GFP-labeled MAV-1 (Spindler et al., unpublished) or an antibody specific for MAV-1. Currently, we know that mouse brain vascular endothelial cells are infected by MAV-1 (Charles et al. 1998; Kajon et al. 1998). We also have preliminary evidence that astrocytes are infected *ex vivo*. It will be interesting to test through siRNA knockdown of *Ly6* genes in pmBECs whether expression level differences of these genes contribute to the loss of TEER following MAV-1 infection.

We also hypothesized that LY6 proteins could function as virus receptors or co-factors important for the viral entry process. However, infection of BALB/c-, SJL- and C.SJL-Msq1-derived pmBECs showed no difference in the ability of MAV-1 to replicate in cells from the different mouse strains (Hsu et al. 2012). Intracerebral injection of MAV-1 results in equivalent brain viral loads in SJL and BALB/c mice. Taken together this suggests that the difference in ability of virus to replicate in the brains of different mouse strains is due to a difference in virus trafficking to the organ, and not a difference in replication at the brain endothelial cell level (Spindler et al. 2007).

Functional analysis using monoclonal antibodies to block LY6A, LY6C and LY6G prior to viral infection did not affect MAV-1 viral yield in 3T6 cells (Fig. 6.3). Results from these studies can potentially be misleading due to the high possibility of antibody cross-reactivity between these highly homologous proteins. However, regardless of whether the antibodies cross-reacted with other LY6 proteins, we observed no

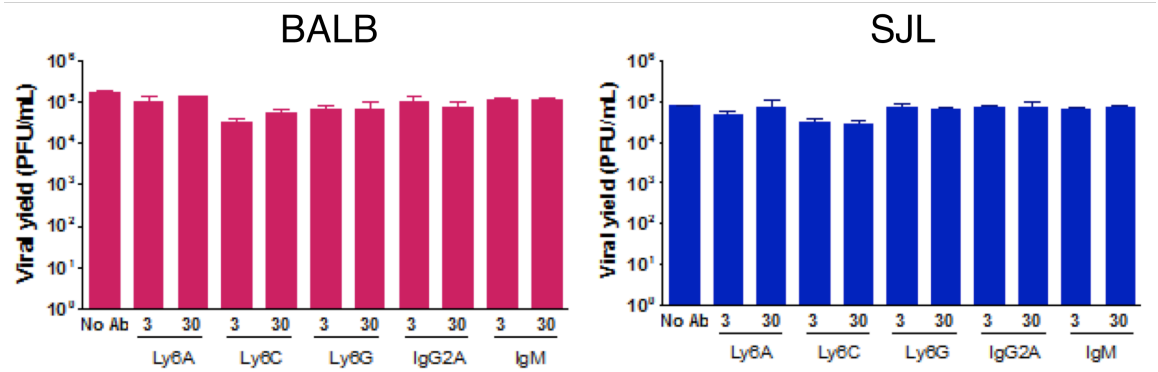

Figure 6.3. Treatment with LY6A, LY6C and LY6G antibodies did not affect viral yields of mouse fibroblast cells. 3T6 cells were treated with Ly6 antibody or a relevant isotype control antibody (IgG2A or IgM) and infected with MOI 5 of MAV-1. Antibody concentrations were either 3 or 30 µg/mL, as indicated; No Ab, no antibody. Cells were harvested 2 dpi and viral yields were determined by plaque assay performed in triplicate. Data are from one experiment with three replicates for each experimental condition. Means and SDs are indicated.

difference between treated and untreated cells. To further test for a receptor function of LY6 proteins, we can also treat pmBECs with phospholipase C (which removes GPI-anchored proteins from the membrane) prior to infection. It is possible that removing LY6 proteins from the cell surface may also disrupt additional functions, for example, if they are important for maintenance of the structural integrity of tight junctions. However, if this is the case, phospholipase C-treated pmBECs should lose their high levels of TEER prior to MAV-1 infection.

The type I and II interferon (IFN) responses are important for protection against pathogens. IFNs are important for both survival of the host and the control of MAV-1 replication (Spindler et al., unpublished). The protein products of interferon stimulated genes (ISGs) carry out anti-viral defense. MAV-1 increases the steady-state level of ISG mRNAs, interferon regulatory factors 1 and 7 (IRF-1 and IRF-7) and signal transducer and activator of transcription 1 (STAT-1), *in vitro* and *in vivo* (Spindler et al. 2007). STAT-1, IRF-1 and IRF-7 are important regulators of other ISGs and help establish the antiviral state (Samuel 2001). Since *Ly6* genes are ISGs, it would be interesting to determine whether expression of *Ly6* genes is affected by the addition of exogenous interferon or during MAV-1 infection, and whether *Ly6* gene regulation is different between susceptible and resistant mouse strains.

Alternative hypothesis to explain why transgenic mice are resistant to MAV-1

Thus far, none of the transgenic mice that we generated using BACs from a 129S6/SvEv BAC library introduced onto a resistant recipient mouse background were susceptible to MAV-1. We used 129S6/SvEv BAC DNA because the BAC library was

readily available from Children's Hospital Oakland Research Institute. No SJL BAC library was available. Susceptibility to MAV-1 for 129S6/SvEv mice was also mapped to a region on Chr 15 that includes $Msq1^{SJL}$ (Spindler et al. 2010). This locus in 129S6/SvEv mice accounts for 54% of the brain viral load variance. These data demonstrate that 129S6/SvEv mice are an appropriate susceptible donor strain for the BAC transgenesis approach.

The resistant phenotype of our transgenic mouse strains is contrary to our expectations because we hypothesized that the addition of a BAC containing the susceptibility gene to a resistant mouse background would render the recipient mouse susceptible to MAV-1. Currently, we are determining whether the transgenes in our BAC transgenic strains are being expressed, and whether a larger region is necessary to confer susceptibility. Careful assessment of transgene expression levels will need to be performed. We are also working to generate mice that contain more than one BAC construct.

However, we are also considering an alternative hypothesis, in which the susceptibility phenotype could be due to haploinsufficiency of the resistant allele. In the case of haploinsufficiency, the presence of both functional alleles is required in order to express a certain phenotype. In yeast, around 3% of the tested genes were founds to be haploinsufficient for growth in rich media (Deutschbauer et al. 2005). In humans, there have been several transcription factors identified with haploinsufficient mutations, for e.g., *GATA*, *Nkx21* and *TWIST* (Johnson et al. 1998; Seidman and Seidman 2002; van Looij et al. 2005). Holt-Oram syndrome is another example where haploinsufficiency of a transcription factor results in disease; it has also been shown in other animal model

systems that sufficient TBX5 gene expression levels are important for proper heart and limb development (Simon et al. 1997; Tamura et al. 1999; Hatcher and Basson 2001). In humans, a mutation in the TBX5 gene (important for heart and forelimb development) leading to a truncated protein product results in decreased TBX5 activity and cardiac and limb defects (Basson et al. 1997). Heterozygous mutations in *ATM* and *BLM* have also been shown to result in increased tumor susceptibility (Goss et al. 2002; Spring et al. 2002).

Both (BALB/c×SJL)F_1 mice (Welton et al. 2005) and C.SJL-Msq1$^{BALB/SJL}$ mice heterozygous for *Msq1* (Hsu et al. 2012) have an intermediate susceptibility phenotype. According to our original hypothesis, these mice are susceptible because the susceptibility phenotype is semi-dominant. However, it may be that the resistant allele does not produce enough gene product to make the mouse resistant to MAV-1. If the susceptibility phenotype of (BALB/c×SJL)F_1 and C.SJL-Msq1$^{BALB/SJL}$ congenic mice is due to haploinsufficiency of the BALB allele, the transgenic mouse strains should not be susceptible to MAV-1, since they have two copies of the BALB/c (resistant) allele. The hypothesis that susceptibility is brought about by haploinsufficiency of the resistant allele would mean that the presence of two copies of the resistant allele should be sufficient to confer the resistant phenotype, regardless of the number or expression levels of susceptible strain-derived genes. To test if the resistance gene has such an effect, we will need to make transgenic mice using BALB/c-derived transgenes and a recipient susceptible strain.

However, regardless of whether susceptibility is semi-dominant or if the susceptibility phenotype is due to haploinsufficiency of the resistant allele, *Msq1* is still

strongly linked to MAV-1 disease outcome. Our previous findings regarding the relative contribution of *Msq1* to brain pathogenesis during MAV-1 infection remain valid under both hypotheses. Identification of the gene within *Msq1* that accounts for these aspects of MAV-1 morbidity is an important step in uncovering the mechanism behind BBB breakdown and viral encephalitis. Defining the components in the pathway may improve diagnosis of additional cases of viral encephalitis and may provide avenues for development of therapeutics to treat cases of human adenovirus CNS infections in immunocompromised individuals.

References

Alliot, F., J. Rutin and B. Pessac. 1998. Ly-6C is expressed in brain vessels endothelial cells but not in microglia of the mouse. Neuroscience Letters 251: 37-40.

Ashley, S. L., A. R. Welton, K. M. Harwood, N. Van Rooijen and K. R. Spindler. 2009. Mouse adenovirus type 1 infection of macrophages. Virology 390: 307-314.

Bamezai, A. 2004. Mouse Ly-6 proteins and their extended family: markers of cell differentiation and regulators of cell signaling. Arch Immunol Ther Exp (Warsz) 52: 255-266.

Bamezai, A. and K. L. Rock. 1995. Overexpressed Ly-6A.2 mediates cell-cell adhesion by binding a ligand expressed on lymphoid cells. Proc Natl Acad Sci U S A 92: 4294-4298.

Basson, C. T., D. R. Bachinsky, et al. 1997. Mutations in human TBX5 [corrected] cause limb and cardiac malformation in Holt-Oram syndrome. Nat Genet 15: 30-35.

Brass, A. L., D. M. Dykxhoorn, Y. Benita, N. Yan, A. Engelman, R. J. Xavier, J. Lieberman and S. J. Elledge. 2008. Identification of host proteins required for HIV infection through a functional genomic screen. Science 319: 921-926.

Candelario-Jalil, E., Y. Yang and G. A. Rosenberg. 2009. Diverse roles of matrix metalloproteinases and tissue inhibitors of metalloproteinases in neuroinflammation and cerebral ischemia. Neuroscience 158: 983-994.

Charles, P. C., J. D. Guida, C. F. Brosnan and M. S. Horwitz. 1998. Mouse adenovirus type-1 replication is restricted to vascular endothelium in the CNS of susceptible strains of mice. Virology 245: 216-228.

Chen, F., N. Ohashi, W. Li, C. Eckman and J. H. Nguyen. 2009. Disruptions of occludin and claudin-5 in brain endothelial cells in vitro and in brains of mice with acute liver failure. Hepatology 50: 1914-1923.

Cray, C., R. W. Keane, T. R. Malek and R. B. Levy. 1990. Regulation and selective expression of Ly-6A/E, a lymphocyte activation molecule, in the central nervous system. Brain Res Mol Brain Res 8: 9-15.

Deutschbauer, A. M., D. F. Jaramillo, M. Proctor, J. Kumm, M. E. Hillenmeyer, R. W. Davis, C. Nislow and G. Giaever. 2005. Mechanisms of haploinsufficiency revealed by genome-wide profiling in yeast. Genetics 169: 1915-1925.

Engelhardt, B. and L. Sorokin. 2009. The blood-brain and the blood-cerebrospinal fluid barriers: function and dysfunction. Semin Immunopathol 31: 497-511.

Eugenin, E. A., K. Osiecki, L. Lopez, H. Goldstein, T. M. Calderon and J. W. Berman. 2006. CCL2/monocyte chemoattractant protein-1 mediates enhanced transmigration of human immunodeficiency virus (HIV)-infected leukocytes across the blood-brain barrier: a potential mechanism of HIV-CNS invasion and NeuroAIDS. J Neurosci 26: 1098-1106.

Getts, D. R., R. L. Terry, et al. 2008. Ly6c+ "inflammatory monocytes" are microglial precursors recruited in a pathogenic manner in West Nile virus encephalitis. J Exp Med 205: 2319-2337.

Gordon, S. and P. R. Taylor. 2005. Monocyte and macrophage heterogeneity. Nat Rev Immunol 5: 953-964.

Goss, K. H., M. A. Risinger, et al. 2002. Enhanced tumor formation in mice heterozygous for Blm mutation. Science 297: 2051-2053.

Gralinski, L. E., S. L. Ashley, S. D. Dixon and K. R. Spindler. 2009. Mouse adenovirus type 1-induced breakdown of the blood-brain barrier. J Virol 83: 9398-9410.

Guida, J. D., G. Fejer, L. A. Pirofski, C. F. Brosnan and M. S. Horwitz. 1995. Mouse adenovirus type 1 causes a fatal hemorrhagic encephalomyelitis in adult C57BL/6 but not BALB/c mice. J Virol 69: 7674-7681.

Hänninen, A., I. Jaakkola, M. Salmi, O. Simell and S. Jalkanen. 1997. Ly-6C regulates endothelial adhesion and homing of CD8(+) T cells by activating integrin-dependent adhesion pathways. Proc Natl Acad Sci U S A 94: 6898-6903.

Hatcher, C. J. and C. T. Basson. 2001. Getting the T-box dose right. Nat Med 7: 1185-1186.

Hijazi, A., M. Haenlin, L. Waltzer and F. Roch. 2011. The Ly6 protein coiled is required for septate junction and blood brain barrier organisation in Drosophila. PLoS One 6: e17763.

Hijazi, A., W. Masson, B. Auge, L. Waltzer, M. Haenlin and F. Roch. 2009. boudin is required for septate junction organisation in Drosophila and codes for a diffusible protein of the Ly6 superfamily. Development 136: 2199-2209.

Holmes, C. and W. L. Stanford. 2007. Concise review: stem cell antigen-1: expression, function, and enigma. Stem Cells 25: 1339-1347.

Hsu, T. H., I. W. Althaus, O. Foreman and K. R. Spindler. 2012. Contribution of a single host genetic locus to mouse adenovirus type 1 infection and encephalitis. MBio 3(3), e00131–12–e00131–12. doi:10.1128/mBio.00131-12.

Johnson, D., S. W. Horsley, et al. 1998. A comprehensive screen for TWIST mutations in patients with craniosynostosis identifies a new microdeletion syndrome of chromosome band 7p21.1. Am J Hum Genet 63: 1282-1293.

Kajon, A. E., C. C. Brown and K. R. Spindler. 1998. Distribution of mouse adenovirus type 1 in intraperitoneally and intranasally infected adult outbred mice. J Virol 72: 1219-1223.

Kring, S. C., C. S. King and K. R. Spindler. 1995. Susceptibility and signs associated with mouse adenovirus type 1 infection of adult outbred Swiss mice. J Virol 69: 8084-8088.

Krishnan, M. N., A. Ng, et al. 2008. RNA interference screen for human genes associated with West Nile virus infection. Nature 455: 242-245.

Lewin, B. 2007. Cells. Sudbury, Mass., Jones and Bartlett Publishers.

Liu, H. C., M. Niikura, J. E. Fulton and H. H. Cheng. 2003. Identification of chicken lymphocyte antigen 6 complex, locus E (LY6E, alias SCA2) as a putative Marek's disease resistance gene via a virus-host protein interaction screen. Cytogenet Genome Res 102: 304-308.

Liu, S. Y., D. J. Sanchez, R. Aliyari, S. Lu and G. Cheng. 2012. Systematic identification of type I and type II interferon-induced antiviral factors. Proc Natl Acad Sci U S A 109: 4239-4244.

Loeuillet, C., S. Deutsch, A. Ciuffi, D. Robyr, P. Taffe, M. Munoz, J. S. Beckmann, S. E. Antonarakis and A. Telenti. 2008. In vitro whole-genome analysis identifies a susceptibility locus for HIV-1. PLoS Biol 6: e32.

Malim, M. H. 2009. APOBEC proteins and intrinsic resistance to HIV-1 infection. Philos Trans R Soc Lond B Biol Sci 364: 675-687.

Matullo, C. M., K. J. O'Regan, H. Hensley, M. Curtis and G. F. Rall. 2010. Lymphocytic choriomeningitis virus-induced mortality in mice is triggered by edema and brain herniation. J Virol 84: 312-320.

McKenzie, I. F., J. Gardiner, M. Cherry and G. D. Snell. 1977. Lymphocyte antigens: Ly-4, Ly-6, and Ly-7. Transplant Proc 9: 667-669.

Moore, M. L., C. C. Brown and K. R. Spindler. 2003. T cells cause acute immunopathology and are required for long-term survival in mouse adenovirus type 1-induced encephalomyelitis. J Virol 77: 10060-10070.

Moore, M. L., E. L. McKissic, C. C. Brown, J. E. Wilkinson and K. R. Spindler. 2004. Fatal disseminated mouse adenovirus type 1 infection in mice lacking B cells or Bruton's tyrosine kinase. J Virol 78: 5584-5590.

Morgan, R. W., L. Sofer, A. S. Anderson, E. L. Bernberg, J. Cui and J. Burnside. 2001. Induction of host gene expression following infection of chicken embryo fibroblasts with oncogenic Marek's disease virus. J Virol 75: 533-539.

Moussian, B., E. Tang, A. Tonning, S. Helms, H. Schwarz, C. Nusslein-Volhard and A. E. Uv. 2006. Drosophila Knickkopf and Retroactive are needed for epithelial tube growth and cuticle differentiation through their specific requirement for chitin filament organization. Development 133: 163-171.

Pirofski, L., M. S. Horwitz, M. D. Scharff and S. M. Factor. 1991. Murine adenovirus infection of SCID mice induces hepatic lesions that resemble human Reye syndrome. Proc Natl Acad Sci U S A 88: 4358-4362.

Reijerkerk, A., G. Kooij, S. M. van der Pol, S. Khazen, C. D. Dijkstra and H. E. de Vries. 2006. Diapedesis of monocytes is associated with MMP-mediated occludin disappearance in brain endothelial cells. FASEB J 20: 2550-2552.

Rock, K. L., H. Reiser, A. Bamezai, J. McGrew and B. Benacerraf. 1989. The LY-6 locus: a multigene family encoding phosphatidylinositol-anchored membrane proteins concerned with T-cell activation. Immunol Rev 111: 195-224.

Samuel, C. E. 2001. Antiviral actions of interferons. Clin Microbiol Rev 14: 778-809, table of contents.

Schoggins, J. W., S. J. Wilson, M. Panis, M. Y. Murphy, C. T. Jones, P. Bieniasz and C. M. Rice. 2011. A diverse range of gene products are effectors of the type I interferon antiviral response. Nature 472: 481-485.

Seidman, J. G. and C. Seidman. 2002. Transcription factor haploinsufficiency: when half a loaf is not enough. J Clin Invest 109: 451-455.

Shevach, E. M. and P. E. Korty. 1989. Ly-6: a multigene family in search of a function. Immunol Today 10: 195-200.

Simon, H. G., R. Kittappa, P. A. Khan, C. Tsilfidis, R. A. Liversage and S. Oppenheimer. 1997. A novel family of T-box genes in urodele amphibian limb development and regeneration: candidate genes involved in vertebrate forelimb/hindlimb patterning. Development 124: 1355-1366.

Spindler, K. R., L. Fang, M. L. Moore, G. N. Hirsch, C. C. Brown and A. Kajon. 2001. SJL/J mice are highly susceptible to infection by mouse adenovirus type 1. J Virol 75: 12039-12046.

Spindler, K. R. and T. H. Hsu. 2012. Viral disruption of the blood-brain barrier. Trends Microbiol doi:10.1016/j.tim.2012.03.009.

Spindler, K. R., M. L. Moore and A. N. Cauthen. 2007. Mouse adenoviruses. The mouse in biomedical research. American College of Laboratory Animal Medicine series. Amsterdam ; Boston, Elsevier. 2: 49-65.

Spindler, K. R., A. R. Welton, E. S. Lim, S. Duvvuru, I. W. Althaus, J. E. Imperiale, A. I. Daoud and E. J. Chesler. 2010. The major locus for mouse adenovirus susceptibility maps to genes of the hematopoietic cell surface-expressed LY6 family. J Immunol 184: 3055-3062.

Spring, K., F. Ahangari, et al. 2002. Mice heterozygous for mutation in Atm, the gene involved in ataxia-telangiectasia, have heightened susceptibility to cancer. Nat Genet 32: 185-190.

Suspene, R., D. Guetard, M. Henry, P. Sommer, S. Wain-Hobson and J. P. Vartanian. 2005. Extensive editing of both hepatitis B virus DNA strands by APOBEC3 cytidine deaminases in vitro and in vivo. Proc Natl Acad Sci U S A 102: 8321-8326.

Tamura, K., S. Yonei-Tamura and J. C. Izpisua Belmonte. 1999. Differential expression of Tbx4 and Tbx5 in Zebrafish fin buds. Mech Dev 87: 181-184.

van Looij, M. A., H. van der Burg, R. S. van der Giessen, M. M. de Ruiter, J. van der Wees, J. H. van Doorninck, C. I. De Zeeuw and G. A. van Zanten. 2005. GATA3 haploinsufficiency causes a rapid deterioration of distortion product otoacoustic emissions (DPOAEs) in mice. Neurobiol Dis 20: 890-897.

Van Rooijen, N. 1989. The liposome-mediated macrophage 'suicide' technique. J Immunol Methods 124: 1-6.

Vartanian, J. P., D. Guetard, M. Henry and S. Wain-Hobson. 2008. Evidence for editing of human papillomavirus DNA by APOBEC3 in benign and precancerous lesions. Science 320: 230-233.

Venter, M., T. G. Myers, M. A. Wilson, T. J. Kindt, J. T. Paweska, F. J. Burt, P. A. Leman and R. Swanepoel. 2005. Gene expression in mice infected with West Nile virus strains of different neurovirulence. Virology 342: 119-140.

Walunas, T. L., D. S. Bruce, L. Dustin, D. Y. Loh and J. A. Bluestone. 1995. Ly-6C is a marker of memory CD8+ T cells. J Immunol 155: 1873-1883.

Wang, P., J. Dai, F. Bai, K. F. Kong, S. J. Wong, R. R. Montgomery, J. A. Madri and E. Fikrig. 2008. Matrix metalloproteinase 9 facilitates West Nile virus entry into the brain. J Virol 82: 8978-8985.

Welton, A. R., E. J. Chesler, C. Sturkie, A. U. Jackson, G. N. Hirsch and K. R. Spindler. 2005. Identification of quantitative trait loci for susceptibility to mouse adenovirus type 1. J Virol 79: 11517-11522.

Zhang, H., B. Yang, R. J. Pomerantz, C. Zhang, S. C. Arunachalam and L. Gao. 2003. The cytidine deaminase CEM15 induces hypermutation in newly synthesized HIV-1 DNA. Nature 424: 94-98.

Zhang, W., H. Li, G. Cheng, S. Hu, Z. Li and D. Bi. 2008. Avian influenza virus infection induces differential expression of genes in chicken kidney. Res Vet Sci 84: 374-381.

Zhou, J., S. A. Stohlman, D. R. Hinton and N. W. Marten. 2003. Neutrophils promote mononuclear cell infiltration during viral-induced encephalitis. J Immunol 170: 3331-3336.